Universidade do Minho
Escola de Ciências

João Carlos Canossa Ferreira

Characterization of vacuole permeabilization and HMGB1 nuclear release in the yeast cell death induced by a benzo[a]phenoxazine derivative

Março de 2017

Characterization of vacuole permeabilization and HMGB1 nuclear release in the yeast cell death induced by a benzo[a]phenoxazine derivative
João Carlos Canossa Ferreira
UMinho | 2017

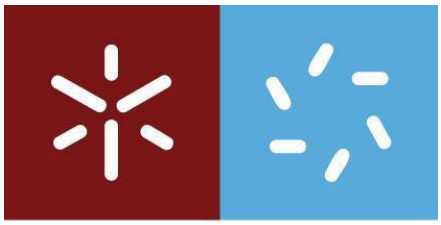

Universidade do Minho
Escola de Ciências

João Carlos Canossa Ferreira

Characterization of vacuole permeabilization and HMGB1 nuclear release in the yeast cell death induced by a benzo[*a*]phenoxazine derivative

Tese de Mestrado
Mestrado em Genética Molecular

Trabalho realizado sob orientação de
Professora Doutora Maria João Marques Ferreira Sousa Moreira
Professora Doutora Maria Sameiro Torres Gonçalves

Agradecimentos

Apesar deste trabalho deste trabalho ter sido de caracter individual, não poderia deixar de exprimir o meu mais sincero agradecimento a todos os que me ajudaram e apoiaram na sua realização.

Em primeiro lugar, agradeço as minhas orientadoras, Doutora Maria João Sousa e Doutora Maria do Sameiro Gonçalves, pela possibilidade de realização deste trabalho. À Doutora Maria João, por todo o apoio, toda a disponibilidade e orientação prestada e pelos ensinamentos, aconselhamentos e criticas ao longo deste trabalho que foram muito importantes para o meu crescimento cientifico. À Doutora Sameiro, por se ter mostrado sempre disponível em ajudar e por ter sido incansável em disponibilizar o composto com que trabalhei, sem ela seria impossível a realização deste trabalho.

Agradeço a todos os colegas da Micro I, Lisandra Castro, Cátia Fernandes, Joana Guedes, Anabela Ferreira, Paulo Veloso, Nuno Machado, António Rego, Filipa Dias, Diana Silva, Catarina Afonso e Vasco Lobato muito obrigado pela ajuda e pelo bom ambiente que sempre criaram no laboratório.

Ao departamento de biologia, a todos os técnicos e funcionários, em especial ao Sr. Luís por ser incansável em garantir todas as condições de trabalho.

Obrigado aos meus amigos, em especial ao João Pacheco, Luís Ferraz, Bruno Oliveira, Carlos Eloy, Henrique Ribeiro, João Ferreira, Rui Sousa e Beatriz Domingues por estarem sempre presentes e por me terem apoiado em todos os momentos. Agradeço também aos meus amigos da terra, Miguel Moreira, Hugo Moreira, Ana Luísa, Sandrina Rodrigues, Fábio Daniel, Rosa Silva e Kelly Dias por me terem ajudado a ultrapassar mais esta etapa.

Á minha família, o meu muito obrigado, por terem acreditado em mim e por terem permitido esta oportunidade, sem vocês nada disto seria possível.

A todos Muito Obrigado!!!

Abstract

The number of antifungal agents approved for use in humans is still very limited and resistance to the existing ones is often found, thus revealing the need for the development of new antifungal drugs.

Phenoxazine derivatives have assumed an increasing importance in life sciences since they present antiproliferative proprieties which potentiate their utilization as antitumor and antimicrobial agents. We have recently found that one new phenoxazine derivative (MSG-111-cd3), induces cell death in *Saccharomyces cerevisiae* and accumulates at the vacuolar membrane and endoplasmic reticulum. Initial studies revealed that MSG-111-cd3 toxic effect may be mediated through vacuolar membrane damage and vacuolar permeabilization. Furthermore, it was observed that the compound lead to Nhp6Ap (the yeast HMGB1 orthologue) release from the nucleus to the cytosol, where it displayed a punctuated pattern, without loss of plasma membrane integrity.

Aiming to further elucidate the cell death mechanism we analyzed the consequences of vacuolar permeabilization, the role of the HMGB1 protein in the cell death process and the mechanisms underlying its nuclear release. We find out that MSG-111-cd3 yeast cell death is dependent on the vacuolar protease Pep4p and that the vacuole permeabilization resulted in its translocation from the vacuole to the cytosol. We observed that autophagy is not involved in the cell death process, and although MSG-111-cd3 leads to mitochondrial network fragmentation, apparently, the cell death process is independent of the mitochondrial pathway, since no other alterations were significantly induced in this organelle. Our results suggest that Nhp6Ap is apparently not crucial for the cell death process. Furthermore, we found out that Nhp6Ap is not the only DNA binding protein to be released into cytosol, since the histone Hta2p also suffer translocation exhibiting the same phenotype as Nhp6Ap. Furthermore, the treatment lead to nuclear envelope disorganization, which show the high susceptibility of the nucleus to the MSG-111-cd3 effects.

Resumo

O número de agentes antifúngicos aprovados para utilização em seres humanos é ainda muito limitado e é frequentemente encontrada resistência aos existentes, revelando assim a necessidade de desenvolvimento de novos fármacos antifúngicos.

Os derivados de fenoxazina assumiram uma importância crescente nas ciências da vida, uma vez que apresentam propriedades antiproliferativas que potenciam a sua utilização como agentes antitumorais e antimicrobianos. Recentemente descobrimos que um novo derivado de fenoxazina (MSG-111-cd3) induz morte celular em *Saccharomyces cerevisiae* e acumula-se na membrana vacuolar e no retículo endoplasmático. Estudos iniciais revelaram que o efeito tóxico de MSG-111-cd3 parece ser mediado através de danos na membrana vacuolar e permeabilização vacuolar. Além disso, observou-se que o composto conduziu à libertação de Nhp6Ap (o ortólogo de HMGB1 em levedura) do núcleo para o citosol, onde apresenta um padrão pontuado, sem perda da integridade da membrana plasmática.

Com o objetivo de melhor clarificar o mecanismo de morte celular induzido pelo composto MSG-111-cd3, analisamos as consequências da permeabilização vacuolar, o papel da proteína HMGB1 e os mecanismos subjacentes à sua liberação nuclear em resposta ao tratamento com este composto. Descobrimos que a morte das células de levedura causada pelo composto MSG-111-cd3 é dependente da protéase vacuolar Pep4p e que a permeabilização do vacúolo resultou na sua translocação para o citosol. Observamos que a autofagia não está envolvida no processo de morte celular e, embora o MSG-111-cd3 leve à fragmentação da rede mitocondrial, aparentemente, o processo de morte celular é independente da via mitocondrial. Os resultados sugerem que Nhp6Ap aparentemente não é crucial para o processo de morte celular. Além disso, mostrámos que Nhp6Ap não é a única proteína de ligação ao DNA a ser libertada do núcleo para o citosol, uma vez que a histona Hta2p também sofre translocação exibindo o mesmo fenótipo que Nhp6Ap. Além disso, o tratamento conduz à desorganização do envelope nuclear, o que mostra a elevada suscetibilidade do núcleo aos efeitos do MSG-111-cd3.

Table of contents

List of abbreviations and acronyms

AcLi	Lithium acetate
AIF	Apoptosis inducing factor
APC	Antigen-presenting cell
ATP	Adenosine triphosphate
CFU	Colony formation units
DAPI	4',6-diamidino-2-phenylindole
DIC	Differential Interference Contrast
DMSO	Dimethyl sulfoxide
DPM	Double point mutation
ENDOG	Endonuclease G
H_2O_2	Hydrogen Peroxide
HMGB1	High Mobility group box 1
LAMP	Lysosome-associated membrane proteins
LC3	Light chain 3
LIMP	Lysosomal integral membrane proteins
LMP	Lysosomal membrane permeablization
LPS	Lipopolysaccharides
MIC	Minimum inhibitory concentration
MMP	Mitochondrial membrane permeabilization
MSG	MSG-111-cd3

NLS	Nuclear localizations signals
O.D	Optical density
PCD	Programed cell death
PEG	Polyethylene glycol
PI	Propidium iodide
PMSF	Phenylmethylsulfonyl fluoride
PVDF	Polyvinylidene fluoride membrane
RAGE	Receptor for advanced glycation end products
ROS	Reactive oxygen species
S. cerevisiae	*Saccharomyces cerevisiae*
SDS-PAGE	Sodium dodecyl sulphate polyacrilamide gel electophoresis
ssDNA	Salmon sperm DNA
TUNEL	Terminal deoxynucleotidyl transferase dUTP nick end labeling
WT	Wild type
YEPD	Yeast Extract Peptone Dextrose
Z-VAD-fmk	N-benzyloxycarbonyl-Val-Ala-Aspfluoromethylketone

List of figures

List of tables

1. Introduction

1.1 Cell death

1.1.1 Cell death Pathways

All living organisms from the simplest to the most complex share the same structural and functional base unit - the cell. Starting from this basic unit of life and through more or less complex biological processes, the cellular organization and its rearrangement will give the enormous biodiversity of living beings that exist today. The final stage of a living organism after reaching its maturity is death. However, at the cellular level the dying process is not always associated with something bad and neither should be unwanted (Baehrecke, 2002). In reality, cells also need to die to allow the development and to contribute to the homeostasis of the individual. Thus, cell death is an important biological process in the development of an organism, being involved in eliminating abnormal cells, in the control of cell numbers, and also in the formation and deletion of structures (Jacobson *et al.*, 1997). In fact, genetics studies have shown that organisms so different as worms and humans have conserved genes that encode the core cell death machinery (Aravind *et al.*, 2001).

On the other hand, aberrant cell death is associated with the occurrence of various complex diseases such as cancer, autoimmune diseases, neurodegenerative syndromes and myelodysplastic syndromes (Thompson, 1995; Krammer, 2000; Sastry and Rao, 2000). Cell death can be classified taking into account the morphological appearance of the process without a reference to precise biochemical mechanisms, but also taking into account the enzymological criteria (with or without the involvement of nucleases, or proteases, such as calpains, caspases, cathepsins, and transglutaminases), functional aspects (if the lethal process is accidental or programed, pathological or physiological), and considering the immunological characteristics (immunogenic or non-immunogenic) (Melino *et al.*, 2001; Kroemer *et al.*, 2009).

The first descriptions of programmed cell death mechanisms date back to around the mid 1960's (Lockshin and Williams, 1964, 1965). Since then, there has been much research in order to classify the cell death modalities based on morphological characteristics. Schweichel and Merker were able to propose a classification of the several cell death processes, that includes the type I cell death that is an heterophagic processes also known as apoptosis, the type II cell death that is associated

with autophagy, and also the type III cell death known as necrosis, that does not involve any type of digestion (Schweichel and Merker, 1973).

Apoptosis or type I cell death is an active form of PCD (programed cell death), that was first presented by Kerr (Kerr *et al.*, 1972). It is a process that has a direct involvement in several fundamental biological events, and is characterized by specific alterations in the dying cells, both morphological and biochemical. In terms of morphological alterations apoptotic cells present reduction of cellular volume, nuclear condensation (pyknosis) and fragmentation (karyorhexis) (Kroemer *et al.*, 2009). Apoptotic cells also present a few or no ultrastructural modifications of cytoplasmic organelles, loss of adhesion to neighbors cells and plasma membrane blebbling that results in the formation of apoptotic bodies but with the maintenance of the cell integrity until the final stages of the process (Nishida *et al.*, 2008). In terms of biochemical alterations, apoptotic cells display expression of cell surface markers such as phosphatidylserine externalization, internucleosomal cleavage of chromosomal DNA, protein cross-linking and also cleavage of a number of intracellular substrates by specific proteolysis (Cohen *et al.*, 1994; Martin and Green, 1995). However, is important to consider that apoptosis and programed cell death are not synonyms, since when cell death occurs in a context of physiological development, can manifest non-apoptotic features (Roach and Clarke, 2000; Baehrecke, 2002). Apoptosis is a highly sophisticated and complex process, that involves an energy-dependent cascade of molecular events. There are two main apoptotic pathways, the intrinsic (mitochondrial pathway) that is dependent or independent of caspases, and the extrinsic also known as the death receptor pathway (figure1) (Galluzzi *et al.*, 2012).

Mitochondrial membrane permeabilization (MMP) and caspase activation are the two prominent processes responsible for the occurrence of these pathways. MMP determines the point of no return of the intrinsic pathway, and is regulated by Bcl-2 proteins that can act as inducers or blockers of the process, the result of MMP is the release of pro-apoptotic molecules like cytochrome *c*, that acts as an activator of caspases which are responsible for the degradation of many nuclear and cytoplasmic proteins in the apoptotic cell (Youle and Strasser, 2008). However, the activation of caspases is not strictly dependent on MMP, and, for example, in the death receptor pathway caspase 8 can undergo an autocatalytic activation when it is recruited by the activated dead receptors, leading then to the directly cleavage and activation of the effector caspases 3 and 7 (Taylor *et al.*, 2008). During MMP,

besides cytochrome *c*, there are other mitochondrial proteins that can be released, such as apoptosis inducing factor (AIF) and endonuclease G (ENDOG). These proteins translocate to the nucleus and originate a large-scale DNA fragmentation leading to occurrence of apoptosis in a caspase-independent intrinsic pathway (Modjtahedi *et al.*, 2006).

Furthermore, there is evidence of the crosstalk between the intrinsic and extrinsic pathways, one example is the role of the BCL-2-family member BID, that when cleaved by caspase 8 is capable of activating the mitochondrial pathway acting as way to amplify the apoptotic signal (figure 1) (Galluzzi *et al.*, 2009b).

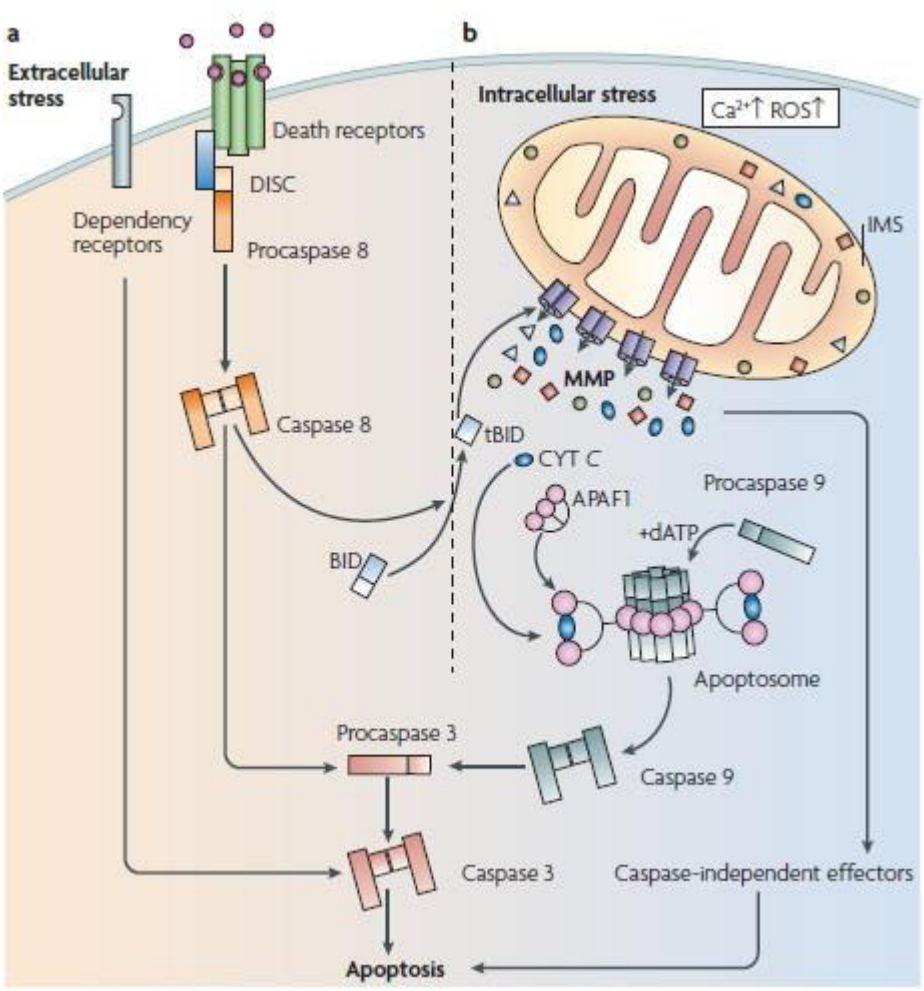

Figure 1 – Representation of extrinsic a) and intrinsic apoptotic pathways b) The activation of the extracellular pathway occurs at the level of the plasma membrane by some specific transmembrane receptors, followed by the activation of the initiator caspase 8 that can catalyze the proteolytic maturation of executioner caspases, such as caspase 3. The mitochondrial pathway is activated by intercellular alterations such as ROS accumulation or Ca^{2+} overload, that results in MMP. MMP is the point of no return in this pathway, since this permeabilization leads to the occurrence of cell death by the activation of both caspase-dependent and caspase-independent mechanisms. Adapted from (Galluzzi *et al.*, 2009b).

Autophagy is associated with another form of programmed cell death, also known as type II cell death, first introduced by Deter and Duve (Duve, 1967). Autophagy which means "self-eating" is a lysosomal degradative pathway that allows cells to recycle and degrade macromolecules and organelles, and has as primary functions the maintenance of cell homeostasis and the protection of cells under stress conditions, such as the presence of toxic substances and starvation (Klionsky, 2007). Furthermore, this process is also involved in normal organism development (Levine and Klionsky, 2004), lifespan extension (Vellai *et al.*, 2009), senescence (Young *et al.*, 2009), immunity and defense against microbial incursion (Deretic and Levine, 2009). On the other hand, autophagy is also involved in several human diseases, such as gastrointestinal disorders, myopathies, neurodegeneration, liver and heart diseases and cancer (Klionsky, 2005; Mizushima *et al.*, 2008).

Researchers have found that this process is highly conserved since genes that regulate autophagy in yeast have been conserved in organisms that are as different as humans (Levine and Klionsky, 2004). There are three main types of autophagy, microautophagy, chaperone-mediated autophagy and macroautophagy. Among those, macroautophagy is the process that is mostly associated with type II autophagic cell death (Baehrecke, 2005).

During macroautophagy (Figure 2), proteins, organelles and other cytoplasmic components are sequestered within a double-or multi-membrane structure (the autophagosome) that then fuses with hydrolase and protease containing lysosomes forming the autolysosomes for bulk degradation (Maiuri *et al.*, 2007). The resulting products are then recycled and used for synthesis of other molecules and ATP production. During the last decade, extensive research has shown the existence of at least 38 autophagy-related proteins that are involved in the autophagy initiation, elongation, cargo recruitment and fusion with lysosomes (Rubinsztein *et al.*, 2012). However, besides the high level of regulation, in some cases, autophagy is excessively induced, in an attempt to eliminate toxic molecules or damaged organelles, and this excessive induction can result in an autophagic cell death (Maiuri *et al.*, 2007).

Morphologically, autophagic cell death is defined by the high amount of autophagic vacuolization of the cytoplasm, which often, but not always, is associated with an increase in the autophagic flux (Stunkard, 2009). However, is incorrect to assume the occurrence of autophagic cell death based on this morphological alteration since in most cases autophagy is induced in a

cytoprotective way, in an attempt to cope with stress, and the inhibition will result with an increase in the cell death (Boya *et al.*, 2005). So, the occurrence of 'autophagic cell death' should be defined considering functional and biochemical aspects. It's only possible to assume that autophagic is responsible for the death process if it can be suppressed by the inhibition of the autophagic pathway (Galluzzi *et al.*, 2012). This could be achieved using autophagy inhibitor agents (such as agents that target PI3K), and/or using gene knockout/mutations or RNAi targeting in essential autophagic modulators like *ATG1*, *ATG5* and *ATG12* (Galluzzi *et al.*, 2012).

So, we should not classify as an autophagic cell death process the cases where the autophagy inhibition does not result in a decreases of cell death even if is possible to observe autophagy occurrence both through morphological alterations, or by an increased degradation of autophagic substrates.

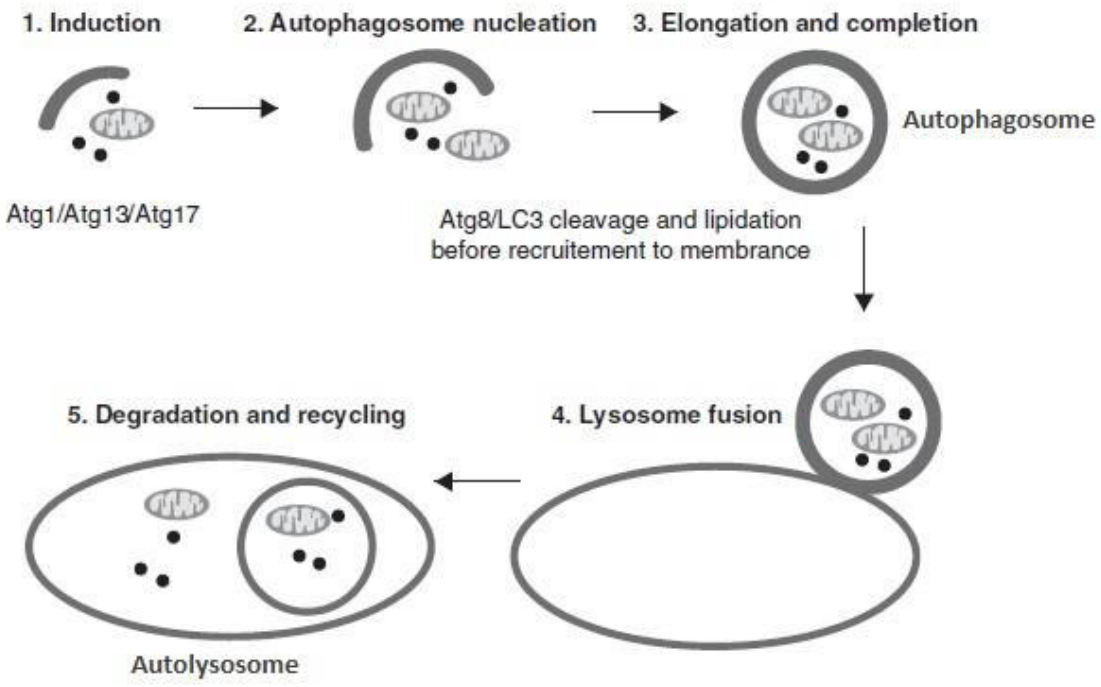

Figure 2 - Macroautophagy process. Macroautophagy is inducted by the formation of the ATG1 complex followed by the recruitment of protein and lipids mediated by the class-III phosphatidylinositol-3-kinase (Vps34) and Beclin-1/Atg6 necessary for autophagosome formation. Elongation and autophagosome completion is regulated by the conjugation of microtubule-associated protein 1 light chain 3 (LC3). In yeast this function is performed by Atg8p. Autolysosome formation occurs when the completed autophagosome fuses with the lysosome. Adapted from (Denton *et al.*, 2012)

Necrosis or type III cell death has been defined over the years as an accidental, uncontrolled type of cell death, that occurs when cells are subjected to an excessive external stress, such as a pathogen infection, ischemia and heat (Galluzzi *et al.*, 2012). This type of cell death exhibits several morphological alterations such as an increase in the cellular volume, swelling of organelles, rupture of plasma membrane and release of cytosolic contents (such as high mobility group Box 1 - HMGB1, that is a pro-inflammatory factor) (Ziegler, 2004). The leak of the cellular contents to the extracellular environment usually acts as a 'danger signal' that alerts the innate immune system and leads to an inflammatory process (Zitvogel *et al.*, 2004).

Despite its importance in human pathology, necrosis has been referred as a passive and unregulated process and therefore very little efforts had been made to investigate its mechanism. However, evidences have emerged that necrosis occurrence and course might be regulated. Today, there are several data that support both programmed course and programmed occurrence of necrosis: necrosis can occur during development (example of that is the death of chrondrocytes that control the longitudinal growth of bones) (Roach and Clarke, 2000) and in tissue homeostasis (in intestinal epithelial cells) (Barkla and Gibson, 1999). Furthermore, the facts that necrosis can be triggered by plasma membrane surface receptors when they are bound with their ligands, the inhibition of some enzymes and processes can prevent necrosis and also that genetic and epigenetic factors can regulate the susceptibility of necrotic cell dead are some of evidences that necrosis is not strictly an accidental type of cell death (Golstein and Kroemer, 2007).

More recently there has been a substantial advance in the comprehension of the molecular pathways that regulate and execute the cell dead processes, which have allowed the classification of cell dead not only based on morphological characteristics but also using biochemical assays for monitoring cell death-related phenomena (Galluzzi *et al.*, 2009a). Besides, those advances have allowed to observe that similar cell death morphologies present high biochemical, immunological and functional heterogeneity (Green *et al.*, 2009; Kroemer *et al.*, 2009). So, now it becomes clear that we cannot apply the equation "programmed cell death – apoptosis – caspase activation – non-immunogenic cell death" in all the cases, because it will constitute an incorrect generalization. Supporting this conclusion is fact that necrosis may occur and be regulated by a programed process (Galluzzi *et al.*, 2007). Also, apoptosis can lead to a lethal occurrence without caspase activation, and

caspase activation does not necessarily mean that will occur a death process (Galluzzi *et al.*, 2007). These examples clearly show the complexity of the cell death subroutines, and that a lot of work is still necessary in order to improve the knowledge of these processes with the main goal to improve treatments of diseases associated with deregulated cell death.

1.1.2 Cell death in yeast

Yeast has been used as an excellent model in the understanding of basic cellular processes such as intracellular trafficking (Nakano, 2004), protein folding (Coughlan and Brodsky, 2003), autophagy (Abeliovich and Klionsky, 2001) and cell cycle regulation (Hartwell, 2004). After the first description of apoptosis in a *Saccharomyces cerevisiae* strain, that dates from more than eighteen years ago (Madeo *et al.*, 1997), yeast, mainly *S. cerevisiae*, has also been used as an experimental model for cell death study. In fact, *S. cerevisiae* has several characteristics that enhance its use as an excellent model for cell death study, such as being inexpensive and non-pathogenic, displaying rapid growth and easy genetic manipulation accompanied by simple mutant isolation (Carmona-Gutierrez *et al.*, 2010b).

Furthermore, researchers found out that the apoptotic core machinery is conserved in yeast, which makes this organism a great model to approach human apoptosis and its deregulation in several human diseases (Carmona-Gutierrez *et al.*, 2010b). Today, crucial molecular apoptotic regulators have been identified in yeast such as the apoptosis inducing factor (AIF) (Wissing *et al.*, 2004), effector caspases like caspase 7 (Madeo *et al.*, 2002), endonuclease G (yeast Nuc1p) (Buttner *et al.*, 2007), as well as complex apoptotic scenarios such as chromatin modifications, mitochondrial fragmentation and depolarization, cytochrome *c* release and cytoskeleton perturbations (Carmona-Gutierrez *et al.*, 2010b). Furthermore, yeast is a 'clean room system' to heterologously express some mammalian apoptotic proteins that retain their function but do not have obvious orthologues in yeast, in a way to analyze and to elucidate their role (Greenwood and Ludovico, 2010) . Example of that is the expression of pro-apoptotic protein Bax in yeast, that results in cell death that can be prevented by the co-expression of Bcl-2 protein, suggesting the protective role of Bcl-2 in the process (Ligr *et al.*, 1998; Renault *et al.*, 2016). Moreover, yeast undergoes nonapoptotic types of cell death such as programmed

necrosis and autophagic cell death. In fact, programmed necrosis has recently been described as an important regulatory mechanism during chronological aging in yeast (Eisenberg *et al.*, 2010). Furthermore, yeast undergo autophagic cell death following activation of protein phosphatase 2A or when cells arrested at any stage of the cell cycle (Ludovico *et al.*, 2005).

Today there is a large amount of cell death markers that can be used to evaluate the yeast cell death process (Figure 3). The cell death rate is usually obtained by the quantification of Colony Formation Units (CFU) or using fluorescent vital and dead dyes (Carmona-Gutierrez *et al.*, 2010a). Apoptotic cells can be identified by the 'terminal deoxynucleotidyl transferase dUTP nick end-labeling' (TUNEL), that allows to determine DNA fragmentation and the existence of DNA stand breaks a hallmark of apoptotic cell death (Madeo *et al.*, 1997). Furthermore, DAPI staining is usually used to observe DNA condensation. Alternatively, externalization of phosphatidylserine by Annexin V staining is also used to visualize apoptotic cells. Mitochondrial fragmentation, changes in the mitochondrial membrane potential, ROS accumulation and cytochrome *c* are also some common apoptotic markers (Carmona-Gutierrez *et al.*, 2010a).

Necrotic yeast cells are characterized by alterations in the plasma membrane integrity by propidium iodide staining (PI). Furthermore, PI staining is usually combined with Annexin V staining, in a way to distinguish early apoptotic (AnnV+/PI-) from late apoptotic and secondary necrotic (AnnV+/PI+) as well as primary necrotic cells (AnnV-/PI+). The nuclear-cytosolic translocation of HMGB1 yeast ortholog Nhp6Ap has been also used as a necrotic marker in yeast cell death (Eisenberg *et al.*, 2010).

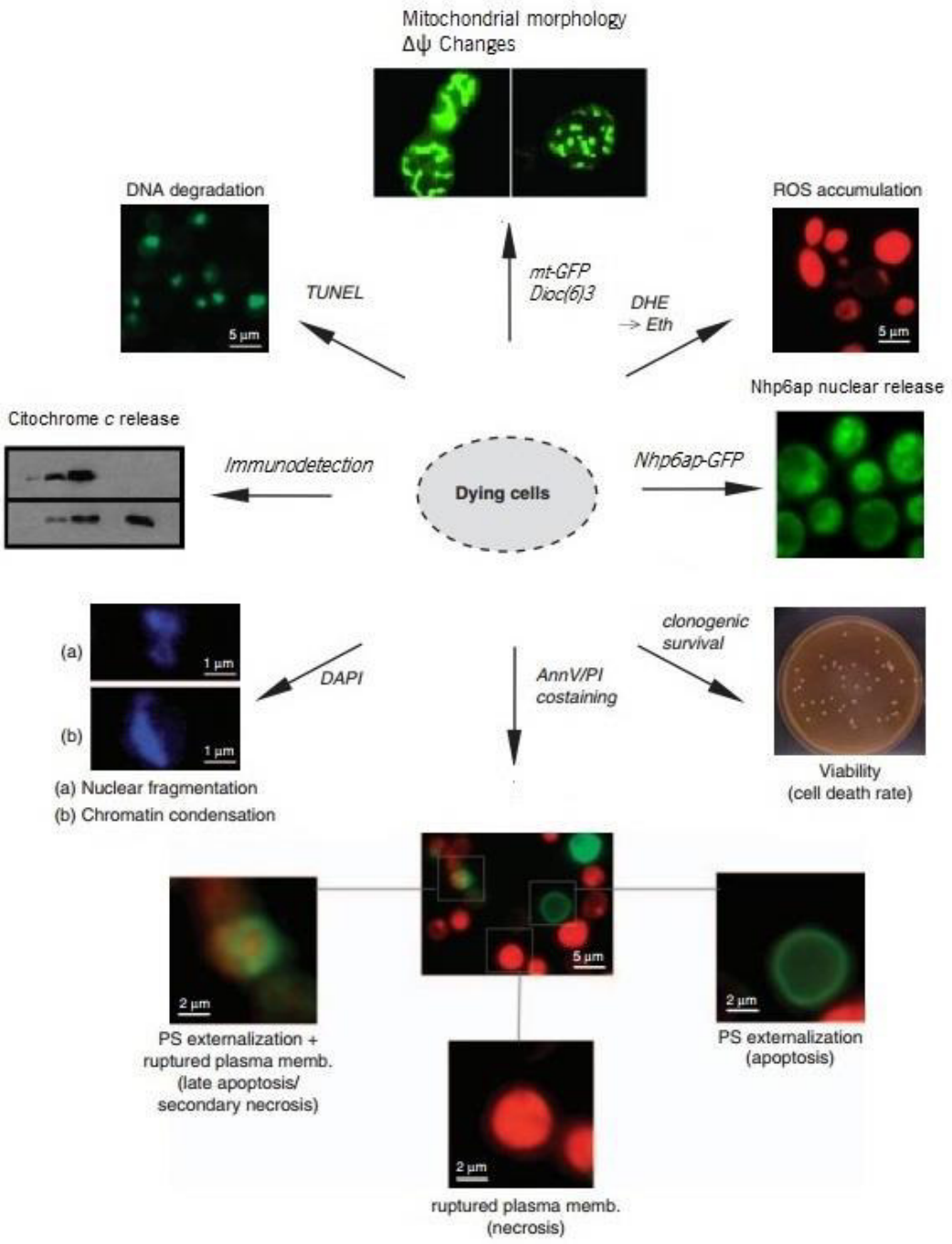

Figure 3 - Assays routinely used in the field of yeast cell death. Viability assays are used to determine the cell death rate. Co-staining of Annexin V and propidium iodide (PI) allows the distinction between early apoptotic (AnnV+/PI-) from late apoptotic and secondary necrotic (AnnV+/PI+) as well as primary necrotic cells (AnnV-/PI+). TUNEL is used to analyze DNA fragmentation and chromatin condensation and fragmentation is observed by DAPI staining. ROS accumulation is commonly detected using dihydroethidium (DHE). Mitochondrial morphology can be evaluated using a GFP labeled protein as well as the Nhp6Ap nuclear-cytosolic translocation can be evaluated using a GFP bonded to Nhp6Ap, whereas changes in the mitochondrial membrane potential are usually assessed using a probe that accumulates on mitochondria upon membrane potential such as $DiOC_6(3)$. Cytochrome *c* release can be assessed by immunodetection or by spectroscopy. In all the cases stained cells are usually analyzed by flow cytometry and/or florescence microscopy observations. Adapted from (Carmona-Gutierrez et al., 2010a)

1.2 Cell death by lysosomal permeabilization

Lysosomes are single membrane-enclosed cytoplasmic organelles that are present in almost all kinds of eukaryotic cells and were discovered in 1955 by Christian de Duve (De Duve and Wattiaux, 1966) . They are the main digestive organelle in eukaryotic cells and are characterized by the presence of a high amount of hydrolytic enzymes, as they contain more than 50 different hydrolases that include proteases, glycosidases, lipases, nucleases, phosphatases, phospholipases and sulfatases, and which usually have their maximal enzymatic activity at low pH (Turk *et al.*, 2002). The lysosomes are also characterized by the presence of an acidic milieu (pH - 3.8 - 5) maintained by a vacuolar ATPase that pumps protons from the cytosol into the lysosomal lumen using metabolic energy derived from ATP (Eskelinen *et al.*, 2003).

They are the major degradative compartment of the endosomal/lysosomal system and have as prime function the degradation of organelles, proteins, nucleic acids and glycoconjugates. However, they also present some other functions, being involved in the repair of plasma membrane, in the release of endocytosed material, in the removal of pathogens as well as central hubs for signal transduction in the control of cellular responses to nutrients and energy metabolism (Luzio *et al.*, 2007; Puertollano, 2014). Besides, lysosomes are essential organelles in autophagy. In macroautophagy they fuse with autophagosomes to form autolysosomes, where the degradation and recycling of the autophagosome material occurs (Mizushima *et al.*, 2008). As referred above, in microautophagy lysosomes form surface invaginations in order to trap cytosolic material destined for degradation whereas in chaperone-mediated autophagy, certain proteins are recognized by chaperones such as the heat shock cognate 70 (Hsc70) which deliver the substrate to the membrane of the lysosome (Boya *et al.*, 2013).

As stated above, there is a large arsenal of hydrolytic enzymes in the lysosome lumen, which makes it a potentially harmful organelle for the cell. In fact, 50 years ago, Christian de Duve described lysosomes as “suicide bags” that can lead to an indiscriminate degradation of cellular components if they release their contents into the cytosol due to a lysosomal membrane damage (Turk and Turk, 2009). However, the inner leaflet of the lysosome is coated by a thick glycocalyx, composed by heavily glycosylated lysosomal integral membrane proteins (LIMPs) and lysosome-associated membrane

proteins (LAMPs) such as LAMP1 and LAMP2 that protect the lysosomal membrane from the acidic hydrolases avoiding an intrinsic membrane damage and accidental release of the lysosomal content. Furthermore, compared with other cellular organelles, lysosome membranes present a different lipid composition characterized by a low percentage of cholesterol and sphingolipids which contribute for its stability (Eskelinen *et al.*, 2003; Eskelinen, 2006).

Today, there are evidences that show that lysosomes play a major role in cell death, both necrosis and apoptosis, due to the occurrence of lysosomal membrane permeabilization (LMP). LMP can be induced by several agents and molecules (figure 3) such as ROS that are one of the principal inducers (Terman *et al.*, 2006), lysosomotropic agents (molecules that accumulate inside the lysosomes and act as detergents) such as sphingosine (Kagedal *et al.*, 2001), photodamage, acidotropic antibiotics (Ichinose *et al.*, 2006), lipids, such as fat acids, sphingosine and bile salts as

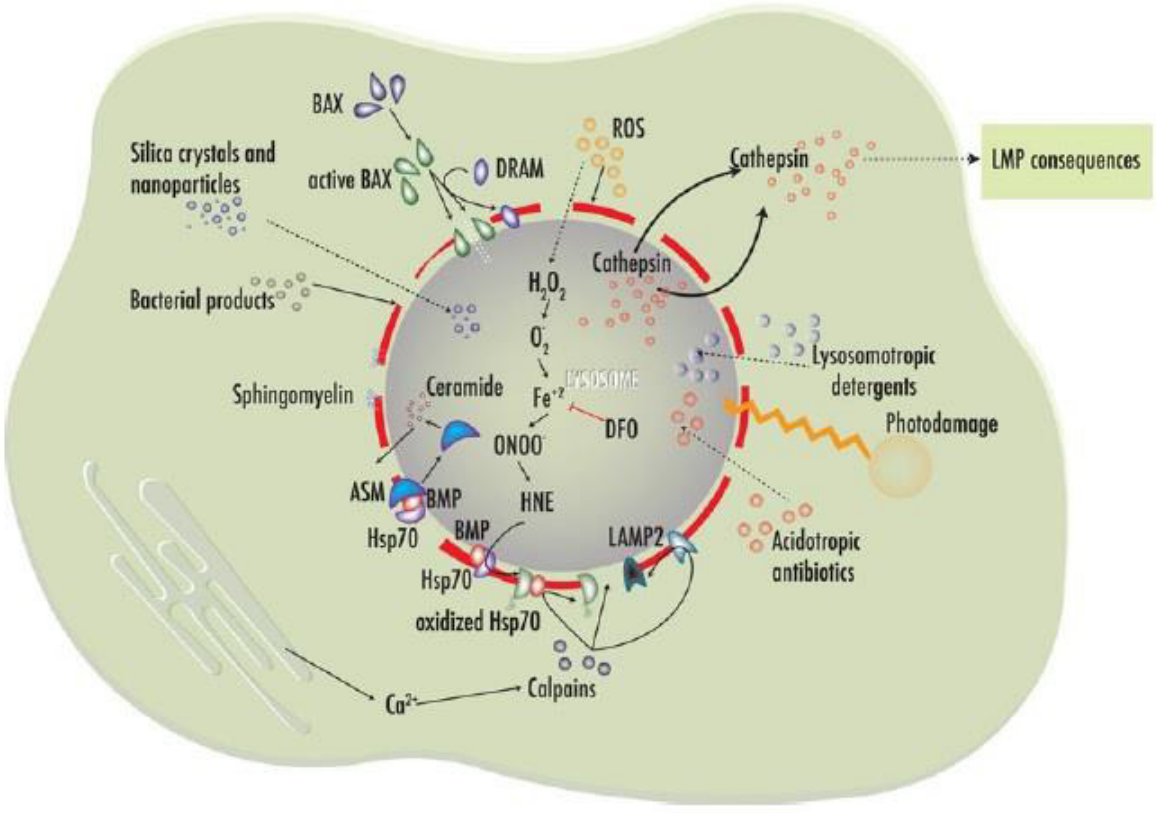

Figure 4 – Inducers of lysosomal membrane permeabilization. ROS accumulation in vacuole lumen is associated with the production of toxic intermediates that damage lysosomal protective proteins such as Hsp70, calpain calcium activation also leads to cleavage and damage in lysosomal protective proteins. Bax is capable to induce lysosomal membrane permeabilization by the rupture of the vacuolar membrane. Lysosomotropic agents and acidotropic antibiotics are able to enter in the vacuole lumen and induce LMP, this effect is enhanced by photodamage. Silica crystals, nanoparticles and bacterial products are other agents capable to induce LMP. Adapted from (Serrano-Puebla and Boya, 2016).

well as by some pro-apoptotic Bcl-2-like proteins such as Bax. In fact, it was shown that Bax translocates from the cytosol to lysosomes and induces permeabilization of the lysosomal membranes via a mechanism analogous to Bax mediated pore formation in mitochondria during apoptosis (Kagedal *et al.*, 2005). Calpain calcium activation has also been reported to participate in cell death by LMP, example of this is the cleavage of several lysosomal associated membrane proteins such as LAMP2 and Hsp70 that normally confer lysosomal stability (Villalpando Rodriguez and Torriglia, 2013). Furthermore, researchers found out that LMP can be induced by some apoptotic regulators such as p53 that is activated by DNA damage (Paquet *et al.*, 2005), as well as by the activation of dead receptors of tumor necrosis factor (TNF) receptor family (Werneburg *et al.*, 2004).

The factor that determines the type of cell death is the extent of LMP caused by the distinct agents. Complete disruption of lysosomes and release of all its content is usually associated with uncontrolled cell death by necrosis due to the cytosolic acidification and indiscriminate degradation of cellular components, whereas partial and selective LMP induces a controlled cell death process by apoptosis (Bursch, 2001). Furthermore, LMP has also been associated with autophagy blockade. In fact, is already stablished that lysosomal dysfunction by LMP leads to autophagosome accumulation and the blockade of autophagic flux (Serrano-Puebla and Boya, 2016).

As referred above the lysosomal lumen is fully packed with lysosomal proteases. Among them, cathepsins that are cysteine proteases represent the largest group of proteolytic enzymes in the lysosomes and assume a large importance in the cell death process when LMP occurs. In humans there are 11 cysteine cathepsins (cathepsin B, L, H, K, S, F, C, W, X, V and O), and also the only lysosomal aspartic protease cathepsin D (Turk *et al.*, 2002). They all share the same core structure and are all monomers of 30 kDa, with the exception of cathepsin C, which is a homotetramer. Furthermore, cathepsins are recycle enzymes exhibiting considerable redundancy, presenting a broad specificity for substrates (Turk *et al.*, 2012).

The cathepsins that have been mostly implicated in cell death are cathepsins B (CB), cathepsin D (CD) and cathepsin L (CL) mostly due to the fact that they remain active at neutral cytosolic pH (Turk *et al.*, 2012). When these proteins are present in the cytosol they are responsible for the activation of apoptotic effectors such as caspases and mitochondria. There are several studies that show that cathepsin B, D and L are capable to activate the BH3-only protein (Bid) by a proteolytic cleavage, which

results in conformational changes in the pro-apoptotic Bcl-2 family proteins members Bax and Bak leading to MMP with cytochrome *c* release and caspase-dependent apoptosis (Reiners *et al.*, 2002; Blomgran *et al.*, 2007). Moreover, several reports have shown that cathepsins degrade the anti-apoptotic Bcl-2 family proteins Bcl2, Mcl-1, Bcl-xL and XIAP, which means that lysosomal cathepsins have a large role in apoptosis mediated by LMP (Droga-Mazovec *et al.*, 2008).

However, the type of cell death does not only depend on the type of cathepsin that is present in the cytosol after LMP induction, but also on the amount of cathepsins, on the intensity of LMP as well as on the presence of cathepsin inhibitors such as cystatins. There is a range of distinct modalities of cellular dismantling processes that depend on these properties. Thus, LMP associated with cathepsin release can lead to the occurrence of different lethal pathways that include: cell death through direct activation of calpains and caspases, MMP followed by caspase-dependent cell death, MMP followed by a caspase-independent cell death as well as caspase-independent cell death (figure 5) (Boya and Kroemer, 2008). Is also important to note that the role of cathepsins in cell dead is not

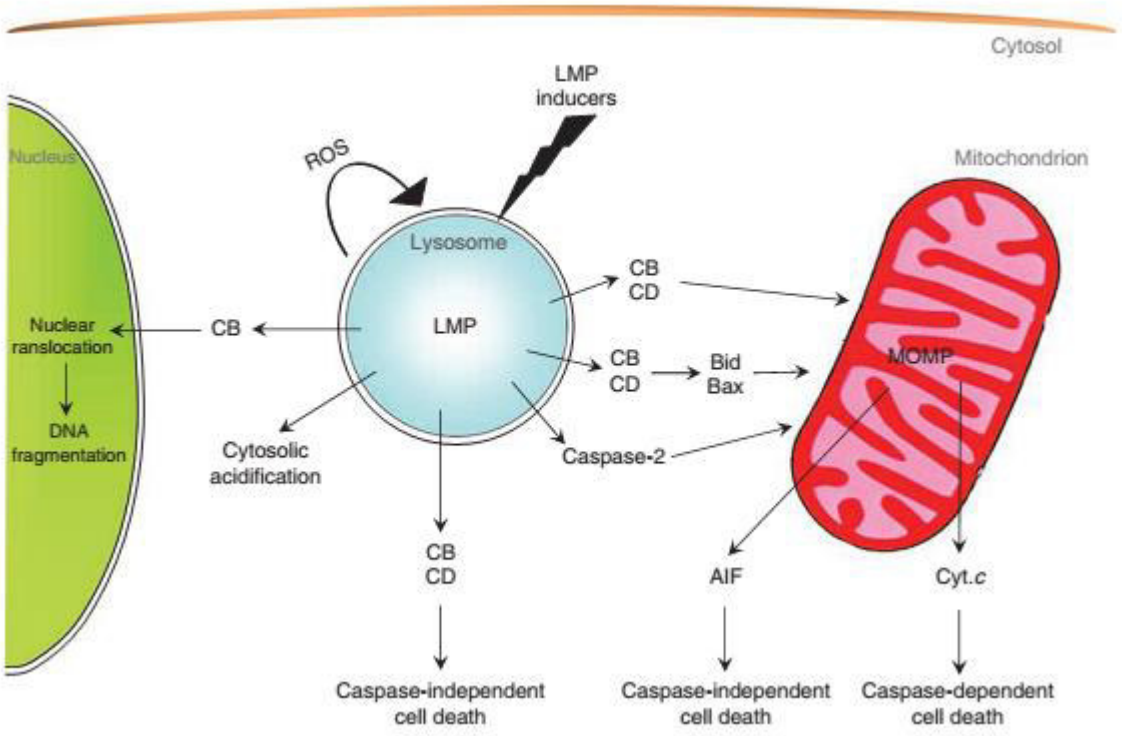

Figure 5 – LMP downstream lethal pathways. The LMP inducer, the expression level of lysosomal hydrolases, the cytosolic concentration of cathepsins as well as cathepsins inhibitors, the MMP, AIF and cytochrome *c* concentration, determinates the effector pathway that leads to cell death. Adapted from (Boya and Kroemer, 2008)

completely understood especially in the case of cathepsin D, where its role is cell type and context dependent, in some situations it enhances apoptosis whereas in others situations it inhibits apoptosis (Sagulenko *et al.*, 2008). Additionally, it was demonstrated that in cancer cells when CD is present outside the cells, it induces proliferation, angiogenesis, invasion and metastasis (Benes *et al.*, 2008). So it is clear that the molecular mechanisms underlying LMP and cathepsin release associated with cell death are very complex and are not completely understood and an intense research in this field is still necessary.

Yeasts do not possess lysosomes, but they also present membrane-bound acidic organelles the vacuoles, which share many similarities with lysosomes, and these organelles were also shown to be directly involved in cell death. There are several studies that relate cell death with vacuolar permeabilization. One of them was the study made by Cunningham group, were they show that tunicamycin (a drug that induce endoplasmic reticulum stress) leads to vacuolar membrane permeabilization of yeast cells, that resulted in a nonapoptotic cell death by a process that involves the vacuolar V-ATPase activity (Kim *et al.*, 2012).

Furthermore, Mason et al. observed the translocation of vacuolar Pep4p (the yeast ortholog of cathepsin D) to cytosol, leading to the degradation of nucleoporins during H_2O_2-induced apoptosis (Mason *et al.*, 2005). Another study, found that Pep4p is released from intact vacuoles by a partial permeabilization of the vacuolar membrane when yeast cells undergo acetic acid induced apoptosis (Pereira *et al.*, 2010). However, in this case the authors observed that Pep4p has a protective role in the cell death process, since the deletion of Pep4p leads to a higher vulnerability to acetic acid treatment (Pereira *et al.*, 2010). Importantly, similar results were then also observed in colorectal carcinoma cells (Marques *et al.*, 2013), which supports the use of yeast as a model to understand the function of lysosomes in cell death.

1.3 HMGB1 protein

HMGB1 (High-mobility group box 1) also known as amphoterin, was originally identified as a highly conserved nuclear DNA-binding protein and was the first member of the HMGB family identified (Štros, 2010). This family is composed by HMGB1, -2 and -3. HMGB4 was also identified as a member of this family, however, it was found that this protein is identical to HMGB3, so its name remained HMGB3 (Štros, 2010; Yang *et al.*, 2013). These proteins have a highly conserved structure showing over 80% of sequence identity.

However, HMGB1 has assumed a greater importance due to its ubiquitous presence in all nucleated eukaryotic cells in comparison with HMGB2 which expression is limited to lymphoid tissues and testis of adult animals (Ronfani *et al.*, 2001; Muller *et al.*, 2004), and with HMGB3 which expression is restricted to embryos and hematopoietic stem cells (Nemeth *et al.*, 2003).

Structurally, the human HMGB1 is a 30 kDa protein with 216 amino acids that contains two folded helical DNA-binding motifs, called A-Box and B-Box, followed by a negatively charged acidic tail that contains a string of glutamic and aspartic acid (figure 6) (Weir *et al.*, 1993; Hardman *et al.*, 1995). HMGB1 contains two nuclear localizations signals (NLS), one in A-Box and another in B-Box that are responsible for its nuclear localization (Yang *et al.*, 2013). However, this protein is not always present in the nucleus, since the NLS's are susceptible to suffer acetylation modifications in there conserved lysine residues, which results in the protein exclusion from the nucleus (Bonaldi *et al.*, 2003; Lu *et al.*, 2012). In fact, HMGB1 is a protein with two functions. Inside the cell it is bound to DNA, while outside the cell it acts as a cytokine.

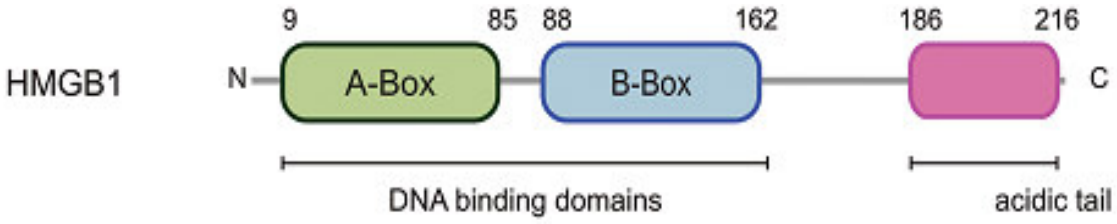

Figure 6 – HMGB1 structure. The human HMGB1 protein is composed by 216 amino acids and is characterized by the existence of two DNA binding domains the A-Box and the B-Box, followed by a C terminal negatively charged acidic tail. Adapted from (Vande Walle *et al.*, 2011).

Although its nuclear role it is still incompletely understood, it is known that in the nucleus HMGB1 acts as a non-histone DNA-binding factor, where it supports the structure of chromatin by binding to the DNA minor grove in a nonspecific manner, being involved in: chromatin stabilization (Gerlitz *et al.*, 2009), transcription regulation (Bianchi and Agresti, 2005), chromosome assembly (Celona *et al.*, 2011), cell replication (Bianchi and Agresti, 2005), DNA repair (Lange *et al.*, 2008) and also in the assembly of site-specific DNA binding proteins like p53 at their binding sites within the chromatin (Thomas and Travers, 2001).

On the other hand, HMGB1 is an example of an alarmin molecule (molecules that can alarm the innate immune system) (Bianchi, 2007), since outside the cells this protein act as a cytokine and binds to RAGE (receptor for advanced glycation end products) and to Toll-like receptors (TLR-2 and -4) of effector cells, mediating inflammatory and repair responses caused by both infectious and

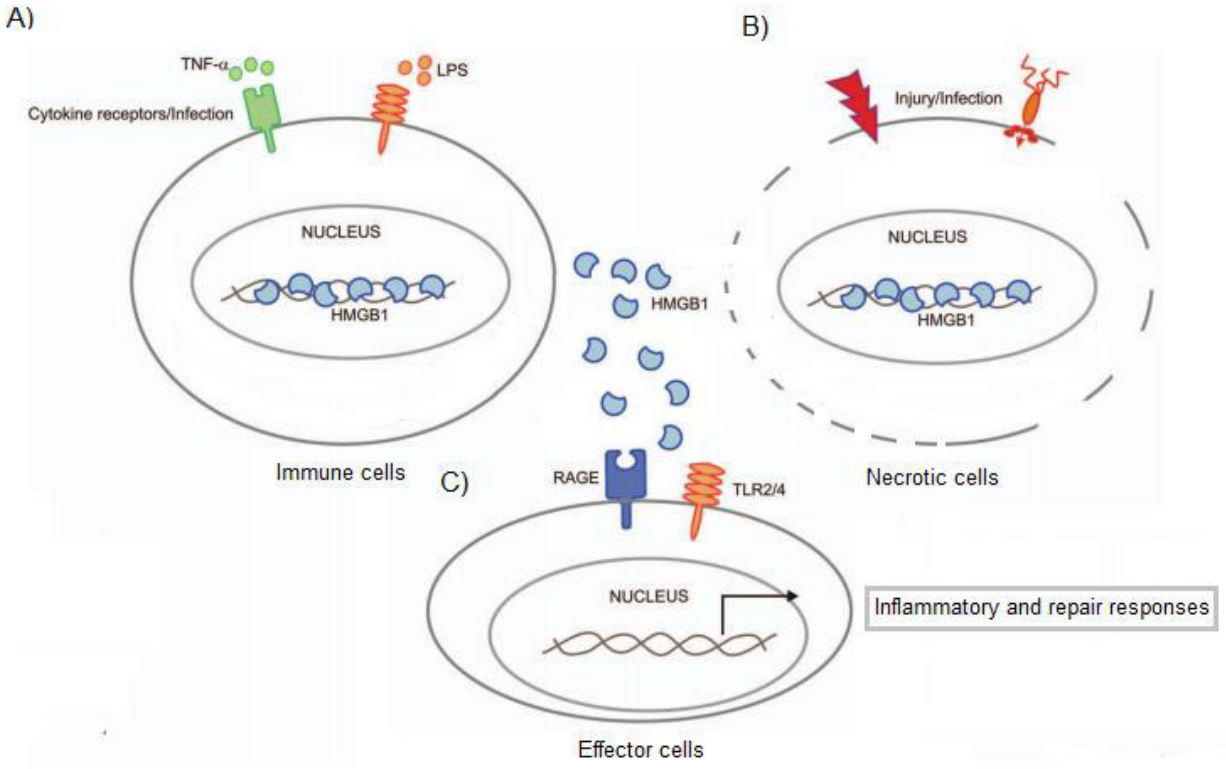

Figure 7 – Release of HMGB1 protein. A) HMGB1 is secreted by LPS and TNF-α activated immune cells (monocyte and macrophage cell lines). The translocation of HMGB1 protein from the nucleus to the cytoplasm is accompanied by post-translational modifications, such as acetylation, phosphorylation and methylation. Once in the cytoplasm HMGB1 is encapsulated in secretory lysosomes for secretion (Gardella *et al.*, 2002). **B)** HMGB1 is released in necrotic cells usually by a passive mechanism. **C)** Outside the cells, HMGB1 acts as an alarmin molecule and bind to its receptors RAGE and TLR2/4 on effector cells in order to induce inflammation and repair responses. Adapted from (Vande Walle *et al.*, 2011)

autoimmune disorders (figure 7) (Vande Walle *et al.*, 2011). Actually, several studies have shown that HMGB1 is secreted by LPS (lipopolysaccharides) and TNF-α activated monocyte and macrophage cell lines, which is consistent with its role as a prototypical alarmin (Figure 7 A)) (Kaminska *et al.*, 1999; Andersson *et al.*, 2000). However, to exert its alarmin role, HMGB1 must translocate from the nucleus to the extracellular medium.

Although this transition was first observed in immune cells activated by LPS, several studies subsequently showed that necrotic cells also release this protein (figure 7 B). One of these studies, was made by Paola Scaffidi group, were they used a chimeric protein (HMGB1-GFP) to observe the location of the HMGB1 protein (Scaffidi *et al.*, 2002). In fact, in necrotic HeLa cells the researchers observed a rapid dissociation of the chimeric protein from the chromatin followed by its leak into the extracellular medium (Scaffidi *et al.*, 2002). As such, HMGB1 has been implicated as a cause of inflammation that occurs secondary to necrotic cell death. This is supported by Patrizia Rovere-Querini work, where the authors showed that necrotic HMGB1-/- cells have reduced ability to activate antigen-presenting cells (APCs). This was concluded by comparing the activation of APCs by supernatants from necrotic HMGB1-/- or will-type cells (Rovere-Querini *et al.*, 2004).

However, it should be noted that more recent studies showed that the extent of HMGB1 release during necrosis might depend on the agent used for the induction. In these studies it is shown that certain agents cause a drastic extracellular protein translocation whereas other agents may lead to a small or event inexistent release (Beyer *et al.*, 2012). Regarding the apoptotic release of these proteins, both studies referred above (Scaffidi *et al.*, 2002; Rovere-Querini *et al.*, 2004), observed that HMGB1 release did not occur during apoptotic cell death, in contrast to necrosis. Interestingly, Scaffidi group showed that in HeLa cells treated with etoposide to induce apoptosis, post-translational modifications on HMGB1 occur, which increased the protein adherence to chromatin, resulting in the fixation of the protein in the nucleus. Moreover, in cells that transit to a late apoptotic state (where it occurs cell permeabilization) it was observed retention of HMGB1 in the nucleus. Indeed, the failure to release HMGB1 in apoptotic cells can explain why apoptosis is an immunological silence non-inflammatory process.

Today, is established that cells undergoing apoptosis can release several molecules from the nucleus as well as DNA fragments (Li *et al.*, 2003; Choi *et al.*, 2005). As stated above, in an apoptotic

process there is an increase in the adherence of HMGB1 to chromatin, so if apoptotic cells can release DNA fragments from the nucleus the failure of apoptotic cells to show HMGB1 externalization is surprising. More recent studies have been based on this problematic. In fact, Bell et al. showed that in Jurkat cells induced to undergo apoptosis by different apoptotic stimuli, HMGB1 is released in a time-dependent manner, during late apoptosis (a state where the cell membrane permeability increase and nuclear molecules such as DNA and histones shift to an extracellular location). Besides, they observed that this release is blocked when cells are treated whit apoptotic inhibitors (Bell *et al.*, 2006). These results demonstrate that we cannot generalize that HMGB1 release only occurs in necrotic cells.

Although HMGB1 nuclear release can occur during cell death and cell activation an intriguing question that has attracted researchers' attention is how this protein travel from the nucleus to the extracellular medium. Actually, it does not present the classical peptide secretion signals that allow the exit of proteins to the extracellular medium in Golgi-derived secretory vesicles by the classic Endoplasmic reticulum – Golgi secretory pathway (Lee *et al.*, 2004). There are already several models that have been proposed to explain the extracellular release of this kind of proteins like HMGB1 in lysosomes, microvesicles and exosomes (Nickel and Rabouille, 2009).

Studies have shown that in cell activation, HMGB1 suffers post-translation modifications like phosphorylation, acetylation and methylation which lead to the loss of chromatin adherence and subsequent cytoplasmic release followed by the protein entry into secretory lysosomes that lead to their extracellular release (Gardella *et al.*, 2002; Bonaldi *et al.*, 2003). In contrast, in necrosis, the process of protein release is passive, since there is a huge increase of nuclear and cellular membrane permeability that may allow the protein exit (Figure 7 A and B).

Furthermore, recent studies made by Pisetsky (Pisetsky, 2014) showed that HMGB1 appears to be present on microparticles (small membrane bound vesicles, that contain nuclear and cytoplasmic components), which appear to be extracellularly released by blebbing processes during cell activation and cell death. In this study RAW 264.7 macrophages were stimulated with LPS and treated with apoptotic inducers (staurosporine and etoposide); after the treatments the microparticles were isolated by centrifugation and the presence of HMGB1 was determined by Western blotting. The results showed that in both treatments HMGB1 was present in the microvesicles (Pisetsky, 2014). So it is clear that a

lot of research is still necessary to fully understand the molecular mechanisms underlying the extracellular release of HMGB1 both in cell activation and cell death.

Although yeasts do not express HMGB1, they express a homologue protein, the Nhp6Ap (Kolodrubetz *et al.*, 1988). The nuclear release of this protein has also been observed in necrotic yeasts and has therefore being used as a marker of necrosis in this organism (Eisenberg *et al.*, 2009; Santos *et al.*, 2012).

1.4 Phenoxazine derivatives

Over the last years there has been a huge research in the design and synthesis of novel organic compounds for life science applications. Among these, are the cationic polycyclic phenoxazine derivatives, that are florescent markers emitting at long wavelength light and that have assumed a large importance as probes but have also attracted interest as antiproliferative compounds. They absorb and emit florescence in the 600-900 nm region of the spectrum, where there is minimum the interference caused by the natural auto-fluorescence of the biological molecules (Jose and Burgess, 2006). Their applications include the covalent labeling of amino acids (Frade *et al.*, 2007) and proteins (Salomi *et al.*, 2005), however they have assumed a more common utilization in non-covalent labeling of nucleic acids in various contexts such as blotting experiments, gel electrophoresis and also living cell assays (Soto *et al.*, 2002).

Phenoxazine dyes, namely benzo[*a*]phenoxazines are derived from the oxazin heterocycle (figure 8a). Structurally, they are characterized by presenting a benzene ring fused with the *a* face of the phenoxazine structure (figure 8b and 8c) (Jose and Burgess, 2006). The main similarity between

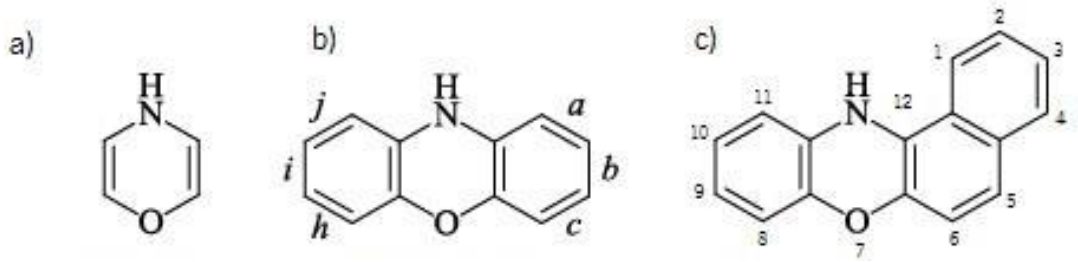

Figure 8 – Molecular structure of a) Oxazine, **b)** Phenoxazine and **c)** Benzo[*a*]phenoxazine.

them, apart from the central structure of benzophenoxazine, is the presence of an amine function at the 9-position of the system (which may be primary, secondary or tertiary and positively charged or neutral) (Jose and Burgess, 2006). Furthermore, some benzo[*a*]phenoxazines also present a functional group (amine, carboxyl or hydroxyl group) at the position 5 (figure 8c) that is essential for covalent labelling molecules, but also confer them the possibility of other chemical modifications, in addition to its intrinsic noncovalent character (Frade *et al.*, 2007).

As referred above, besides their use as fluorophores, oxazine heterocycles, such as phenoxazine and benzo[*a*]phenoxazine derivatives have assumed also significance in life sciences due to their antiproliferative proprieties that have prompted their study as antimicrobial (Patil *et al.*, 2015) or antitumor agents (Shimamoto *et al.*, 2001; Bolognese *et al.*, 2006). In fact, there are several reports in literature that reveals that this compounds possess a wide spectrum of biological activities as antibacterial, antifungal (Kumar *et al.*, 2006), cytotoxic (Motohashi *et al.*, 1991), antitumor (Hendrzak-Henion *et al.*, 1999), anti-inflammatory (Silva *et al.*, 2004), etc.

Usually, these compounds exert their antiproliferative activity by the formation of stable complexes with DNA established by the intercalation of their aromatic planar structure between the DNA base pairs. This leads to the formation of hydrogen bounds and π–π stacking interactions that disrupt the normal function of DNA, leading to cell death (Bolognese *et al.*, 2002). In addition, Alberti group showed that some phenoxazine derivatives can suffer a metabolic conversion into free radical intermediates leading to oxidative stress and DNA damage (Alberti *et al.*, 2003).

Studies made by Lewis group showed that benzo[*a*]phenoxazines derivatives administered orally to neoplastic rats lead to tumor labeling and shrinkage, showing that this class of compounds accumulate in neoplastic cells in comparison with normal cells and induce cell death (LEWIS *et al.*, 1949). Besides, they were able to observe the huge versatility of this class of compounds, since they find out that different substitutions in the positions 5 and 9 originate significant differences in the tumoral labeling, toxicity and selectivity.

Suzuki group compared the cytotoxicity of several phenoxazine derivatives on tumor cells and normal human cells and they observed that two benzo[*a*]phenoxazine salts the WM7 and WM8, presented one of the highest specificity indices for the tumor cells among the tested compounds

(Suzuki *et al.*, 2007). Furthermore, they observed that the type of cell death caused by the two benzo[*a*]phenoxazine salts did not lead to the appearance of apoptotic features such as caspase activation and DNA fragmentation, and rather inhibited autophagosome formation.

Furthermore, there are some benzo[*a*]phenoxazines derivatives that have been shown to lead to an apoptotic cell death in different neoplastic cell lines, both in a caspase-dependent and independent manner (Abe *et al.*, 2001; Shirato *et al.*, 2007). Akihisa Abe observed that the addiction of Z-VAD-fmk, a caspase family inhibitor, reverted the apoptotic cell death induced by a novel phenoxazinone in human lung carcinoma cells. Whereas, Shirato group showed that the addiction of Z-VAD-fmk didn't affect the apoptotic cell death process induced by two benzo[*a*]phenoxazines derivatives on human glioblastoma cell lines, suggesting that the cell death process is mediated by the caspase-independent apoptotic cell death pathway.

So it is clear that there is an enormous potential in the use of these phenoxazine derivatives as antimicrobial and antitumor agent for therapeutic purposes. However, information available about their use is very limited so a deeper research in the synthesis and application of these compounds is still necessary in order to maximize their use.

In these context, in the pass years our group have synthesized several Benzo[*a*]phenoxazine compounds, and have found their interesting for used as antifungal agents (Frade *et al.*, 2007, 2008). Among those, one in particular has attracted our interest, due to its high antifungal activity, the N-(5-((4-ethoxy-4-oxobutyl)amino)-10-methyl-9H-benzo[a]phenoxazin-9-lidene), also designated as MSG-111-cd3 (Figure 9) (Frade *et al.*, 2007). So far, the studies using *Saccharomyces cerevisiae* as a model, suggest that MSG-111-cd3 accumulates at the vacuolar membrane and leads to vacuolar membrane damage and vacuolar permeabilization (Carvalho, 2011; Lopes, 2015). Furthermore, it was also observed that the treatment led to the release of Nhp6Ap (the yeast ortholog of the mammalian HMGB1) from the nucleus to the cytoplasm, however, no loss of plasma membrane integrity was observed (Ferreira, 2014; Lopes, 2015). Furthermore, the release pattern of the Nhp6Ap appears to be different in comparison to the cells undergoing necrosis, the results evidencing a punctuated disposition of the protein in the cytoplasm instead of being uniformly dispersed as is observed in necrotic cells (Eisenberg *et al.*, 2009; Santos *et al.*, 2012). These observations may be due to a possible vesicular localization of Nhp6Ap (perhaps similar to the one recently described for the HMGB1

in microparticles by David S. Pisetsky) that is dependent of the cell death process induced by the compound. So this protein can have a crucial role in the cell death process induced by MSG-111-cd3. So further studies will be necessary to clarify the role of these proteins in the *S. cerevisiae* cell death induced by MSG-111-cd3.

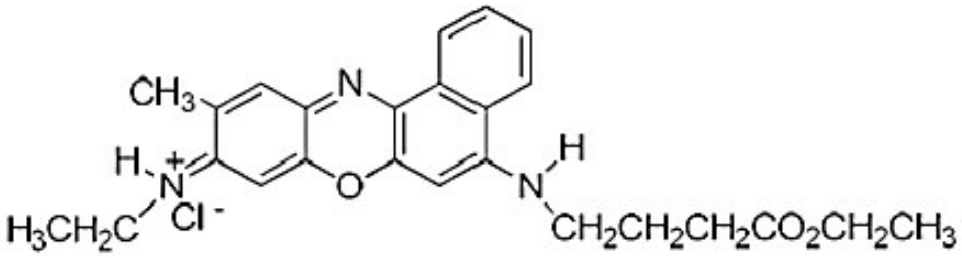

Figure 9 - N-(5-((4-ethoxy-4-oxobutyl)amino)-10-methyl-9H-benzo[a]phenoxazin-9-lidene) (MSG-111-cd3)

2. Aim

As previously referred, in the pass years our group have synthetized several benzo[*a*]phenoxazines compounds, and the N-(5-((4-ethoxy-4-oxobutyl)amino)-10-methyl-9H-benzo[a]phenoxazin-9-lidene), also designated as MSG-111-cd3, have attracted our interest, due to its high antifungal activity. So based on its great potential we have tested its effect on the yeast *S. cerevisiae*. Used as a model of eukaryotic cell. In previous work, we observed that at concentrations close to the minimum inhibitory concentration (MIC), MSG-111-cd3 accumulates in the vacuolar membranes and in the endoplasmic reticulum (Carvalho, 2011). At higher concentrations, it was observed that MSG-111-cd3 leads to loss of viability of several yeast strains and mutants by a process that is partial dependent on protein synthesis.

Several cell death markers, have already been tested, such as ROS accumulation, chromatin condensation, nuclear release of Nhp6Ap, loss of plasma membrane integrity, vacuole membrane permeabilization and fragmentation. It was observed that the compound lead to Nhp6Ap release from the nucleus to the cytosol in yeast cells without loss of plasma membrane integrity (Ferreira, 2014; Lopes, 2015). However, the previous results suggest that MSG-111-cd3 toxic effects may be mediated through the vacuolar membrane damage and vacuolar permeabilization (Lopes, 2015).

So, based on these previous observations, the goal of this work was to further elucidate the cell death process mechanism. To achieve this goal, we analyzed the consequences of vacuolar permeabilization, mainly the role of Pep4p in the cell death process. We assessed several cell death markers such as intracellular calcium fluctuation, DNA fragmentation, mitochondrial fragmentation, alterations on mitochondrial potential, and also the involvement of autophagy by evaluation of the processing of a GFP-ATG8 fusion. We also study the role of the HMGB1 protein in the cell death process and the mechanisms underlying its nuclear release, evaluating the compound effect on the nuclear envelope and assessing if other DNA binding protein, in this case the histone Hta2p, suffer any localization alteration.

3. Material and Methods

3.1 Yeast strains

The *Saccharomyces cerevisiae* strains used in this work are listed below in the table 1. As wild type strains were used the BY 4741 and the W303-1A. BY 4741 WT, BY 4741 *Δnhp6a*, BY 4741 *Δpep4*, BY 4741 *Δpep4* pESC(Ø), BY 4741 Δ*pep4* pESC-Pep4p(FL) and BY 4741 *Δpep4* pESC-DPM-Pep4p were used in viability assays.

For florescence microscopy assays the following strains were used, BY 4741 pUG35-nhp6a-GFP, BY 4741 *Δstp22* pUG35-nhp6a-GFP, BY 4741 *Δsnf7* pUG35-nhp6a-GFP, W303-1A pYX-mt-GFP, W303-1A p416 ADH-pep4-EGFP, W303-1A GFP-ATG8, W303-1A *Δatg5* GFP-ATG8, W303-1A *Δatg32* GFP-ATG8, MEY 337, SCY 363.

3.2 Media and Growth conditions

Cells of the *S. cerevisiae* strains, BY 4741 WT, BY 4741 *Δnhp6a*, BY 4741 *Δpep4*, MEY 337 and SCY 363 were grown on YEPD (Yeast Extract Peptone Dextrose) medium plates (1% yeast extract, 2% bactopeptone, 2% glucose and 2% agar) at 30 °C during 2 days. Then, they were transferred to liquid YEPD (without agar) at 30 °C with agitation at 200 rpm, and allowed to reach the exponential phase (OD_{640} nm ≈ 0.5).

The strains that were transformed with plasmids, were selected and grown in synthetic complete medium (SC: 2% glucose; 0.5% (W/V) ammonium sulphate; 0.7% yeast nitrogen base w/o amino acids; 0.2% dropout mix; 0.01% histidine, uracil and tryptophan; 0.02% leucine). In the case of BY 4741 *Δpep4* pESC(Ø), BY 4741 *Δpep4* pESC-Pep4p(FL), BY 4741 *Δpep4* pESC-DPM-Pep4p and W303-1A pYX-mt-GFP strains, the same medium with galactose 2% instead of glucose was used in order to induce the expression of the proteins. All the strains were growth at 30 °C with agitation at 200 rpm, until they reach the exponential phase (OD_{640} nm ≈ 0.5). For solid media, 2% of agar was added.

Table 1 – *S. cerevisiae* strains used in this study.

Yeast strains	Genotype	Source
BY 4741	MATa, *his3Δ1, leu2Δ0, met15Δ0, ura3Δ0*	EUROSCARF
W303-1A	MATa, *ura3-52, trp1Δ2, leu2-3, 112 his3-11, ade2-1*	EUROSCARF
BY 4741 *Δnhp6a*	MATa, *his3Δ1, leu2Δ0, met15Δ0, ura3Δ0; YPR052c::kanMX4*	EUROSCARF
BY 4741 *Δpep4*	MATa, *his3Δ1, leu2Δ0, met15Δ0, ura3Δ0; YPL154c::kanMX4*	EUROSCARF
BY 4741 *Δpep4* pESC (Ø)	MATa, *his3Δ1, leu2Δ0, met15Δ0, ura3Δ0; YPL154c::kanMX4*, pESC (Ø) (HIS3)	This study
BY 4741 *Δpep4* pESC-Pep4p(FL)	MATa, *his3Δ1, leu2Δ0, met15Δ0, ura3Δ0; YPL154c::kanMX4*, pESC-Pep4p(FL) (HIS3)	This study
BY 4741 *Δpep4* pESC-DPM-Pep4p	MATa, *his3Δ1, leu2Δ0, met15Δ0, ura3Δ0; YPL154c::kanMX4*, pESC-DPM-Pep4p (HIS3)	This study
BY 4741 pUG35-nhp6a-GFP	MATa, *his3Δ1, leu2Δ0, met15Δ0, ura3Δ0*, pUG35-nhp6a-GFP (URA3)	This study
BY 4741 *Δstp22* pUG35-nhp6a-GFP	MATa, *his3Δ1, leu2Δ0, met15Δ0, ura3Δ0, YCL008c::kanMX4*, pUG35-nhp6a-GFP (URA3)	This study
BY 4741 *Δsnf7* pUG35-nhp6a-GFP	MATa, *his3Δ1, leu2Δ0, met15Δ0, ura3Δ0, YLR025w::kanMX4*, pUG35-nhp6a-GFP (URA3)	This study
W303-1A pYX-mt-GFP	MATa, *ura3-52, trp1Δ2, leu2-3, 112 his3-11, ade2-1*, pYX-mt-GFP (URA3)	Nadine Camougrand
W303-1A p416 ADH-pep4-EGFP	MATa, *ura3-52, trp1Δ2, leu2-3, 112 his3-11, ade2-1*, p416 ADH-pep4-EGFP (URA3)	David Galdfarb
W303-1A GFP-ATG8	MATa, *ura3-52, trp1Δ2, leu2-3, 112 his3-11, ade2-1*, GFP-ATG8 (URA3)	Nadine Camougrand
W303-1A *Δatg5* GFP-ATG8	MATa, *ura3-52, trp1Δ2, leu2-3, 112 his3-11, ade2-1*, *YPL149w::kanMX4*, GFP-ATG8 (URA3)	Nadine Camougrand
W303-1A *Δatg32* GFP-ATG8	MATa, *ura3-52, trp1Δ2, leu2-3, 112 his3-11, ade2-1, YIL146c::kanMX4*, GFP-ATG8 (URA3)	Nadine Camougrand
MEY 337	MATa, *ho::LYS2/ho::LYS2, lys2/lys2, his3::hisG/his3::hisG, leu2::hisG/leu2::hisG, ura3/ura3, trp1::hisG/trp1::hisG*, Hta2-GFP::kanMX6/HTA2, Pep4-mCherry::URA3/PEP4	Marc Meneghini
SCY 363	MATa, *ho::LYS2/ho::LYS2, lys2/lys2, his3::hisG/his3::hisG, leu2::hisG/leu2::hisG, ura3/ura3, trp1::hisG/trp1::hisG*, Nup49-GFP::HIS3/NUP49, Hta2-mCherry::hygMX6/HTA2	Marc Meneghini

3.3 MSG-111-cd3 treatment

A 80.0 mM, stock solution of MSG-111-cd3 was prepared by diluting the compound in dimethyl sulfoxide (DMSO).

As referred above the yeast strains were growth in its respective liquid mediums at 30 °C with agitation at 200 rpm, until they reach the exponential phase ($OD_{640\ nm} \approx 0.5$). After that, the cells were collected, washed and resuspended in filtered YEPD. BY 4741 *Δpep4* pESC(Ø), BY 4741 *Δpep4* pESC-Pep4p(FL), BY 4741 *Δpep4* pESC-DPM-Pep4p and W303-1A pYX-mt-GFP strains were resuspended in filtered YEPG (galactose instead of glucose) to continue the plasmid expression.

The compound treatment was done by adding MSG-111-cd3 to the resuspended cells at final concentration of 300 μM. The same volume of DMSO (≈ 0.35 %) was added to another tube that functioned as negative control. The cells were then incubated at 30 °C with agitation at 200 rpm, until the end of the assay. Cells were collected every 30 mim along 120 minutes, the 0 min sample was collected before adding the compound and the DMSO.

3.4 Viability assays

Cells were treated as described in 3.3. After adding the MSG-111-cd3 and DMSO (negative control) samples of 50 μl of culture were collected every 30 min along 120 minutes and diluted 10^{-4} in sterile deionized water. The 0 min sample was collected before adding the compound or DMSO.

Seven drops of 30 μl from the 10^{-4} dilution were placed on YEPD plates. The plates were incubated during 2 days at 30 °C and cell viability was assessed by measuring the Colony-Forming Units (%CFU).

3.5 Yeast pUG35-nhp6a-GFP, pESC (Ø), pESC-Pep4p(FL) and pESC-DPM-Pep4p transformation

All the plasmids (table 2) were first extracted from *Escherichia coli* strains using GenElute Plasmid Miniprep Kit (Sigma Aldritch).

Table 2 – List of plasmids used in this study.

Plasmid	Description	Source
pUG35-nhp6a	Nhp6a-GFP inserted on pUG35, *URA3*, ampR, *MET25*-Promoter	Frank Madeo
pESC (Ø)	Empty pESC, *HIS3*, ampR, *GAL1*-Promoter	Frank Madeo
pESC-Pep4p(FL)	Pep4p Full length inserted on pESC, *HIS3*, ampR, *GAL1*-Promoter	Frank Madeo
pESC-DPM-Pep4p	Double point mutation Pep4p inserted on pESC, *HIS3*, ampR, *GAL1*-Promoter	Frank Madeo

All the yeast strains (BY 4741, BY 4741 *Δpep4*, BY 4741 *Δstp22* and BY 4741 *Δsnf7*) were grown over-night in YEPD medium (1% yeast extract, 2% bactopeptone and 2% glucose), in the next day they were diluted to an $OD_{640\,nm}$ = 0.2, and incubated until reaching an $OD_{640\,nm}$ = 0.8. After reaching the $OD_{640\,nm}$ = 0.8, for each transformation 100 µl of cells were collected (centrifuged at 5000 rpm for 2 minutes), the pellet was washed with deionized sterile water and centrifuged again.

The transformation of the yeast cells with the plasmids was performed by the lithium acetate method. So, the competent cells pellet was resuspended in 360 µl of the mix presented in the table 3. After resuspension, the mix was incubated at 42 °C for 40 minutes. Cells were then pelleted by centrifugation at 14800 rpm for 1 minute and, resuspended in 200 µl of deionized sterile water. Finally, the cells were plated on appropriate selective medium.

Table 3 – Transformation mix.

Reagents	Negative Control	Plasmid
Lithium acetate (LiAc) (1M)	36 µL	36 µl
PEG (50%)	240 µL	24 µl
H_20	72 µL	72 µl
ssDNA (carrier 10mg/ml)	10 µL	10 µl
Plasmid	———	2 µl

3.6 Assessment of Pep4p, Nhp6Ap, Hta2p and Nup49p localization and vacuole membrane permeabilization

The yeast strains expressing (table1) pep4-EGFP, nhp6a-GFP, hta2-GFP and nup49-GFP were treated with MSG-111-cd3 or with DMSO (negative control) as described in 3.3. Cells were then collected for visualization by epifluorescence microscopy to evaluate the localization of the proteins.

In the case of the strain expressing pep4-EGFP (W303-1A p416 ADH-pep4-EGFP) the cells were stained with Celltracker™ Blue CMAC (Molecular Probes Eugene, OR) at a final concentration of 2 μM and incubated for 15-30 minutes at room temperature, in order to assess the vacuole membrane permeabilization.

3.7 Assessment of calcium fluctuation levels

BY 4741 cells were treated with the MSG-111-cd3 and with the DMSO (negative control) as described in 3.3. For intracellular calcium measurements the cells were stained with 5 μM FLuo4-AM (Molecular Probes, Eugene, OR) for 90 minutes at 30 °C in the dark, subsequently washed in PBS(1x) (10x, 1.27 M NaCl, 70 mM $Na_2HPO_4.7H_2O$, 30 mM $NaH_2PO_4.H_2O$) and assessed by flow cytometry. As positive control, BY 4741 cells were treated with 3 mM H_2O_2 at pH 3.0.

3.8 Terminal deoxynucleotidyl transferase dUTP nick end labeling (TUNEL)

DNA strand breaks were assessed by TUNEL assay with the 'In Situ Cell Death Detection Kit, Fluorescein' (Roche Applied Science) as described previously in Ludovico *et al.*, 2001. BY 4741 cells were treated with MSG-111-cd3 or with DMSO (negative control) as described in 3.3. Then, cells were collected and fixed with 3.7% (v/v) formaldehyde at room temperature for 30 minutes, followed by digestion of the cell walls with zymolyase (750 μg/ml) at 37 °C for 7 minutes. Then, the cells were washed two times with PBS(1x) and applied to poly-lysine-coated slides. The slides were rinsed with PBS(1x), incubated in permeabilization solution (0.1%(v/v) triton x100 and 0.1%(w/v) sodium citrate)

for 2 minutes on ice and rinsed twice with PBS. For a positive control of the TUNEL assay, 30 U of DNAse I was applied to a microscope slide with untreated cells. Then the slides were incubated with 15 μl of TUNEL reaction mixture (1:10 proportion of terminal deoxynucleotidyl transferase and FICT-dUTP) for 60 minutes at 37 °C in the dark in a humidity chamber. The slides were rinsed two times with PBS and incubated with 0.2 mg/ml of DAPI 4',6-diamidino-2-phenylindole (Molecular Probes, SIGMA) for 20 minutes at 37 °C in the dark. Finally, the slides were rinsed two times with PBS and a coverslip was mounted with a drop of anti-fading agent Vectashield (Vector Laboratories), and the cells were observed by epifluorescence microscopy.

3.9 Assessment of mitochondrial fragmentation

Saccharomyces cerevisiae W303 pYX-mt-GFP cells were treated with MSG-111-cd3 or with DMSO (negative control) as described in 3.3. Cells were then collected and visualized by epifluorescence microscopy to evaluate the mitochondrial fragmentation.

3.10 Assessment of mitochondrial potential and plasma membrane integrity

BY 4741 cells were treated with MSG-111-cd3 or with DMSO (negative control) as described in 3.3. For mitochondrial potential $Dioc_5(3)$ (Molecular Probes, Eugene, OR) was used. The treated cells were collected, washed and resuspended in Dioc buffer (0,1mM $MgCl_2$, 10mM MES (2(N-Morpholino)ethanesulfonic acid) and 2% (w/v) glucose, pH 6.0). Then, they were incubated with $Dioc_5(3)$ at a final concentration of 0.24 μM for 30 minutes at 30 °C in the dark. A sample of cells were incubated with 2 μg/ml de PI (propidium iodide) to assess the alterations in the plasma membrane integrity. As positive control, BY 4741 cells were treated with 150 mM Acetic acid at pH 3.0, boiled cells were used as positive control for PI staining.

3.11 Assessment of GFP-ATG8 protein localization

S. cerevisiae W303-1A GFP-ATG8, W303-1A *Δatg5* GFP-ATG8 and W303-1A *Δatg32* GFP-ATG8 cells were treated with MSG-111-cd3 with DMSO (negative control) as described in 3.3. Cells were then collected for visualization of GFP-ATG8 protein by epifluorescence microscopy. As positive control, the cells were treated with the autophagy inductor rapamycin at final concentration of 0.2 μg/ml.

3.12 Evaluation of GFP-ATG8 cleavage by SDS gel electrophoresis/Western Blot

S. cerevisiae W303-1A GFP-ATG8 and W303-1A *Δatg5* GFP-ATG8 cells were treated with MSG-111-cd3 or with DMSO (negative control) as described in 3.3. As positive control, the cells were treated with rapamycin at final concentration of 0.2 μg/ml. After 60 minutes of treatment, 1 ml of cells were collected to prepare the cell extracts.

3.12.1 Cell extracts preparation

The cell extracts were prepared by the resuspension of the cells in 500 μl of water, followed by the addition of 50 μl of β-mercaptoethanol 7.4% (v/v) in NaOH 2 M solution. The cells were vortexed and incubated on ice for 15 minutes. Thereafter, 50 μl of TCA 50% (w/v) was added, followed by a 15-minute incubation on ice. The samples were then centrifuged at 14800 rpm for 5 minutes at 4 °C and the pellets were resuspended in 30 μl of *Laemmli* buffer 1x (4x, 0.25 M Tris-HCl, 9.2% (w/v) SDS, 40% (w/v) glycerol, 5% (w/v) β-mercaptoethanol, 0.5% (w/v) bromophenol blue). To maintain the blue color and the ideal pH, 5 μl of Tris 1 M pH 9.5 was added to the samples. Finally, the extracts were denaturated at 100 °C for 5 minutes and stored in -20 °C until SDS-PAGE analysis.

3.12.2 SDS gel electrophoresis/Western Blot

The protein lysates obtained as described in 3.12.1 were separated by SDS gel electrophoresis on a 12.5% SDS-poly-acrylamide gel, in a Mini-Protean III electrophoresis system (Bio-Rad) at 25 mA per gel, for about 60 to 90 minutes using running buffer 1x (10×, 0.25 M Tris base, 1.92 M Glycine,

1% SDS). The separated proteins were then transferred to a polyvinylidene fluoride membrane (PVDF) (Hybond-ECL, GE Healthcare) at 60 mA during 90 minutes in a semi dry transfer unit (TE77X Hoefer) using transfer buffer (10x, 0.25 M Tris-Base, 1.92 M glycine). Then, the membranes were blocked in 5% (w/v) non-fat milk in PBS(1x) containing 0.05% (v/v) Tween 20, for around 30 minutes at room temperature with agitation. Then, the membranes were incubated with the primary antibodies overnight at 4 °C. For GFP detection it was used a mouse anti-GFP monoclonal primary antibody (1:2000) and for phosphoglycerate kinase (Pgk) detection it was used a mouse monoclonal antibody anti-yeast phosphoglycerate kinase (1:5000). Finally, the membranes were incubated with the anti-mouse peroxidase-coupled secondary antibody (1:5000), for 60 minutes at room temperature, and the signals were detected in the *ChemiDoc* XRS image system.

3.13 Epifluorescence microscopy and flow cytometry

In the experiments using epifluorescence microscopy a Leica Microsystems DM-5000B microscope was used, with appropriate filter settings (red, green, blue and DIC (Differential Interference Contrast)) with a 100x oil immersion objective. Images were obtained with a Leica DFC350 FX Digital Camera and processed with LAS AF Microsystems software. For phenotype quantification, at least 300 cells of at least two independent experiments were evaluated.

Flow cytometry analysis was made in an Epics® XL™ (Beckman Coulter) flow cytometer, equipped with an argon ion laser emitting a 488 nm beam. The FL-1 sensor (505-545 nm) collected the green fluorescence and the FL-3 sensor (605-635 nm) collected the red florescence. Thirty thousand cells were analyzed per sample at low flow rate. Flow cytometry analyses was performed with FlowJo® 7.6 software.

4. Results

4.1 MSG-111-cd3 induces cell death of *S. cerevisiae* by a process that is dependent on Pep4p

In previous studies in our laboratory we observed that MSG-111-cd3 decreases cell survival of several yeast strains and mutants by a process that is partial dependent on protein synthesis (Ferreira, 2014; Lopes, 2015). Furthermore, in a preliminary assay we observed that the vacuolar protease Pep4p is apparently an important mediator in the cell death process induced by the compound.

So, to confirm the role of Pep4p in the cell death process we assessed the effect of the compound on the survival of a strain deficient in Pep4p. For that, we exposed both BY 4741 WT and BY 4741 *Δpep4* strains to 300 μM MSG-111-cd3 and to 0.35% of DMSO (negative control) and assessed the effect on the cell viability by CFU counting.

Pep4p deletion resulted in resistance to the treatment when compared to the wild type strain. At 30 minutes of treatment a significant statistical difference in the CFU counting between the wild type and the Pep4p deficient strains was already observed, and this difference was maintained along the 120 minutes of assay (figure 10A). The fact that *Δpep4* strain is more resistant to the MSG-111-cd3 effect indicates that this protein plays an important role in the mediation of the cell death process contrary to what was found for acetic acid-induced cell death, where it had a protective role (Pereira *et al.*, 2010).

So, in order to confirm the effect of Pep4p in the cell death process and to investigate if this resistance relies on the proteolytic activity of the protein, BY4741 *Δpep4* strains transformed either with pESC-Pep4p(FL) containing a functional Pep4p, the double point mutation, pESC-DPM-Pep4p proteolytic inactive, or the empty plasmid pESC (Ø), were used in viability assays. As it was expected, BY4741 *Δpep4* pESC(Ø) strain showed loss of viability similar to the BY4741 *Δpep4* strain (figure 10A and 10B). The resistance phenotype was reverted in Pep4p(FL) strain and a significant difference between the Pep4p(FL) strain and the strain containing the empty plasmid was observed during the entire assay (figure 10 B). Furthermore, the DPM-Pep4p strain presents a viability loss statistical lower than the Pep4p(FL) strain along the 120 minutes of treatment. This shows the importance of the Pep4p proteolytic activity in the resistance phenotype. However, we can't assume that this phenotype is totally dependent on the proteolytic activity of Pep4p since we observed some statistical differences between

the DPM-Pep4p strain and the pESC (Ø) strain (figure 10B). Taking together, these observations confirm that Pep4p plays a crucial role in the cell death process induced by the MSG-111-cd3.

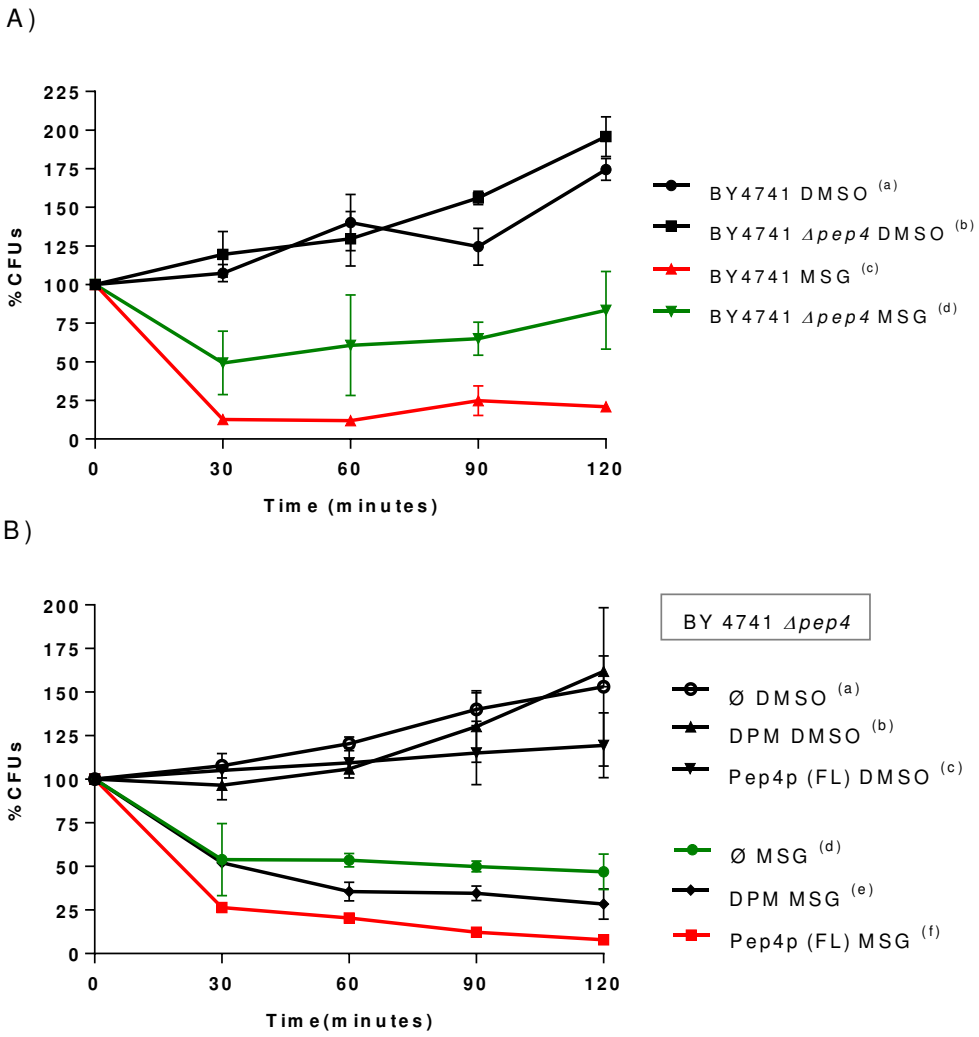

Figure 10 – Influence of Pep4p on the effect of MSG-111-cd3 on yeast cellular viability. A) Effect of MSG-111-cd3 (300µM) and DMSO (0.35%) (negative control) on cell viability of *S. cerevisiae* BY4741 and BY4741 *Δpep4* strains. 30 min: (c vs d)ns; 60 min: (c vs d)**; 90 min: (c vs d)*;120 min: (c vs d)***. **B)** Effect of MSG-111-cd3 (300µM) and DMSO (0.35%) on cell viability of *S. cerevisiae* BY 4741 *Δpep4* pESC(Ø), BY 4741 *Δpep4* pESC-DPM-Pep4p and BY 4741 *Δpep4* pESC-Pep4p(FL) strains. 30 min: (d vs e) ns, (d vs f)**, (e vs f)**; 60 min: (d vs e)*, (d vs f)***, (e vs f) ns; 90 min: (d vs e) ns, (d vs f)***, (e vs f)*; 120 min: (d vs e)* , (d vs f)***, (e vs f)*. Cell viability was assessed by CFU counting at the different time points (0, 30, 60, 90, 120 minutes). The time 0 corresponds to 100% is the CFU counting before MSG-111-cd3 and DMSO treatment. Values are means with SD (n≥2). Statistical analysis was performed by two-way ANOVA. ns non-significant, *P<0.05, **P<0.01, ***P<0.001, ****P<0.0001.

4.2 Pep4p localization and vacuole permeabilization

As was initially observed, the vacuolar protease Pep4p plays an important role in the mediation of the cell death process induced by MSG-111-cd3, so it seems likely that some perturbations are occurring in the vacuole. In fact, this organelle is known to present an acidic lumen and a high content of hydrolytic enzymes. If the vacuole membrane is damaged, it will result in a subsequent released of its content into the cytosol causing degradation of cellular components (Boya *et al.*, 2003). In the work made so far we observed that this compound leads to vacuolar permeabilization and vacuolar membrane disorganization (Lopes, 2015).

So, considering those previous observations and the role of Pep4p in the cell death process it is highly likely the occurrence of Pep4p translocation to the cytosol. To confirm this hypothesis, we treated a *S. cerevisiae* strain expressing a Pep4p fusion with GFP with MSG-111-cd3 and DMSO (negative control) and assessed the cytosolic translocation of Pep4p. Furthermore, in order to observe the occurrence of vacuole permeabilization, the cells were stained with the florescence dye CMAC, which is sequestered within the vacuole lumen if the vacuolar membrane is intact (Stewart and Deacon, 1995).

We were able to observe the translocation of Pep4-EGFP to the cytosol right after 30 minutes of MSG-111-cd3 treatment, characterized by the appearance of a green labeling throughout the cell accompanied by the appearance of small green fragments or spots (figure 12A), in contrast with the observations regarding the DMSO treatment, where the cells present a green labeling in the vacuole lumen, consistent with CMAC staining (figure 11). This translocation was observed throughout all 120 minutes of treatment (figure 12A). Furthermore, in the cells that showed Pep4p cytosolic translocation we were also able to observe the occurrence of vacuole permeabilization, characterized by a dispersed blue staining pattern through the cell (figure 12 A) in contrast with the vacuole lumen staining (figure 11) in the cells treated with DMSO. In fact, after 30 minutes more than 60% of the MSG-111-cd3 treated cells already presented a dispersed staining pattern reaching almost 92% after 120 minutes of

treatment (figure 12B). So, considering these observations, it is clear that vacuole is very susceptible to the MSG-111-cd3 treatment.

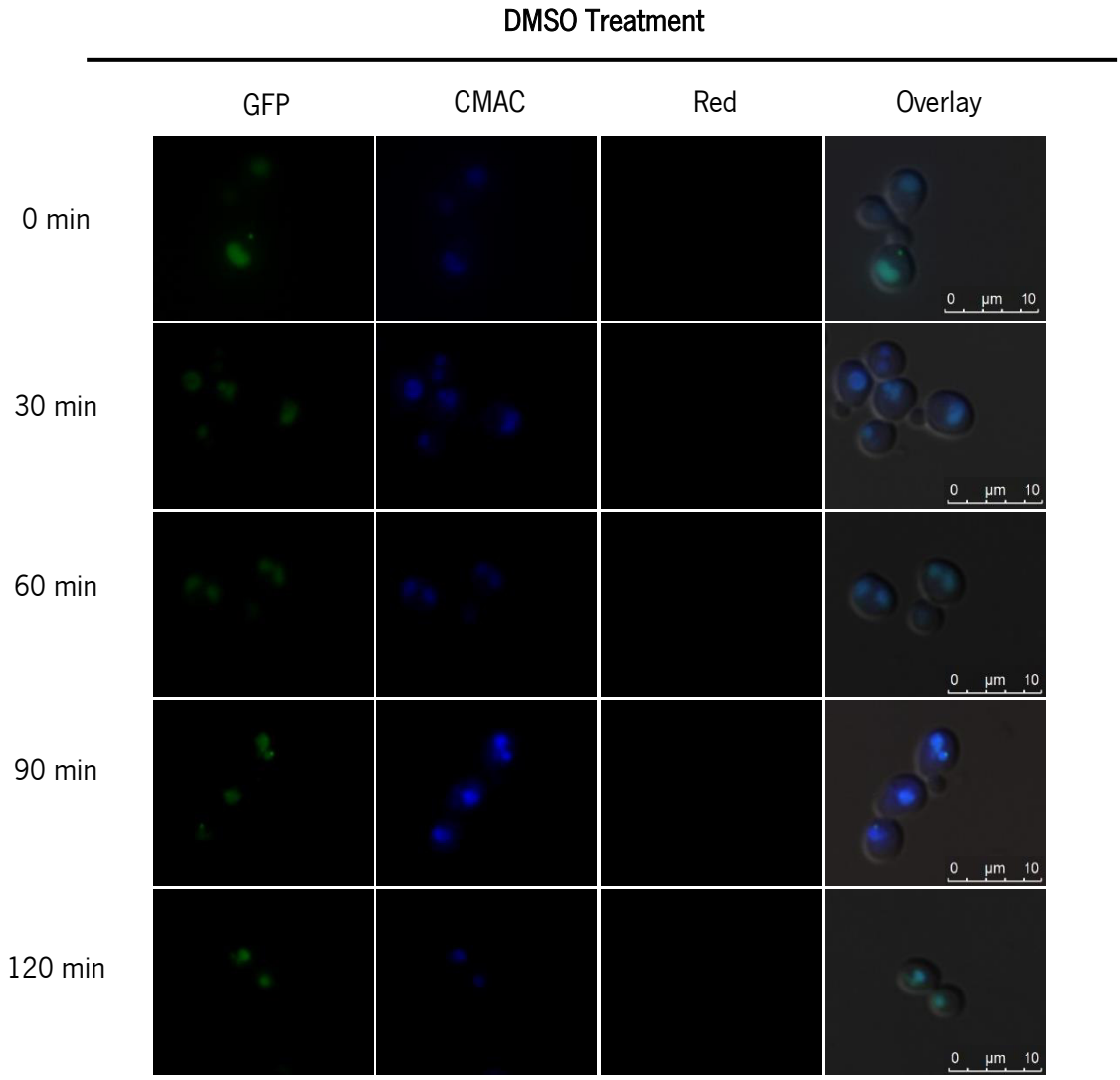

Figure 11 –Effect of DMSO (negative control) on Pep4p localization. Florescence microscopy images of W303-1A p416 ADH-pep4-EGFP cells after treatment with DMSO (0.35%). Cells were stained with CMAC, to observe the vacuole lumen. Samples were collected at different time points, before (time 0) and after 30, 60, 90 and 120 minutes of treatment and then visualized by epifluorescence microscopy with a 100x oil immersion objective.

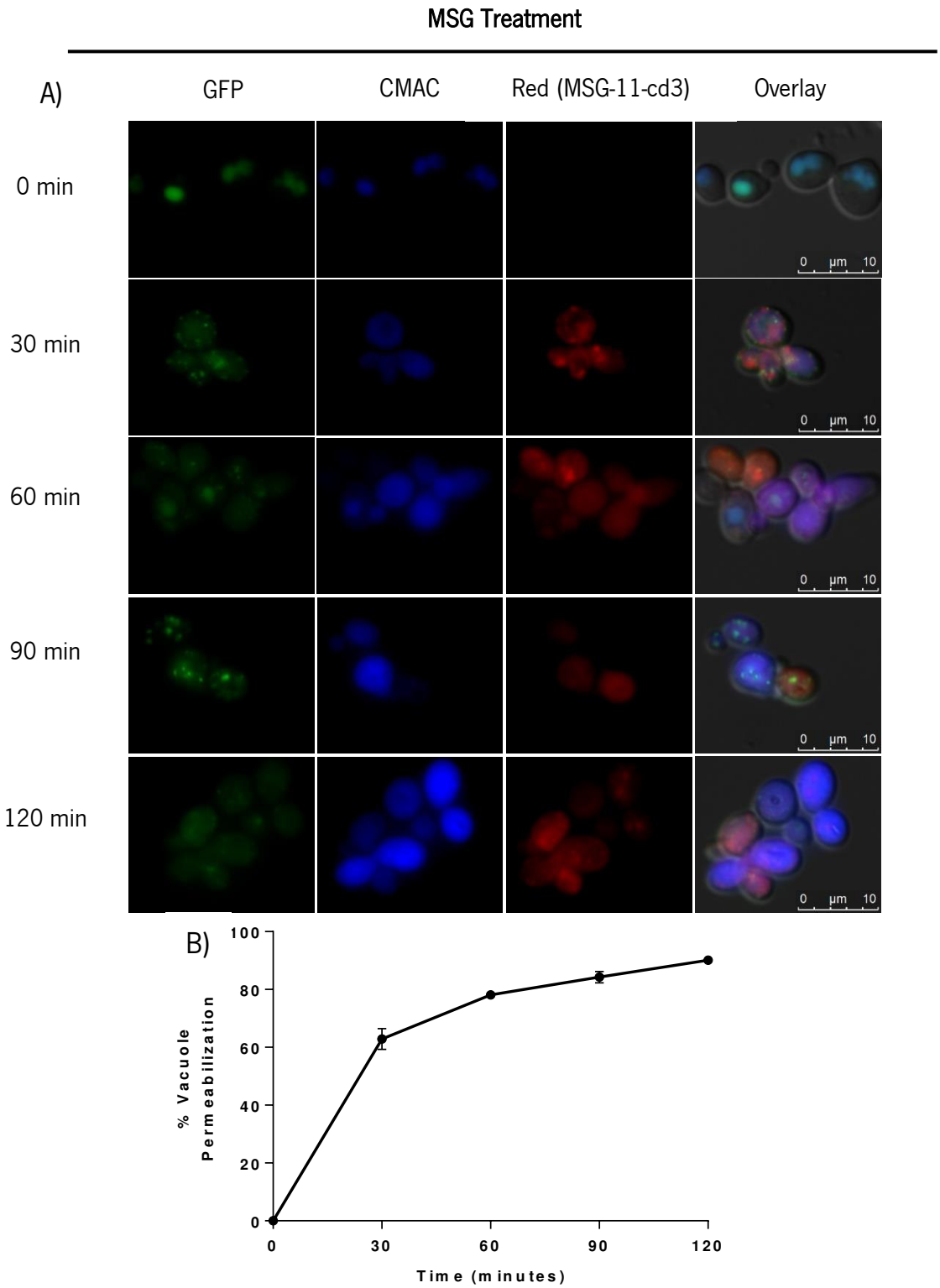

Figure 12 – Effect of MSG-111-cd3 on Pep4p localization. A) Florescence microscopy images of W303-1A p416 ADH-pep4-EGFP cells after treatment with MSG-111-cd3 (300 µM). Cells were stained with CMAC, to observe vacuolar permeabilization. Samples were collected at different time points, before (time 0) and after 30, 60, 90 and 120 minutes of treatment and then visualized by epifluorescence microscopy with a 100x oil immersion objective. **B)** Percentage of MSG-111-cd3 treated cells displaying dispersed blue staining pattern correspondent to vacuole permeabilization. The reported values are means with SD ($n \geq 2$). At least 300 cells were counted for each condition.

4.3 Assessment of calcium fluctuations

Today it is established that calcium signaling is an important mediator in both the initiation and execution of cell death. In fact, intracellular calcium perturbation has been linked to cytotoxicity and to apoptotic, necrotic and autophagic cell death (Orrenius *et al.*, 2003). Furthermore, calcium mobilization has been reported as a signal that leads to calpain activation, which results in the cleavage of several lysosomal associated membrane proteins that normally confer lysosomal stability. Moreover, the increase of calcium concentration is also associated with the activation of cytosolic lipases which affect the osmotic stability of lysosomes (Boya and Kroemer, 2008).

Considering the MSG-111-cd3 effect on the *S. cerevisiae* vacuoles (the yeast organelle equivalent to lysosomes) we next access if the compound led to calcium alterations, which may be associated with the cell death process. For that we used the florescent dye Fluo-4-AM that exhibit an increase in fluorescence upon binding to calcium.

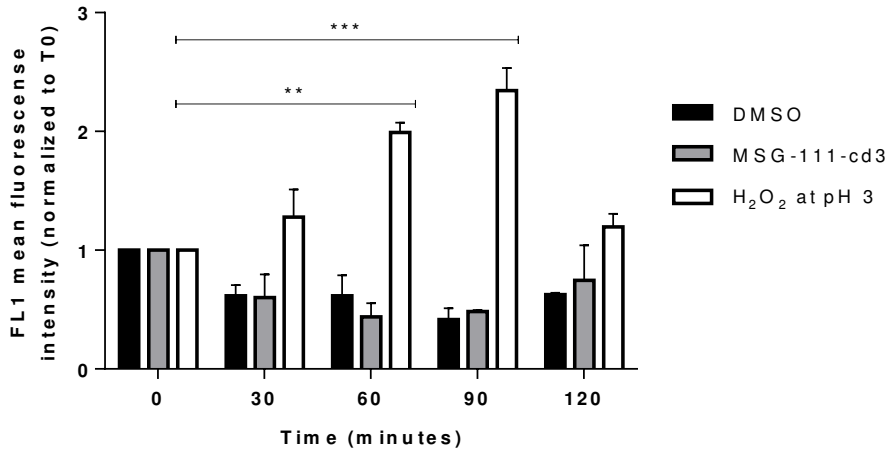

Figure 13 – Effect of MSG-111-cd3 on Intracellular calcium accumulation. Effect of MSG-111-cd3, DMSO (negative control) and H_2O_2 (positive control) on *S. cerevisiae* BY4741 intracellular calcium accumulation. Cells were treated with 300 μM of MSG-111-cd3, 0.35 % of DMSO and 3 mM of H_2O_2 at pH 3.0. For flow cytometry analysis the cells were collected at the different time points, before (time 0) and after 30, 60, 90 and 120 minutes of treatment and then stained with 5 μM FLuo4-AM. Results are expressed as ratio values estimated by dividing the FL1 mean fluorescence intensity of each sample by the FL1 mean of the time 0 sample. MSG-111-cd3: (T0 vs T30) ns, (T0 vs T60) ns, (T0 vs T90) ns and (T0 vs T120) ns; DMSO: (T0 vs T30) ns, (T0 vs T60) ns, (T0 vs T90) ns and (T0 vs T120) ns; H_2O_2: (T0 vs T30) ns, (T0 vs T60)**, (T0 vs T90)*** and (T0 vs T120) ns. Values are means with SD ($n \geq 2$). Statistical analysis was performed by two-way ANOVA. ns non-significant, *P<0.05, **P<0.01, ***P<0.001, ****P<0.0001.

The treatment with MSG-111-cd3 did not lead to calcium accumulation, even for the last time points of treatment, in contrast with the treatment with H_2O_2 (positive control) where we find calcium accumulation after 60 minutes of treatment. In fact, the levels of calcium in the MSG-111-cd3 and DMSO treatment appear to have a decrease compared to the untreated cells (T0) (figure 13), however these values were not statistically different, so it seems unlikely the occurrence of calcium alterations inducted by this compound.

4.4 Assessment of DNA fragmentation by TUNEL assay

DNA condensation and fragmentation is a well-known apoptotic marker. In the previous MSG-111-cd3 studies we observed the existence of a small percentage of cells presenting DNA condensation (Lopes, 2015). However, to further elucidate the cell death process we assessed the occurrence of DNA fragmentation by the appearance of DNA stand breaks using the TUNEL assay.

BY4741 cells were treated both with MSG-111-cd3 and with DMSO, collected and subjected to TUNEL assay. As positive control untreated BY4741 cells were subjected to a 30 U of DNAse I treatment in order to induce DNA stand breaks.

When the treated cells were observed in the epifluorescence microscopy we could not detected the existence of DNA stand breaks (figure 14). Compared with the positive control, 30 U of DNAse I, even after 90 minutes of treatment only a residual population of cells presented DNA fragmentation. In fact, is possible to observe in figure 14 at the 90 minutes of MSG-111-cd3 treatment the presence of a cell showing DNA fragmentation evidence by the nucleus green labeling coincident with DAPI staining. However, this population didn't exceed 1% of the total cells, as such we can conclude that this compound does not lead to DNA fragmentation.

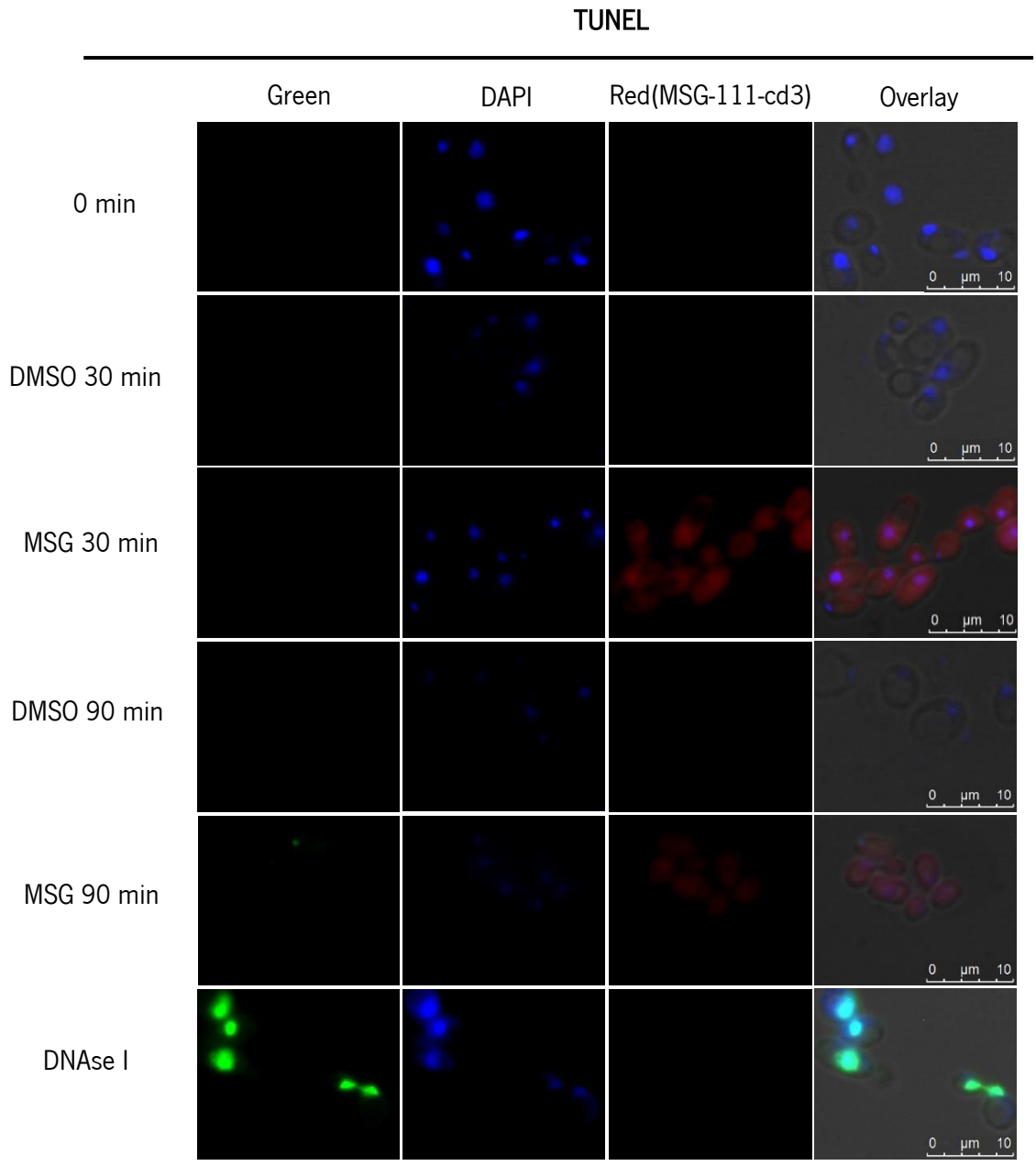

Figure 14 – Effect of MSG-111-cd3 on DNA fragmentation. Florescence microscopy images of BY4741 cells after treatment with MSG-111-cd3 (300 µM), DMSO (0.35%) (negative control) and DNAse I (30 U) (positive control). Samples were collected at different time points, before (time 0) and after 30, 60, 90 and 120 minutes of treatment, subjected to TUNEL protocol and then observed by epifluorescence microscopy with a 100x oil immersion objective.

4.5 Assessment of mitochondrial fragmentation

Mitochondria are a very complex and dynamic organelle, in healthy cells it is characterized by forming an active interconnected network that continually divide and fuse. It is known that mitochondria play a key role in apoptosis mediation, responses to cellular stress and aging (Stunkard, 2009). Furthermore, recent reports have shown that mitochondrial fragmentation (fission) occur during the early stages of apoptosis and is mediated by fission machinery (Suen *et al.*, 2008).

With the aim to investigate if the compound leads to mitochondria network fragmentation we used W303-1A pYX-mt-GFP strain, which express a mitochondrial GFP, and observed cells treated with MSG-111-cd3 by epifluorescence microscopy.

We observed that the compound has a huge effect in the mitochondrial network since after 30 minutes of treatment more than 80% of the total cells presented numerous and smaller mitochondrial in contrast with the negative control where the mitochondria was not affected (figure 15A and 15B). Furthermore, the percentage of cells showing mitochondrial network increased with the treatment time, and after 120 minutes the number of cells showing mitochondrial network fragmentation exceed 90% of the total cells (figure 15B).

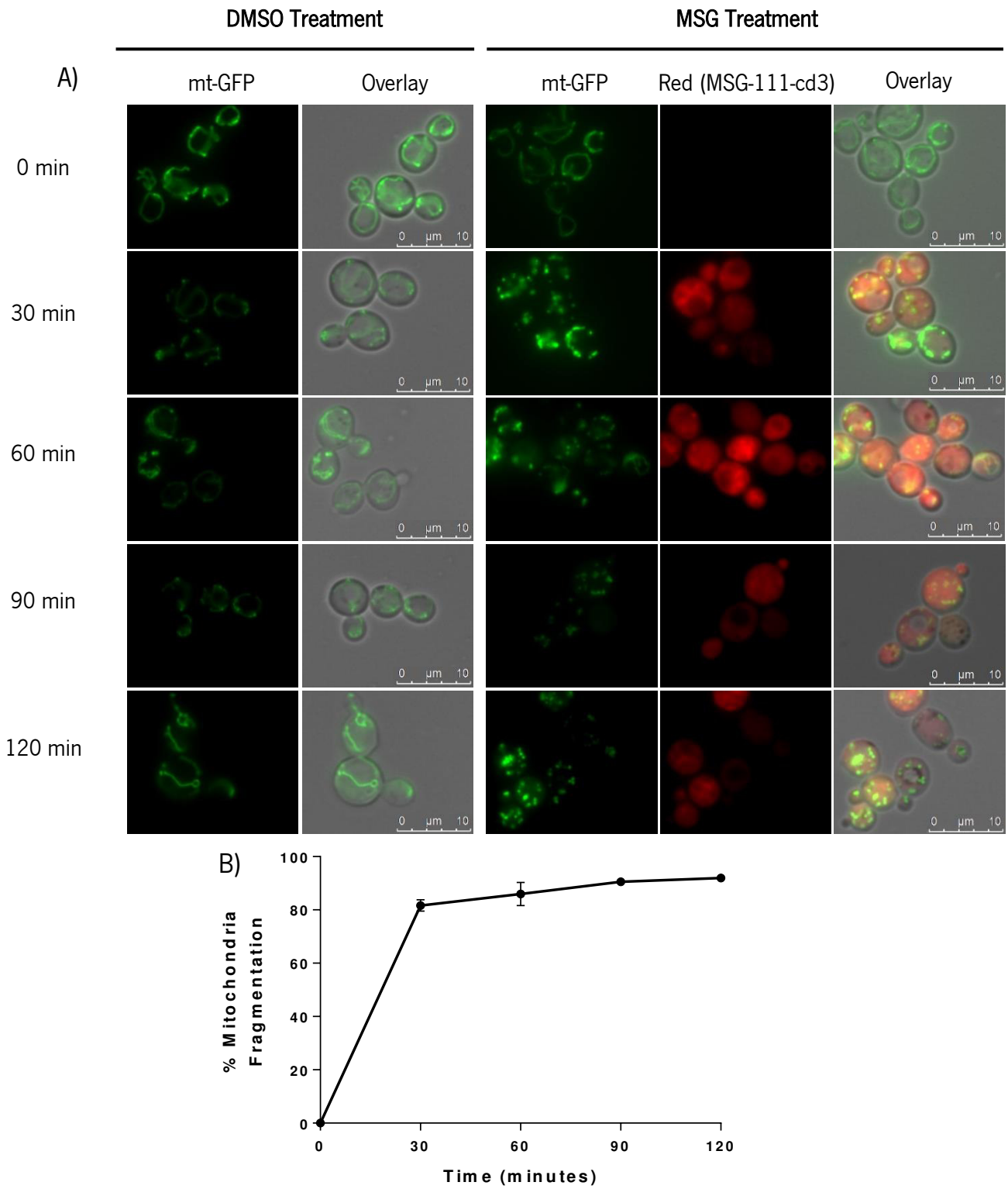

Figure 15 – Effect of MSG-111-cd3 on mitochondrial network. A) Florescence microscopy images of W303-1A pYX-mt-GFP cells after treatment with MSG-111-cd3 (300 µM) and DMSO (0.35%). Samples were collected at different time points, before (time 0) and after 30, 60, 90 and 120 minutes of treatment and then visualized by epifluorescence microscopy with a 100x oil immersion objective. **B)** Percentage of MSG-111-cd3 treated cells displaying mitochondrial network fragmentation. The reported values are means with SD (n≥2). At least 300 cells were counted for each condition.

4.6 Analysis of mitochondrial membrane potential and plasma membrane integrity

Mitochondria are the only know organelles that possesses a significant membrane potential, characterized by an internal negatively charge. In fact, several studies shown that alterations in the mitochondrial membrane potential are implicated in the occurrence of programed cell death. Example of that is the transient hyperpolarization followed by a depolarization of mitochondria membrane in acetic acid-induced apoptosis (Pereira *et al.*, 2010).

Considering the previous observations regarding the mitochondrial network fragmentation it is clear that the MSG-111-cd3 is some way affecting the mitochondria. So, to investigate if this effect isn't only morphological, but also functional, we evaluate if there are changes in the mitochondrial membrane potential.

To assess mitochondrial membrane potential, we used the carbocyanine dye $Dioc_5(3)$ witch accumulates in mitochondria depending on its membrane potential. MSG-111-cd3 and DMSO treated cells were stained with $Dioc_5(3)$ and analyzed by flow cytometry. As positive control BY4741 cells were treated with acetic acid. Furthermore, cells were stained with propidium iodide, to assess if the treated cells suffered any alteration in the integrity of the plasma membrane. Boiled cells were used as positive control.

In the acetic acid treatment, we were able to observe a shift of the $Dioc_5(3)$ fluorescence peak of the acetic acid treated cells to the left (figure 16 A) showing the mitochondrial depolarization of the control cells. Furthermore, it is also possible to observe a small peak in the right side, which corresponds to cells with mitochondrial hyperpolarization. In the MSG-111-cd3 and DMSO treatment we could not observe any shift in the $Dioc_5(3)$ peak. However, we observed the presence of a left peak in the MSG-111-cd3 treated cells (figure 16 B), which shows the existence of a population presenting mitochondrial depolarization. We could observe that after 30 minutes of treatment around 18% of the total cells presented mitochondrial depolarization, however this number did not increase more that 23%, even in the last time points (figure 16 C). Furthermore, the percentage of cells showing PI (propidium iodide) staining was very low. The positive PI staining for the MSG-111-cd3 and DMSO cells did not exceed 1% and the acetic acid cells (positive control) was lower than 3% (figure 17).

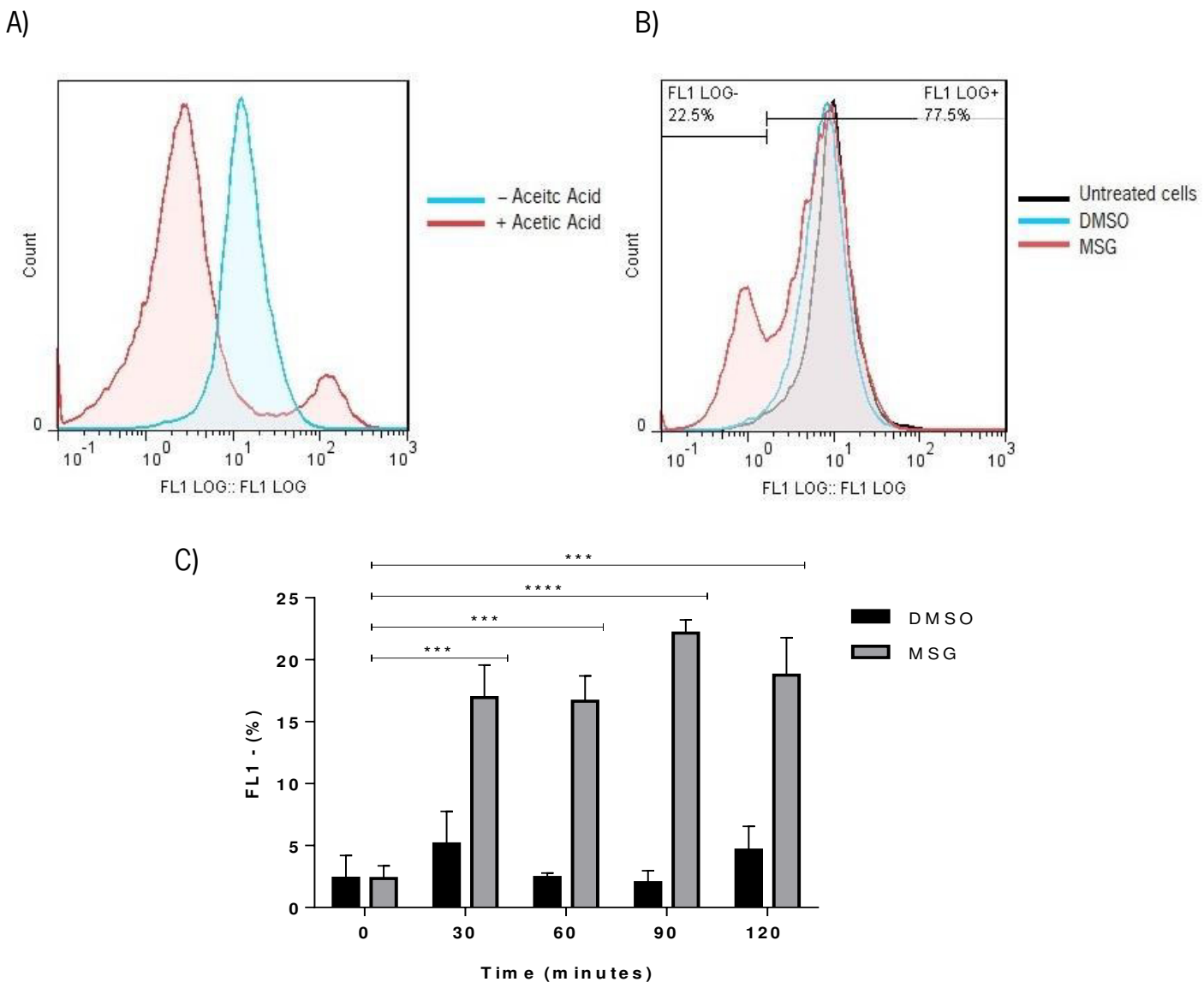

Figure 16 – Effect of MSG-111-cd3 on mitochondrial membrane potential. A) Effect of acetic acid (positive control) on BY4741 mitochondrial membrane potential. Cells were treated with 150 mM of acetic acid at pH 3.0. For flow cytometry analysis, the cells were collected before (- acetic acid) and after 60 minutes of acetic acid treatment (+ acetic acid) and stained with 0.24 μM of $Dioc_5(3)$. Results are expressed as a mono-parametric histogram of $Dioc_5(3)$ fluorescence representing one of three independent experiments. **B)** Effect of MSG-111-cd3 and DMSO (negative control) on BY4741 mitochondrial membrane potential. Cells were treated with 300 μM of MSG-111-cd3 and 0.35 % of DMSO. For flow cytometry analysis the cells were collected before (untreated cells) and after 30, 60, 90 and 120 minutes of treatment and then stained with 0.24 μM of Dioc5(3). The represented result corresponds to the 60 minutes' treatment. Results are expressed as a mono-parametric histogram of $Dioc_5(3)$ fluorescence representing one of three independent experiments. Gate defined by auto-fluorescence sample. **C)** Quantification of FL1 negative population (FL1 LOG –) correspondent to the percentage of cells with mitochondrial depolarization. MSG: (t0 vs t30)***, (t0 vs t60)***, (t0 vs t90)****, (t0 vs t120)***; DMSO: (t0 vs t30) ns, (t0 vs t60) ns, (t0 vs t90) ns, (t0 vs t120) ns. Values are means with SD (n≥2). Statistical analysis was performed by two-way ANOVA. ns non-significant, *P<0.05, **P<0.01, ***P<0.001, ****P<0.0001.

The results showed that there was almost no loss of plasma membrane integrity, which validates the previous results regarding mitochondrial membrane potential. Taken together, these observations suggest that MSG-111-cd3 leads to mitochondrial depolarization in a fraction of the total cells, with no alterations in the plasma membrane integrity.

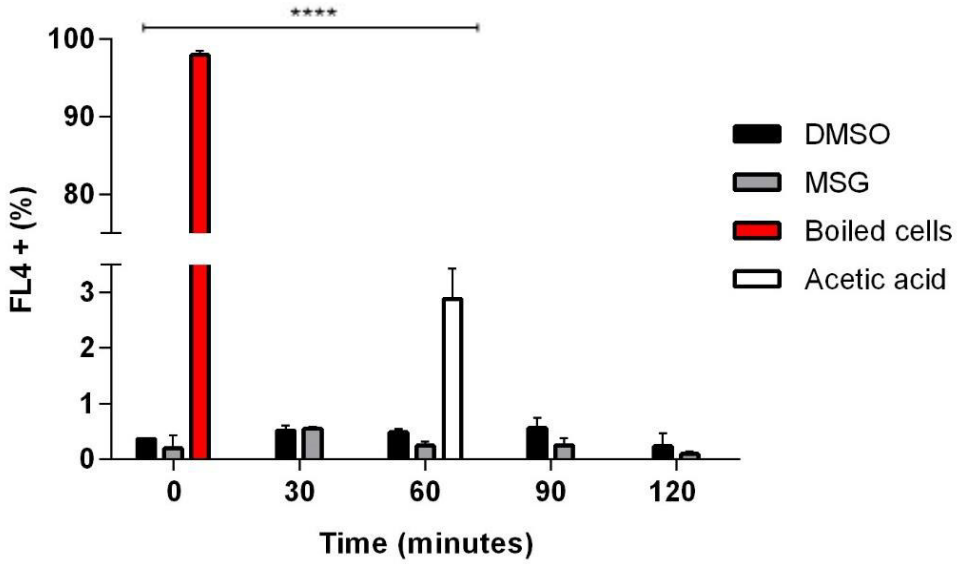

Figure 17 – Effect of MSG-111-cd3 on plasma membrane integrity. Effect of MSG-111-cd3, DMSO (negative control) and acetic acid (positive control) on propidium iodide (PI) staining of BY4741 cells. Cells were treated with 300 μM of MSG-111-cd3, 0.35 % of DMSO and 150 mM of acetic acid at pH 3.0. Boiled cells were used as positive control for PI staining. For flow cytometry analysis the cells were collected at different time points, before (time 0) and after 30, 60, 90 and 120 minutes of treatment and then stained with 2μg/ml of PI. Results are expressed as percentage of FL4 positive population (FL4 LOG +) correspondent to the percentage of cells with loss of plasma membrane integrity. MSG: (t0 vs t30)ns, (t0 vs t60)ns, (t0 vs t90) ns, (t0 vs t120) ns; DMSO: (t0 vs t30) ns, (t0 vs t60) ns, (t0 vs t90) ns, (t0 vs t120) ns; Acetic acid: (t0 vs t60)****. Values are means with SD (n≥2). Statistical analysis was performed by two-way ANOVA. ns non-significant, *P<0.05, **P<0.01, ***P<0.001, ****P<0.0001.

4.7 Analysis of autophagy involvement in the cell death process

Considering the previous results, we could not find a clear apoptotic or necrotic phenotype, so we questioned if the cell death process could involve the autophagy machinery. In the previous studies the dependence of the cell death induced by MSG-111-cd3 on autophagy was assessed using a strain deficient in Atg1p, a serine-threonine kinase that is involved in the formation of the autophagosomal membranes being essential for autophagy induction (Papinski *et al.*, 2014). However, viability assays did not reveal differences between the deleted and wild type strain, indicating that Atg1p does not seem to have a role in the effect of MSG-111-cd3 (Lopes, 2015).

The detection autophagy occurrence can be the evaluation by a commonly used assay that monitors the processing of a GFP-ATG8 fusion protein (Shintani and Klionsky, 2004; Klionsky *et al.*, 2016). When autophagy occurs a part of the membrane bound Atg8p is incorporated into the autophagosome and carried to the vacuolar lumen where it is degraded by the vacuolar hydrolases (Shpilka *et al.*, 2011; Nakatogawa *et al.*, 2012). The hydrolysis of GFP-ATG8 fusion protein results in a free GFP that can be measured as an autophagy indicator. Considering this approach, three strains were used to assess autophagy occurrence the W303-1A GFP-ATG8, W303-1A *Δatg32* GFP-ATG8, blocked in mitophagy, and the W303-1A *Δatg5* GFP-ATG8, blocked in autophagy. The strains were treated with the 300 μM MSG-111-cd3 and/or with 0.2 μg/ml of the autophagy inducer rapamycin, used as positive control. The strains were monitored through florescence microscopy and the extent of GFP-ATG8 cleavage was quantified by western blot analysis (except for the *Δatg32* strain).

After 60 minutes of rapamycin treatment it was possible to observer green fluorescence in the vacuole lumen of the WT and *Δatg32* strain, in contrast to *Δatg5* strain, where green fluorescence remained disperse in the cytosol (figure 18). Western blot analysis confirms autophagy induction in the WT by the appearance of a cleavage band, in contrast with the increase of the GFP-ATG8 band in the *Δatg5* strain (figure 19). However, in the case of the MSG-111-cd3 treatment we could not detect any florescence in the vacuole lumen even after 120 minutes, instead the compound led to an appearance of small green fragments or spots in the cytosol that could correspond to an accumulation of Atg8p in the autophagosomes or simply to aggregation of the protein (figure 18).

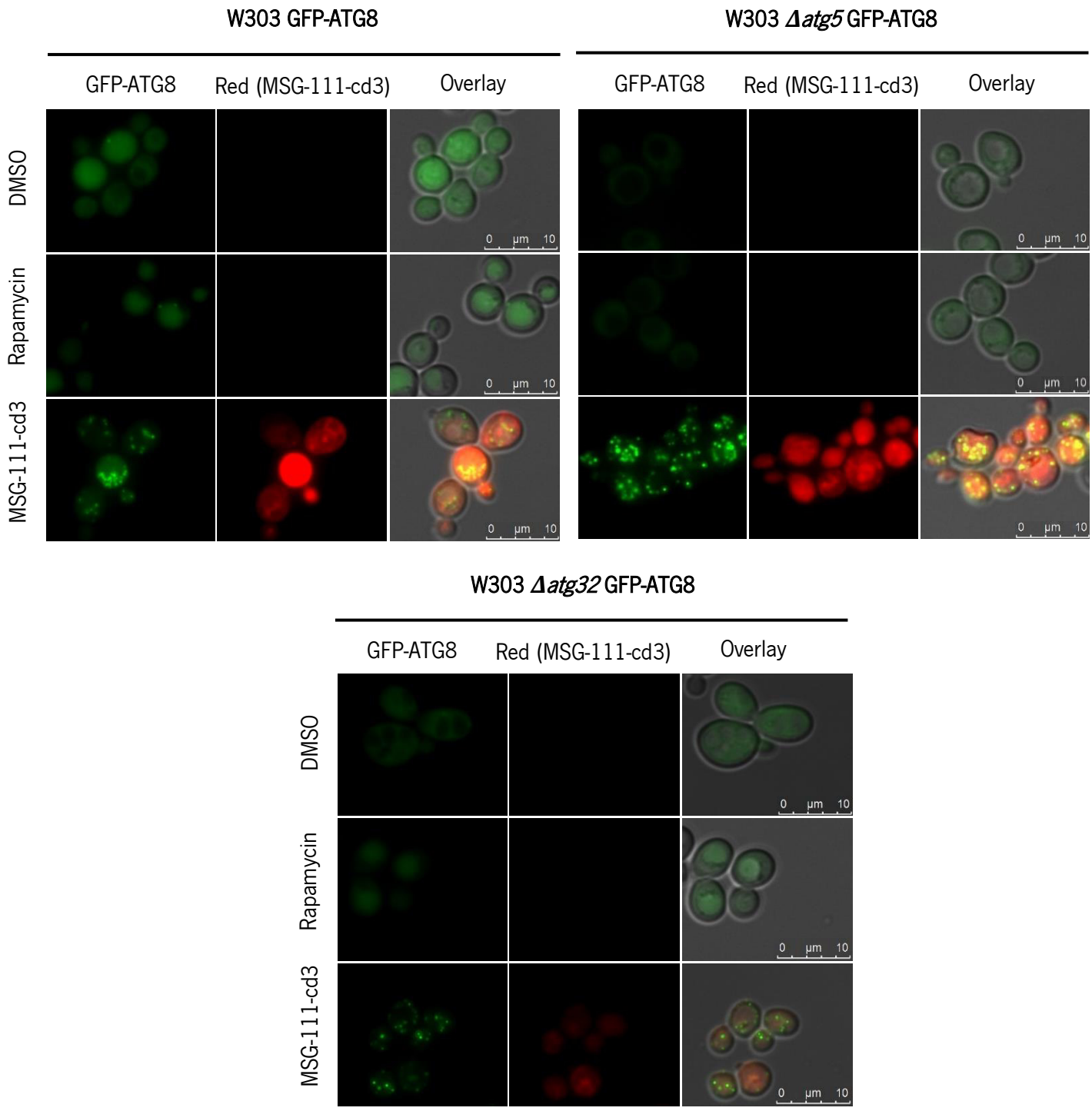

Figure 18 – Analysis of Atg8p localization in response to MSG-111-cd3. Florescence microscopy images of W303-1A GFP-ATG8, W303-1A *Δatg32* GFP-ATG8 and W303-1A *Δatg5* GFP-ATG8 cells after 60 minutes of treatment with MSG-111-cd3, DMSO (negative control) and Rapamycin (positive control). Cells were treated with 300 µM of MSG-111-cd3, 0.35 % of DMSO and 0.2 µg/ml of rapamycin. Samples were collected at different time points, before (time 0) and after 30, 60, 90 and 120 minutes of treatment and then visualized by epifluorescence microscopy with a 100x oil immersion objective.

The western blot analysis did not support the hypothesis of accumulation of Atg8p in the autophagosomes since no increase of the GFP-ATG8 band occur, moreover we couldn't detect any increase in the cleaved GFP band, so the occurrence of autophagy seems very unlikely (figure 19). Furthermore, MSG-111-cd3 appears to block autophagy induction since when we treated *S. cerevisiae* cells with MSG-111-cd3 and rapamycin simultaneously, we detected once again the appearance of green spots in the cytosol instead of the previous observed green florescence in the vacuole lumen (figure 20). This result is in agreement with the previous observed effect of the compound on vacuolar permeabilization.

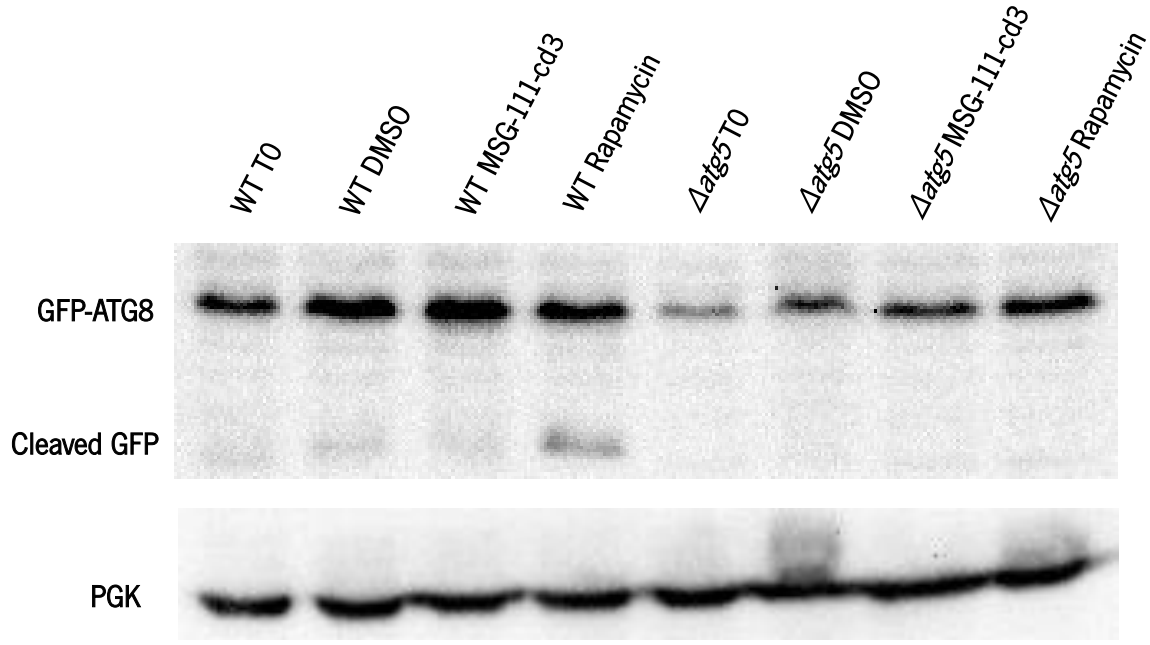

Figure 19 – Western-blot analysis of GFP- ATG8 processing. Effect of MSG-111-cd3, DMSO (negative control) and Rapamycin (positive control) on GFP-ATG8 processing of W303-1A GFP-ATG8 and W303-1A *Δatg5* GFP-ATG8 cells. Cells were treated with 300 μM of MSG-111-cd3, 0.35 % of DMSO and 0.2 μg/ml of rapamycin. Samples were collected before (time 0) and after 60 minutes of treatment. Representative experiment of two independent experiments.

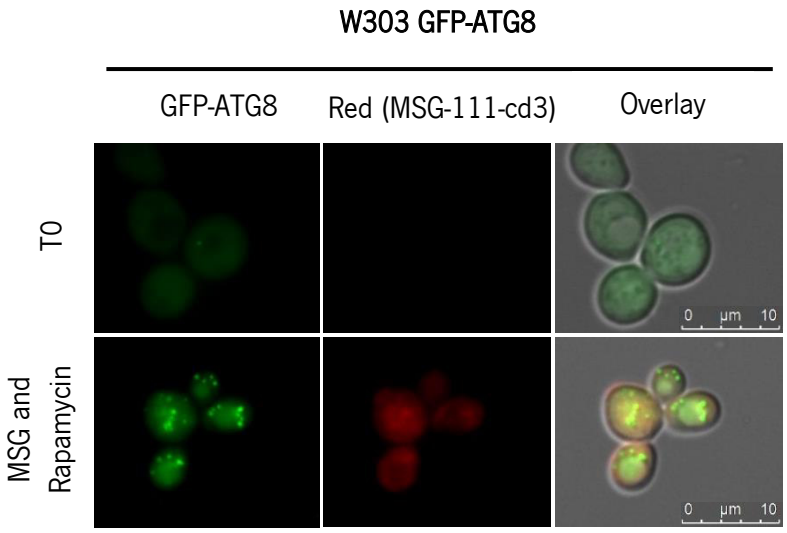

Figure 20 – Analysis of Atg8p localization in response to MSG-111-cd3 and Rapamycin. Florescence microscopy images of W303-1A GFP-ATG8 cells after 60 minutes of treatment with MSG-111-cd3 and Rapamycin. Cells were treated with 300 µM of MSG-111-cd3 simultaneously with 0.2 µg/ml of rapamycin. Samples were collected at different time points, before (time 0) and after 30, 60, 90 and 120 minutes of treatment and then visualized by epifluorescence microscopy with a 100x oil immersion objective.

4.8 Assessment of Nhp6Ap translocation from the nucleus

As referred above, the nuclear release of yeast HMGB1 orthologue Nhp6Ap is usually employed as a marker of necrosis in *Saccharomyces cerevisiae* (Eisenberg *et al.*, 2009; Santos *et al.*, 2012). The cellular localization of Nhp6Ap during treatment with MSG-111-cd3, was previously accessed, the results showing that yeast cells exhibited Nhp6Ap release from the nucleus to the cytosol with punctuated disposition of the protein instead of just being uniformly dispersed as is observed in necrotic cells (Ferreira, 2014; Lopes, 2015).

Furthermore, in a preliminary assay it was observed that the Nhp6Ap release was delayed and reduced in a strain deficient in Pep4p (Lopes, 2015). Those observations reinforced the role of Pep4p in the cell death process, but also suggest that Nhp6Ap release could have a prominent role in the cell death process. So, to further investigate the Nhp6Ap role in the cell death process we assessed the effect of the compound in the survival of a strain deficient in this protein. We exposed both BY 4741 WT and BY 4741 *Δnhp6ap* strains to 300 μM of MSG-111-cd3 or 0.35% of DMSO (negative control) and assessed the effect on the cell viability by CFU counting. The response of the deficient strain was identical to the wild type strain, since we did not find any statistical difference between the CFUs counting along the 120 minutes of treatment (figure 21).

This result could suggest that the Nhp6Ap nuclear release is not crucial for cell death and is just a consequence of the process. However, *S. cerevisiae* contains 7 HMGB protein orthologues, among those, Nhp6Bp is described as a paralog of Nhp6Ap. In fact, the redundancy of Nhp6Bp may replace the Nhp6Ap role in the cell death process (Kolodrubetz and Burgum, 1990; Bustin, 2001).

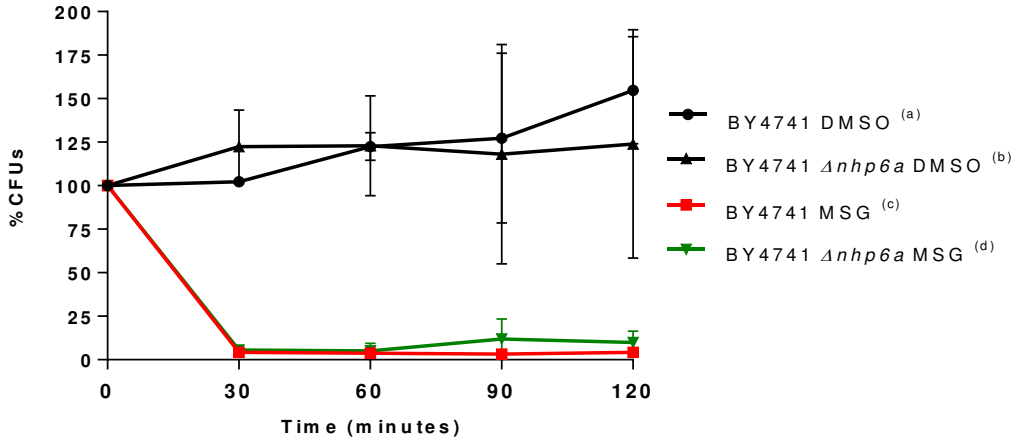

Figure 21 – Effect of MSG-111-cd3 on BY 4741 *Δnhp6a* viability. Effect of MSG-111-cd3 (300µM) and DMSO (0.35%) (negative control) on cell viability of *S. cerevisiae* BY4741 and BY4741 *Δnhp6a* strains. 30 min: (c vs d)ns; 60 min: (c vs d)ns; 90 min: (c vs d)ns; 120 min: (c vs d)ns. Cell viability was assessed by CFU counting at the different time points (0, 30, 60, 90, 120 minutes). The time 0 corresponds to 100% is the CFU counting before MSG-111-cd3 and DMSO treatment. Values are means with SD (n≥2). Statistical analysis was performed by two-way ANOVA. ns non-significant, *P<0.05, **P<0.01, ***P<0.001, ****P<0.0001.

As referred above, the Nhp6Ap nuclear release pattern is totally different from the one observed in other studies (Eisenberg *et al.*, 2009; Santos *et al.*, 2012). In this case, we observe a punctuated disposition of the protein (Ferreira, 2014; Lopes, 2015), that can be a consequence of a vesicular encapsulation of the protein. In fact, recent studies have shown that the mammalian Nhp6Ap homologue HMHB1, can be present in secretory lysosomes and on microparticles that release the protein to the extracellular medium (Gardella *et al.*, 2002; Bonaldi *et al.*, 2003; Pisetsky, 2014; Klionsky *et al.*, 2016).

Considering that Nhp6Ap does not possess the classical peptide secretion signals that allow the protein encapsulation through the Endoplasmic reticulum – Golgi secretory pathway, we next investigated if Nhp6Ap is being encapsulated, possible through an unconventional pathway. More specifically, we assessed the role of the multivesicular body (MVB) pathway in the Nhp6Ap nuclear release pattern. So, we assessed the effect of the compound in the Nhp6Ap nuclear release of two strains deficient in proteins from the Endosomal sorting complexes required for transport (ESCRT) required for the for the MVB pathway. A strain deficient in the Stp22p (BY 4741 *Δstp22* pUG35-nhp6a-GFP) a protein required for the ESCRT I and a strain deficient in the Snf7p (BY 4741 *Δsnf7* pUG35-nhp6a GFP) that is required for the ESCRT III, were used.

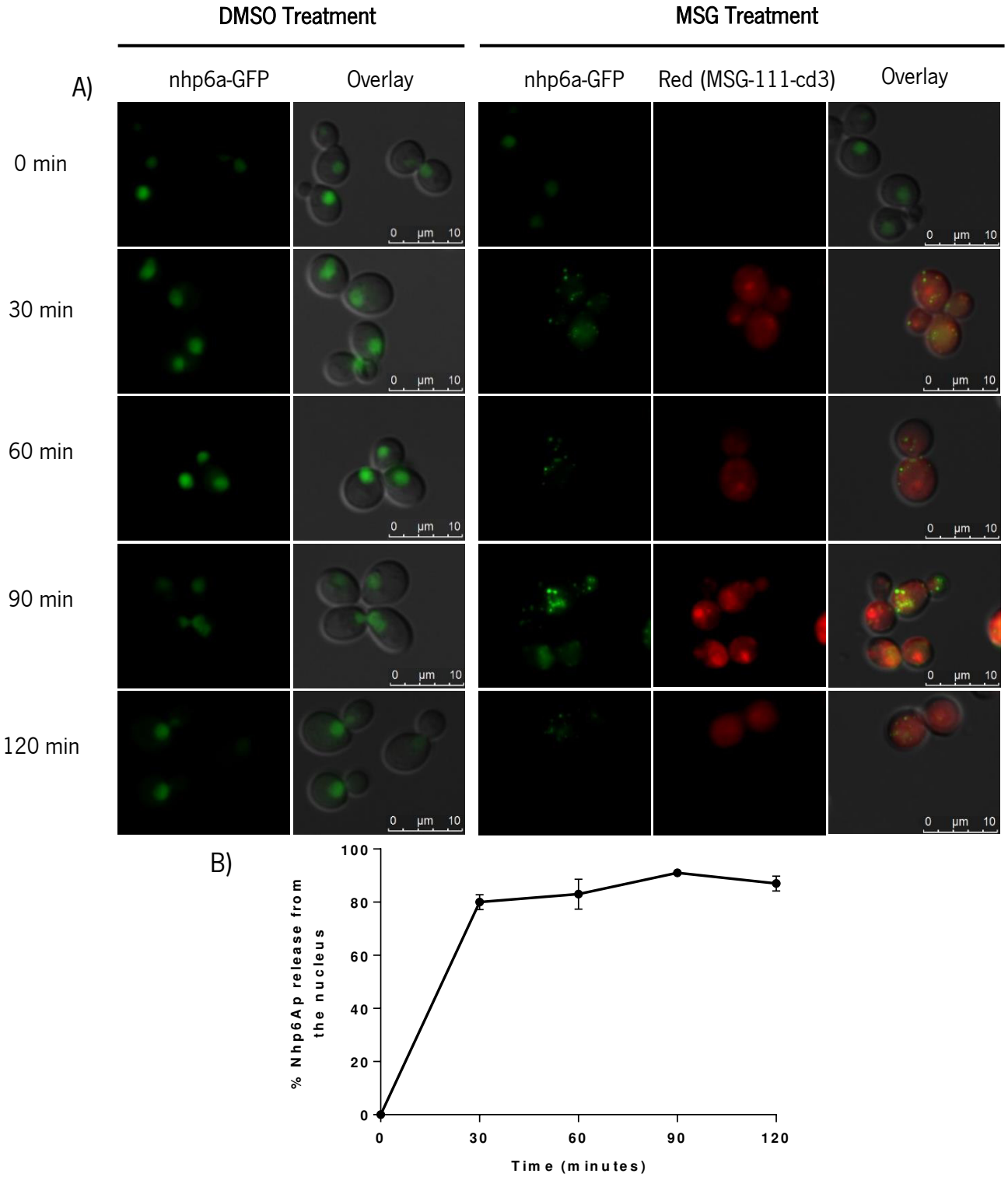

Figure 22 – Effect of MSG-111-cd3 on Nhp6Ap nuclear release. A) Florescence microscopy images of BY 4741 pUG35-nhp6a-GFP cells after treatment with MSG-111-cd3 (300 µM) and DMSO (0.35%). Samples were collected at different time points, before (time 0) and after 30, 60, 90 and 120 minutes of treatment and then visualized by epifluorescence microscopy with a 100x oil immersion objective. **B)** Percentage of MSG-111-cd3 treated cells displaying Nhp6Ap nuclear release. The reported values are means with SD (n≥2). At least 300 cells were counted for each condition.

Initially, we used a BY 4741 pUG35-nhp6a-GFP strain to reproduce the effect of MSG-111-cd3 on the Nhp6Ap localization. After 30 minutes of MSG-111-cd3 treatment we were able to observe that around 80% of the cells exhibited Nhp6Ap release from the nucleus, with the characteristic punctuated disposition, different from the necrotic phenotype (figure 22A and B). This phenotype was observed during the 120 minutes of the assay (figure 22A and B).

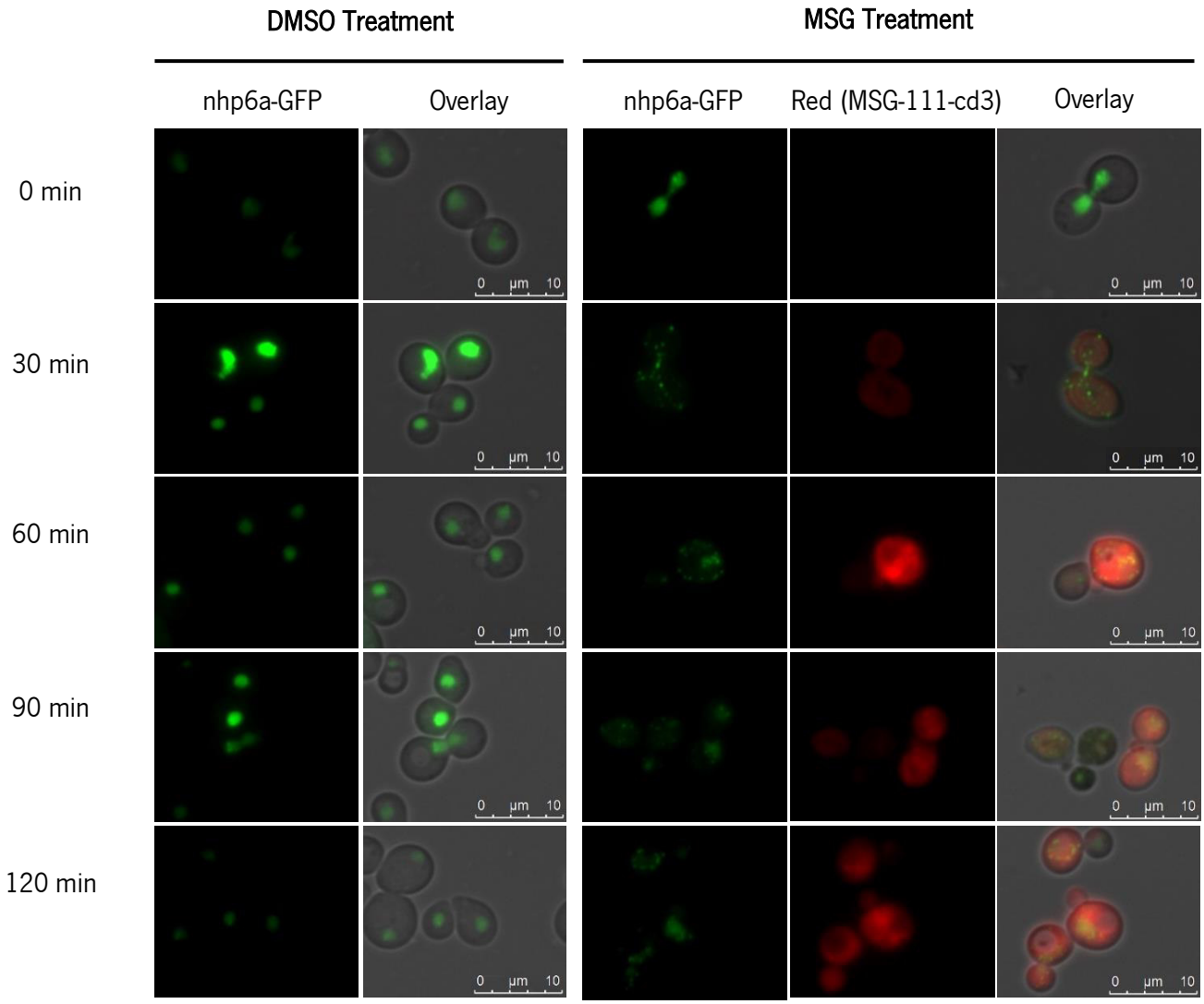

Figure 23 – Effect of MSG-111-cd3 on Nhp6Ap nuclear release of BY 4741 *Δstp22* strain. Florescence microscopy images of BY 4741 *Δstp22* pUG35-nhp6a-GFP cells after treatment with MSG-111-cd3 (300 µM) and DMSO (0.35%). Samples were collected at different time points, before (time 0) and after 30, 60, 90 and 120 minutes of treatment and then visualized by epifluorescence microscopy with a 100x oil immersion objective.

Using the Snf7p and Stp22p deficient strains, we could observe that the absence of these proteins did to disrupt the Nhp6Ap punctuated disposition. As is shown in figure 23 and 24, both

strains continued to display the same phenotype as the wild type strain (figure 22). Furthermore, we could not detect any delay in the Nhp6Ap release nor reduction in the percentage of cells with this phenotype. So, the involvement of the MVB pathway in the Nhp6Ap release process seems unlikely.

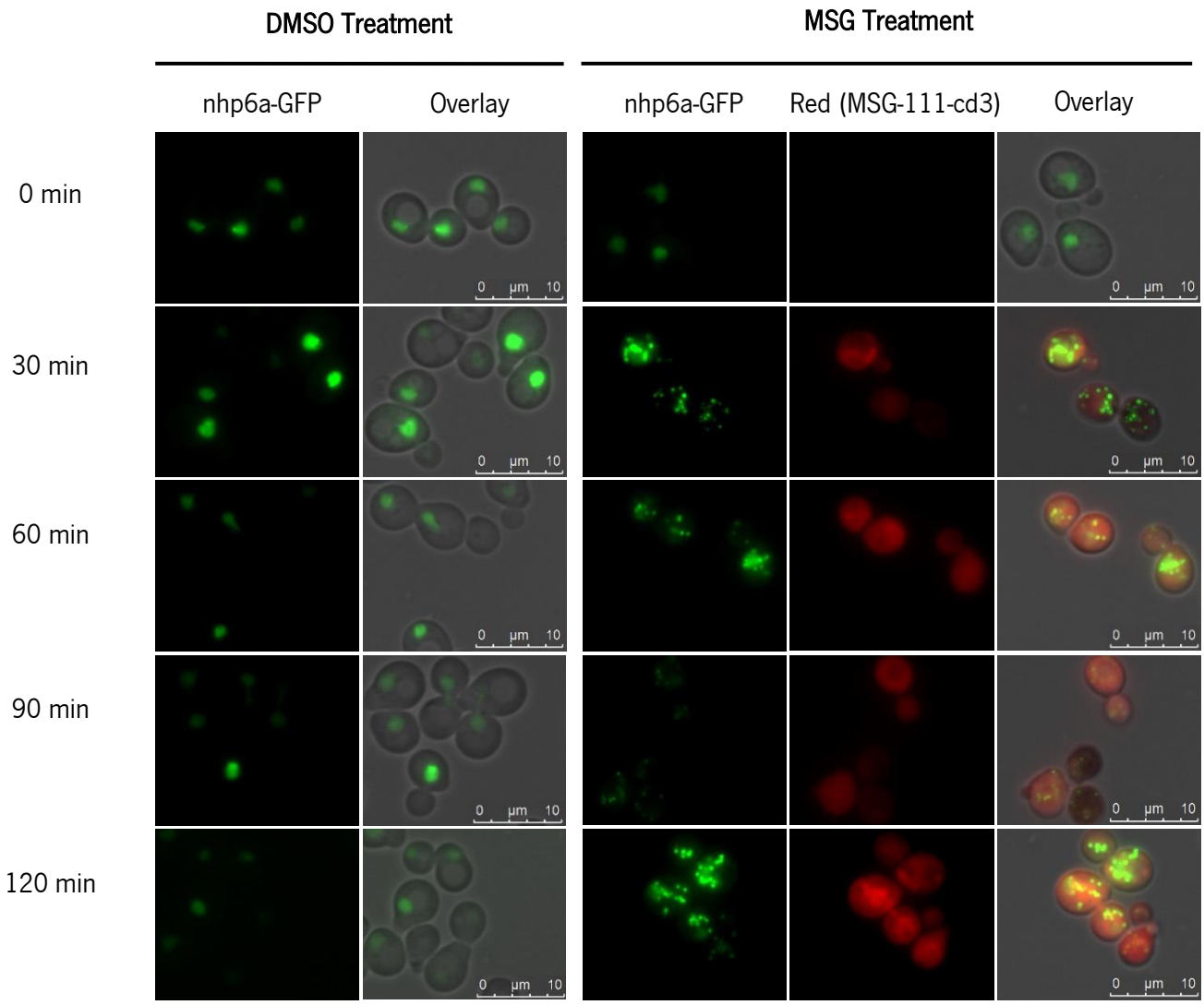

Figure 24 – Effect of MSG-111-cd3 on Nhp6Ap nuclear release of BY 4741 *Δsnf7* strain. Florescence microscopy images of BY 4741 *Δsnf7* pUG35-nhp6a-GFP cells after treatment with MSG-111-cd3 (300 µM) and DMSO (0.35%). Samples were collected at different time points, before (time 0) and after 30, 60, 90 and 120 minutes of treatment and then visualized by epifluorescence microscopy with a 100x oil immersion objective.

4.9 Assessment of Hta2p localization and nuclear envelope disorganization

As referred above, Nhp6Ap is a DNA-Binding factor, being involve in the support of the chromatin structure, so aiming to better understand the mechanism of Nhp6Ap release during MSG-111-cd3 induced cell death, we next investigated if the observed release pattern is specific for this protein or if other proteins involved in chromatin organization were also released. With this aim, we assessed if the histone Hta2p suffered any re-localization in cells treated with MSG-111-cd3 by using a strain expressing a Hta2-GFP hybrid protein. This strain also expresses a Pep4-mchery fusion which could be used to assess movement of the two proteins but in our case this feature of the strain was not useful since MSG-111-cd3 also displays red florescence. We could observe that Hta2p is released from the nucleus to the cytoplasm, presenting a analogous pattern as Nhp6Ap (figure 22A and 25A). However, in this case, the extension of the release was lower in comparison to Nhp6Ap and after 30 minutes of treatment only around 50% of the cells presented this phenotype reaching a maximum of 62% at 120 minutes (figure 25B).

Considering these results, it seemed likely that the nuclear envelop could also be compromised, so the effect of the compound was tested by monitoring the behavior of the nuclear pore complex protein Nup49p. A strain containing Nup49-GFP fusion and a Hta2-mcherry was used. As is possible to observe in the figure 26, the MSG-111-cd3 treatment resulted in the disorganization of the nuclear envelope characterized by the appearance of small green fragments. This phenotype was observed in almost all the MSG-11-cd3 treated cells and maintained during the 120 minutes of treatment, in contrast with the perfect green labeling of the nuclear envelope observed in the negative control (DMSO). Once again the red florescence of the compound did not allow to take advantage of the information provided by Hta2-mcherry.

Taken together, these results show that Nhp6Ap is not the only target of MSG-11-cd3 action but that other nuclear proteins are susceptible to alterations caused by this compound.

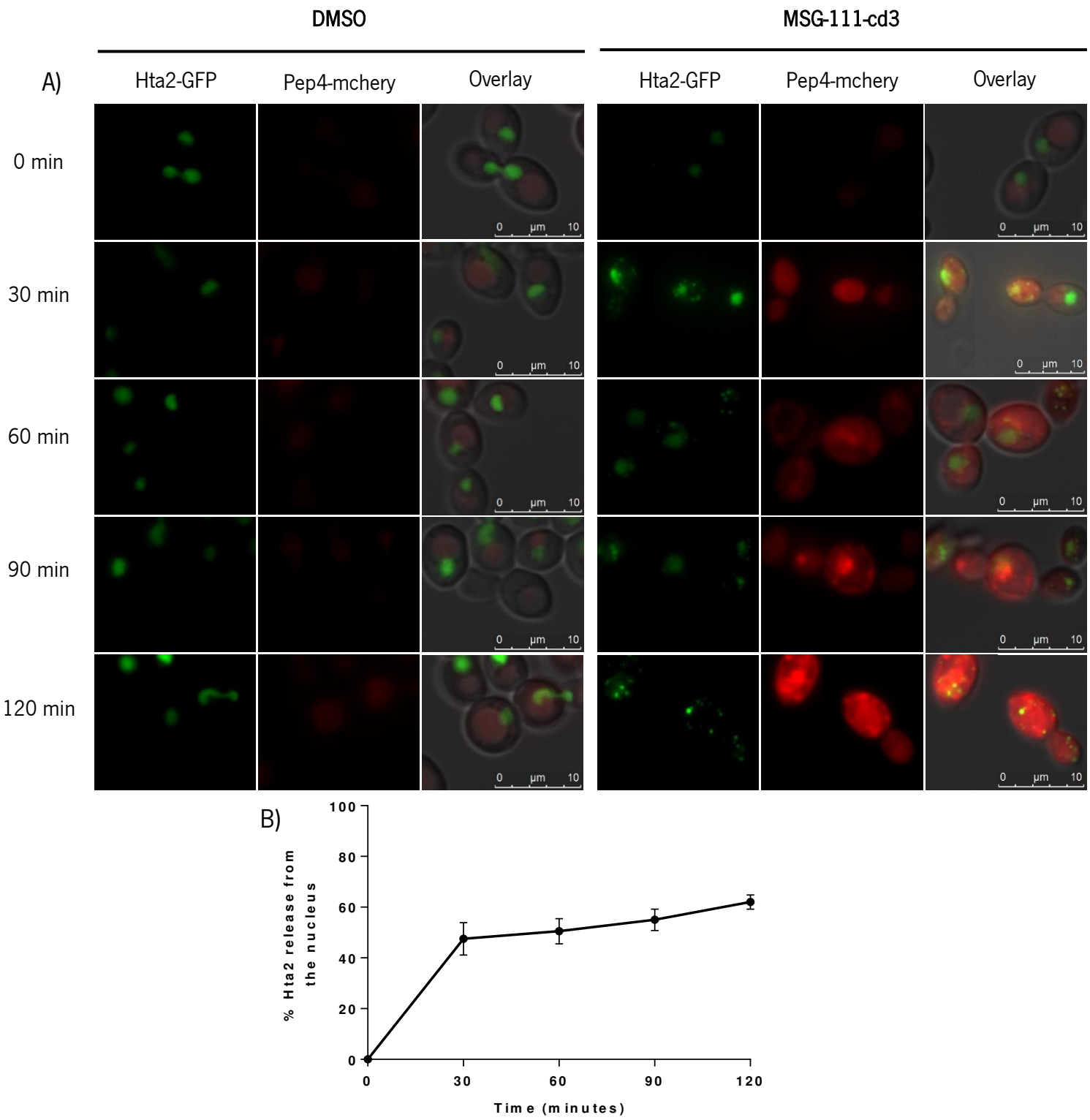

Figure 25 – Effect of MSG-111-cd3 on Hta2p localization. A) Florescence microscopy images of MEY 337 cells after treatment with MSG-111-cd3 (300 µM) and DMSO (0.35%). Samples were collected at different time points, before (time 0) and after 30, 60, 90 and 120 minutes of treatment and then visualized by epifluorescence microscopy with a 100x oil immersion objective. **B)** Percentage of MSG-111-cd3 treated cells displaying Hta2p nuclear release. The reported values are means with SD (n≥2). At least 300 cells were counted for each condition.

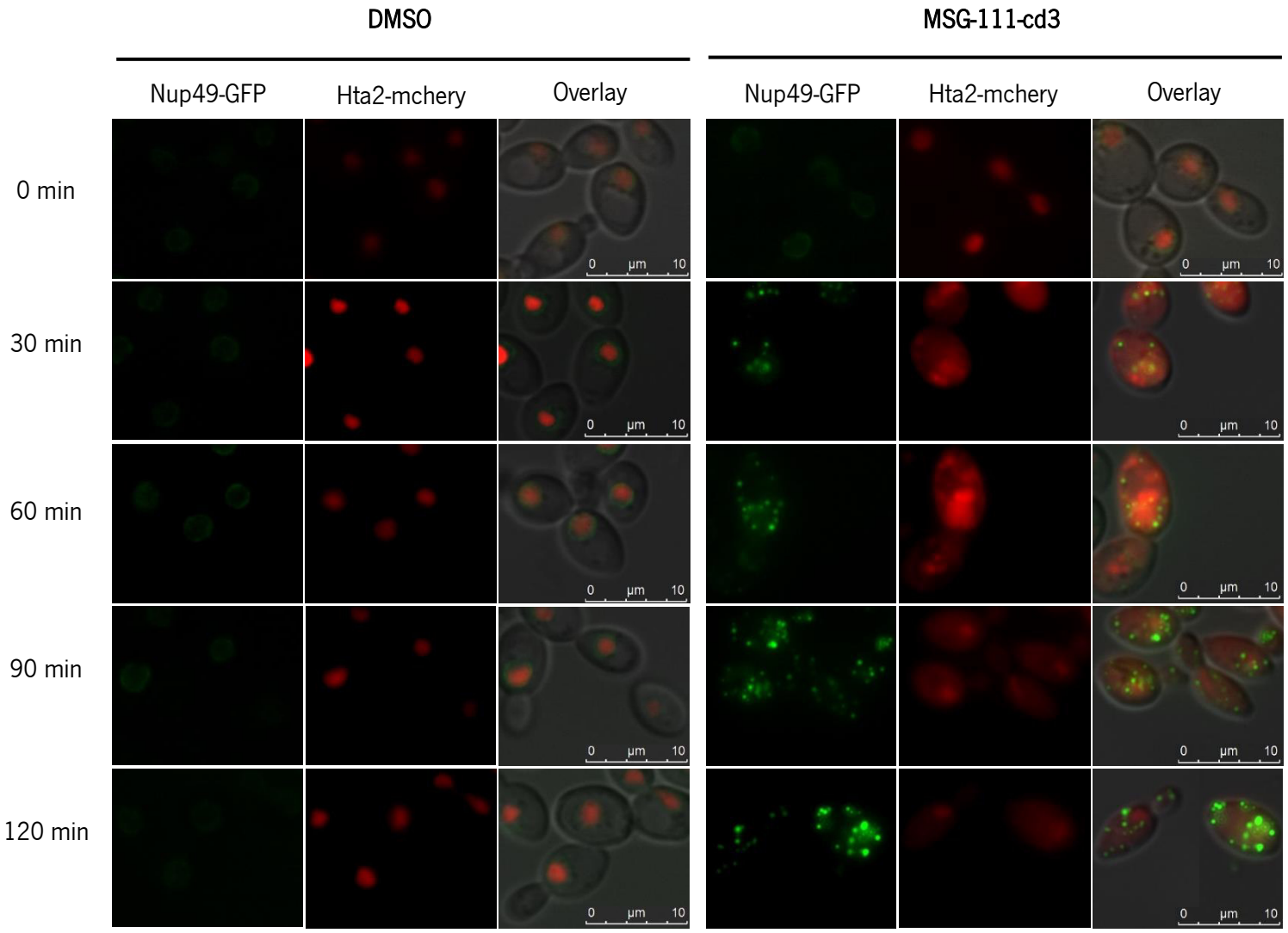

Figure 26 – Effect of MSG-111-cd3 on nuclear envelope organization. Florescence microscopy images of SCY 363 cells after treatment with MSG-111-cd3 (300 µM) and DMSO (0.35%). Samples were collected at different time points, before (time 0) and after 30, 60, 90 and 120 minutes of treatment and then visualized by epifluorescence microscopy with a 100x oil immersion objective.

5. Discussion and Future perspectives

The enormous potential in the use of phenoxazine derivatives as antimicrobial and antitumor agents has stimulated research in this area. In the past years our group have synthesized several Benzo[*a*]phenoxazine compounds, and have found their interesting potential to be used as antifungal agents (Frade *et al.*, 2007, 2008). Among those, MSG-111-cd3 have attracted our interest due to its high antifungal activity. So, in the present work we continue the work made so far in the characterization of the *S. cerevisiae* cell death induced by MSG-111-cd3.

As referred in the above sections, in a previous work (Lopes, 2015) we identified the pepsin-like aspartic protease (Pep4p) as an important protein in the *S. cerevisiae* cell death induced by MSG-111-cd3. The function of this protein in different cell death processes is ambiguous, since depending on the stimulus, it can either have an effector or a protective role. A protective role has been evidenced by the studies performed by Mason group which observed that during H_2O_2-induced apoptosis Pep4p translocates from the vacuole to the cytosol where it degrades the nucleoporins (Mason *et al.*, 2005). Oppositely, Pereira group observed that in acetic acid induced apoptosis the translocation of Pep4p to the cytosol has a protective role (Pereira *et al.*, 2010).

In the present work, we were able to clarify the role of Pep4p in the cell death process induced by MSG-111-cd3, as we observed that a strain lacking Pep4p is significantly more resistance to the compound effects (figure 10A). Furthermore, using strains lacking Pep4p and transformed with different plasmids, pESC-Pep4p(FL), pESC-DPM-Pep4p and pESC(Ø), we were able to revert the resistance phenotype and find out that the catalytic activity of this protein is important for its effect, although the catalytic inactive Pep4p can still partially revert some of the resistance of pep4 deletion strain (figure 10B). These results gave further insights on the role of Pep4p in the process, reinforcing that this protein has an effector role in the cell death induced by the compound. Similar results have also been obtained in cell lines, were the depletion Pep4p mammalian homolog, cathepsin D, inhibit or delayed cell death events (Deiss *et al.*, 1996; Castino *et al.*, 2007).

Our results have also shown that right after 30 minutes of MSG-111-cd3 treatment the vacuolar Pep4p translocates to the cytosol, distributing throughout the cell and leading to the appearance of small spots (figure 12A). Furthermore, the Pep4p translocation was consistent with the observed vacuolar permeabilization, assessed by CMAC staining (figure 12A and B). These observations are in agreement with Lopes' study (Lopes, 2015), and show that the vacuole is highly susceptibility to MSG-

111-cd3. In the future, it would be interesting to analyze the involvement of other vacuolar proteases and assess their possible translocation from the vacuole to the cytosol, to evaluate the extent of vacuolar permeabilization.

As referred above, benzophenoxazine derivatives can exert their antiproliferative activity, by the interaction with DNA, forming hydrogen bounds and π–π stacking interactions, disrupting the DNA normal function (Bolognese *et al.*, 2002). Several studies have demonstrated the great versatility of this type of compounds. In fact, reports show that they are also capable of suffering metabolic conversion in free radical intermediates, leading to oxidative stress and DNA damage. Furthermore, some phenoxazines derivatives induce apoptotic cell death both in a caspase-dependent and independent manner (Abe *et al.*, 2001; Shirato *et al.*, 2007; Pal *et al.*, 2015), whereas other derivatives can lead to a cell death with little or no apoptotic characteristics (Suzuki *et al.*, 2007).

However, there are no reports on the literature regarding vacuole/lysosome permeabilization induced by phenoxazine derivatives. So to our knowledge, the work carried out by our group, previous observations (Carvalho, 2011) and the present thesis, demonstrates by the first time the involvement of vacuolar permeabilization, vacuole membrane disorganization and Pep4p activity in the cell death process induced by a compound of this class.

The consequences of vacuole/lysosome permeabilization are well documented in literature. These "suicide bags" as described by Christian de Duve (De Duve and Wattiaux, 1966), possess a high amount of proteases that when in the cytosol are responsible for the activation of apoptotic effectors such as caspases and mitochondria that signal programed cell death. On the other hand, when LMP is extensive it can lead to widespread hydrolysis in the cytoplasm, which causes non-programmed cell necrosis (Guicciardi *et al.*, 2004). However, the existence of a necrotic process seems unlikely in our case, as no loss of plasma membrane integrity was observed (figure 17). As mentioned above, in the previous works, we already assessed several cell death markers such as ROS accumulation, chromatin condensation and nuclear release of Nhp6Ap (Ferreira, 2014; Lopes, 2015), but we were unable to observe a clear apoptotic or necrotic phenotype. Considering these observations and with the objective to further clarify the cell death process induced by this benzo[*a*]phenoxazine we assessed several other cell death markers.

Research during the past several decades has provided convincing evidence for a crucial role of calcium (Ca^{2+}) signaling in cell death (Zhivotovsky and Orrenius, 2011). Furthermore, calcium signaling is involved in lysosome/vacuole permeabilization. Some reports show that calcium accumulation affects the lysosomal membrane stability by calpain activation and affects the osmotic stability of lysosomes by the activation of cytosolic lipases (Orrenius *et al.*, 2003). However, and in spite of the vacuole permeabilization observed in the MSG-111-cd3 treated cells, we did not find substantial alterations in the calcium levels, so the involvement of calcium signaling in this process seems unlikely.

Similar conclusions could be drawn for one of the most prominent markers in apoptotic processes, the DNA fragmentation. Using TUNEL assay we could only observed a residual percentage of cells displaying DNA fragmentation that did not reach more than 1% of the total cells.

Mitochondria prominent role in programed cell death is thoroughly reported. They exist as dynamic interconnected networks, that are constantly fusing and dividing. More recently, researchers find out that mitochondrial morphology has an important role in the cell function control and in cell death. In fact, in some cell death scenarios, during the early stages of apoptosis, prior to caspase activation and at the time of cytochrome *c* release, mitochondrial network fragmentation occurs, resulting in the appearance of numerous and smaller mitochondria (Suen *et al.*, 2008). Resorting to a strain expressing a mitochondrial-GFP protein, we were able to observe that the initially interconnected mitochondrial network became totally disrupted when the cells were treated with MSG-111-cd3 (figure 15).

Mitochondria network fragmentation is usually accompanied by mitochondrial dysfunction, characterized by loss of membrane potential, permeabilization of the mitochondrial outer membrane, cytochrome *c* release and ROS accumulation (Du *et al.*, 2008; Pereira *et al.*, 2010). So, with the objective to assess alterations that could indicate the involvement of mitochondria in the cell death process, we evaluated if the MSG-111-cd3 leads to any alteration of the mitochondrial membrane potential. We could observed the occurrence of mitochondrial membrane depolarization, but only in a small percentage of cells, that did not exceed more than 23% of the total cells. Indeed, loss of mitochondrial membrane potential may be an early event in an apoptotic process. However, depending on the system analyzed and on the cell death stimulus, the decreases in the mitochondrial membrane

potential may also be a consequence of the signaling pathway (Ly *et al.*, 2003). In this case, since mitochondrial depolarization is present only in a small percentage of cells, significant inferior to the percentage of cell that lost viability, this potential change seems to be a consequence and not determinant for the cell death process.

In the present work, the fact that we did not observed alterations at the level of calcium concentration, an important messenger between the endoplasmic reticulum and mitochondria in programed cell death events (Austriaco Nicanor, 2012) also argues against the mitochondrial involvement. In addition, only a low accumulation of mitochondria ROS has previously been observed (Lopes, 2015). As a whole the results suggest that the MSG-111-cd3 effects on mitochondria appear to be a consequence of the cell death process and perhaps a consequence of the vacuolar permeabilization.

However, we can not ignore the high percentage of mitochondria fragmentation. In fact, several studies show that depending on the cell death stimulus, the deletion of mitochondrial fission factors such as Dnm1p, Mdv1p and Fis1p results in increased resistance against various cell death effectors (Braun and Westermann, 2011). So, to confirm that the mitochondrial network fragmentation is a consequence of the process or has a role in its mediation, it will be necessary to address the effect of the compound in strains lacking these proteins. Besides, it will be interesting to analyze other possible alterations involving the mitochondria, such as mitochondrial membrane permeabilization and cytochrome *c* release.

Since we did not observe a clear necrotic or apoptotic phenotype, we questioned the potential involvement of the autophagy machinery in the cell death process. In the previous work, using an autophagic mutant strain *Δatg1*, we observed that this serine-threonine kinase, that is involved in the formation of the autophagosomal membranes (Papinski *et al.*, 2014), does not seem to have a role in the cell death induced by MSG-111-cd3 (Lopes, 2015).

To further address autophagy occurrence, and knowing that during autophagy Atg8p is incorporated in the autophagosomes and delivered to the vacuole lumen where it is degraded by vacuolar hydrolases (Shpilka *et al.*, 2011; Nakatogawa *et al.*, 2012), we evaluated the processing and localization of a GFP-ATG8 fusion protein in *S. cerevisiae* cells treated with the compound. Resorting

to this analysis, we confirmed that the cell death process does not involve the autophagy machinery. Furthermore, by adding the autophagy inducer rapamycin and MSG-111-cd3 simultaneously to *S. cerevisiae* cells, we found out that MSG-111-cd3 blocks autophagy induction, since after 60 minutes of treatment we did not observe the green labeling in the vacuole. This result is not surprising, since one consequence of lysosomal/vacuole permeabilization is autophagy blockade and autophagosome accumulation (Serrano-Puebla and Boya, 2016). In fact, initially we thought that the GFP green spots in the cytosol corresponded to autophagosome accumulation, however, the western blot analysis does not support this hypothesis. This is not the first report of autophagy blockade by a phenoxazine compound, since Suzuki *et al.* showed that two phenoxazine derivatives the VM7 and VM8 inhibited autophagosome formation and induced cell death on tumor cells and normal human cells by a process with little apoptotic features (Suzuki *et al.*, 2007).

As mentioned above, in the characterization of the MSG-111-cd3 cell death we accessed several cell death markers, among them, the nuclear release of the yeast HMGB1 orthologue Nhp6Ap, a well-known necrotic marker. However, we observed a different release pattern from the one described for necrotic processes (Gardella *et al.*, 2002; Eisenberg *et al.*, 2009; Santos *et al.*, 2012). Instead of a uniformly dispersed localization of Nhp6Ap, the MSG-111-cd3 treatment lead to a punctuated disposition of the protein (figure 20). Furthermore, in a preliminary assay, we observed that Nhp6Ap nuclear release is dependent from the Pep4p protein (Lopes, 2015). These observations not only reinforced the role of Pep4p in the cell death process, but also suggested that Nhp6Ap could have a crucial role in the cell death mechanism induced by this benzophenoxazine.

Following these results, we investigated if the cell death process is dependent of Nhp6Ap, using a strain deficient in this protein and assessing cell viability in response to MSG-111-cd3. However, the deficient strain showed the same behavior as the wild type strain suggesting that Nhp6Ap is not essential for the cell death process. This result is not surprising, since *S. cerevisiae* possess 7 HMGB like proteins (Kolodrubetz and Burgum, 1990; Bustin, 2001), among them Nhp6Bp, a paralog of Nhp6Ap, that can substitute the potential role of Nhp6Ap in the cell death process. So, to confirm this hypothesis it will be necessary to investigate at least the effect of a double deletion of Nhp6Ap and Nhp6Bp in the cell death process.

The release pattern of Nhp6Ap is very intriguing, firstly because its nuclear release is usually observed in necrotic processes, which is not the case, and secondly due to its punctuated disposition in the cytosol. So, we first consider that this disposition could be caused by the encapsulation of Nhp6Ap in a vesicular structure. As referred above, several studies have shown that in cell activation, such as monocytes and macrophages activated by LPS, the mammalian HMGB1 can suffer several prost-translation modifications such as phosphorylation, acetylation and methylation that result in the loss of chromatin adherence and subsequent protein encapsulation in lysosomes that are released to the extracellular medium (Gardella *et al.*, 2002; Bonaldi *et al.*, 2003). In our case we did not assess Nhp6Ap extracellular release, however, the cytosolic punctuated disposition could be caused by a similar encapsulation process. Nevertheless, this cannot be achieved through the Endoplasmic reticulum–Golgi secretory pathway, since Nhp6Ap does not possess the peptide secretion signal that allow the encapsulation of this protein through this pathway (Lee *et al.*, 2004). So, we question the involvement of the endosomal machinery, in this case the involvement of the multivesicular body (MVB) pathway, in the Nhp6Ap punctuated disposition.

MVBs or multivesicular endosomes are formed through invaginations of the plasma membrane that result in early endosomes, the limiting membrane of early endosomes invaginates and buds into its own lumen, by a process that is regulated by the endosomal sorting complexes required for transport (ESCRT). The ESCRT machinery, which is composed by ESCRT-0, -I, -II and -III, assists in sorting ubiquitinated proteins into the early endosomes of multivesicular endosomes for degradation in the lysosome/vacuole or for the fusion with the plasmatic membrane and the extracellular release of MVBs (Piper and Katzmann, 2007; Schmidt and Teis, 2012). So, to assess if Nhp6Ap is being encapsulated in MVBs through a process depend on the ESCRT machinery, we used two strains without two of its proteins, a strain without Stp22p a protein required for the ESCRT I, and a strain without Snf7p required for the ESCRT III, and we assessed the effect in the Nhp6Ap localization. In fact, the results obtained leave no doubt, that the MSG-111-cd3 is not leading to Nhp6Ap vesicular encapsulation at least through this pathway. Additionally, once our results show that MSG-111-cd3 does not induces autophagy and even inhibits its induction an encapsulation through the autophagic pathway is also unlikely.

To get further insights into the mechanism of release of Nhp6A, we next assessed the specificity of the release and the effects of MSG-111-cd3 on the nuclear envelope. We observed that

the histone Hta2p presents the same release phenotype as the Nhp6Ap protein. However, the release was significant lower in comparison to Nhp6Ap, which may result from a stronger association of the histone to DNA. Monitoring the behavior of the nuclear pore complex protein (nucleoporin) Nup49p, we observed that the nuclear envelope became disorganized, since in response to MSG-111-cd3 this protein changed from its distribution delineating the nucleus to a localization in granules, similar to the Nhp6Ap. Similar effects were observed in Lopes work, for Vba1p, a protein from the vacuolar membrane (Lopes, 2015). So, MSG-111-cd3 seems to affect the nuclear envelope similarly to the observed for the vacuolar membrane.

Mason *et al* observed that the permeability of yeast nuclear envelope increased during H_2O_2-induced cell death and that in this process Pep4p migrated out of the vacuole and degraded specific nucleoporins (Mason *et al.*, 2005). Considering the Pep4p role in MSG-111-cd3–induced cell death and the delay and decrease of the Nhp6Ap nuclear release in a the strain defective in Pep4p (Lopes, 2015), it seemed likely that the observed nuclear effects, could result from a similar process to that observed during H_2O_2-induced cell death. To test this hypothesis, we investigate the dependency of Hta2p release and nuclear envelope disorganization on Pep4p. We attempted to observe this effect by treating the MEY 337 and SCY 363 strains, expressing Hta2-GFP and/or Nup49-GFP, with the serine protease inhibitor PMSF (Phenylmethylsulfonyl fluoride) which is an inhibitor of the proteolytic activity of Pep4p (Swaminathan and Sunnerhagen, 2005). However, the effect of PMSF on the distribution of the proteins was null. In the future, it will be necessary to address this hypothesis using a strain without Pep4p, since we could not confirm that the PMSF was effectively inhibiting the catalytic activity of Pep4p, and even if it where, our cell viability results show that the catalytic activity of this protein is important for its effect, but not absolutely required.

Our results show that MSG-111-cd3 induces a common phenotype for several proteins, that organize in a punctuated disposition right after the treatment with the compound. A possible co-localization between the different proteins could be evaluated taking advantage of the information provided by the MEY 337 strain that genomically express both Hta2-GFP and a Pep4p-mchery. However, the red florescence provided by the compound compromised the Pep4p-mchery fluorescence and did not allowed this analysis.

Future studies will be needed to confirm if these proteins actually co-localize. Since our results seem to discard the potential encapsulation of proteins in vesicles, one possibility is that the compound induces protein aggregation, perhaps in aggresome-like structures. However, future analysis is necessary to assess this possibility.

This study provided new insights regarding the *S. cerevisiae* cell death induced by MSG-111-cd3 that are summarized in figure 27. Overall, the results obtained in this work confirm the relevance of vacuolar permeabilization in the cell death process, showing prominent role of Pep4p. Furthermore, we confirmed that autophagy is not involved in the cell death process and apparently this process is independent of the mitochondrial pathway. However, our results show that the nucleus is very susceptible to the effect of the MSG-111-cd3, since the treatment lead to nuclear envelope disorganization and subsequent cytosolic localization of DNA binding proteins.

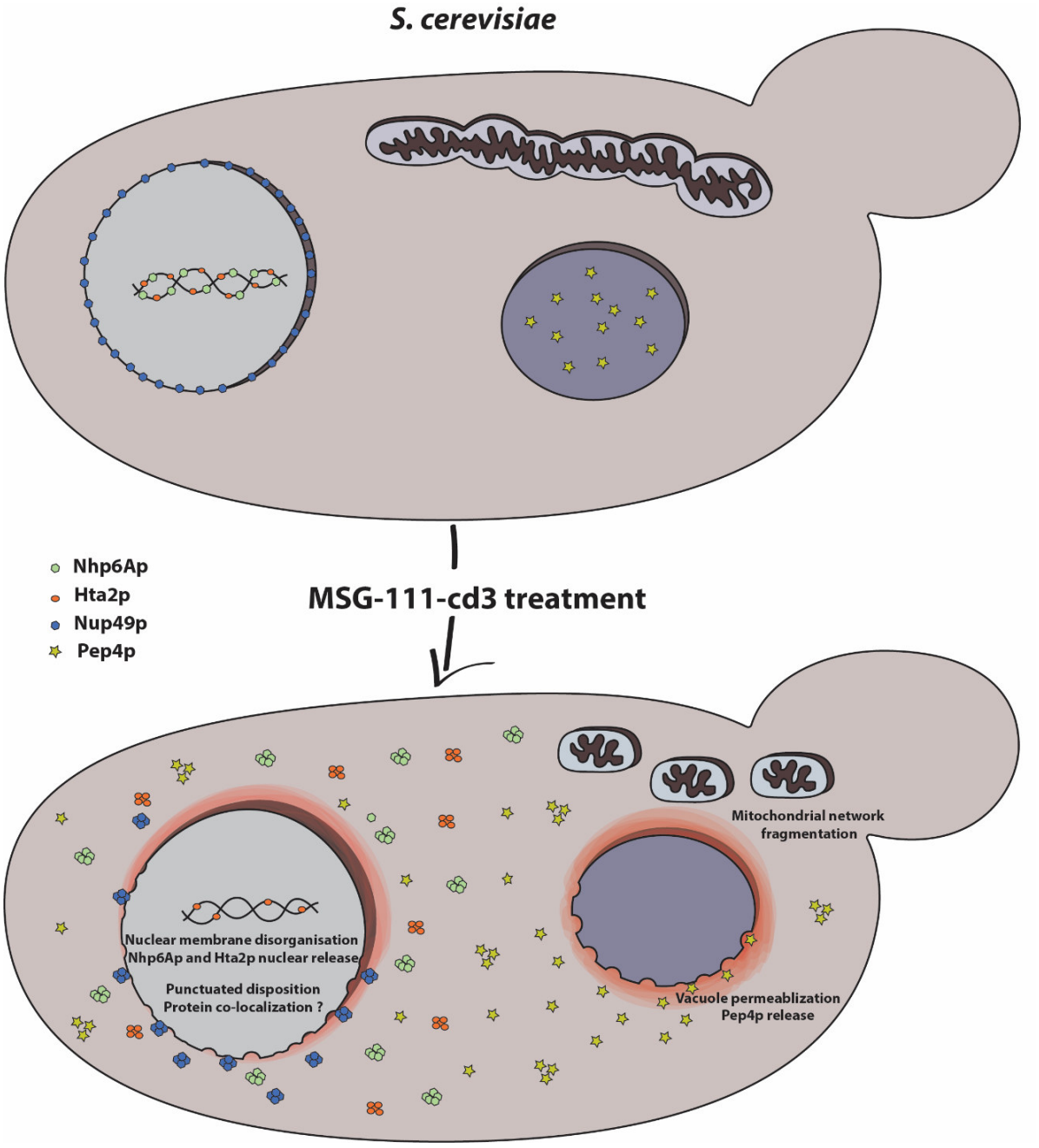

Figure 27 – Effects of MSG-111-cd3 in *S. cerevisiae*. MSG-111-cd3 has a prominent effect both on vacuole and nucleus. In the vacuole, the treatment results in vacuolar permeabilization and consequent translocation of Pep4p to the cytosol. In the nucleus, the effect is similar, since the compound leads to the cytosolic translocation of Nhp6Ap and Hta2p, presenting a punctuated disposition. Furthermore, MSG-111-cd3 has an effect in the nuclear envelope similar to the one observed to the vacuolar membrane in previous works. The nuclear envelope becomes disorganized in response to MSG-111-cd3, characterized by the change of Nup49p distribution, delineating the nucleus, to a localization in granules. Mitochondrial network fragmentation is also caused by MSG-111-cd3 however, this effect appears to be only a consequence of the cell death process.

6. References

Abe, A., Yamane, M., and Tomoda, A. (2001). Prevention of growth of human lung carcinoma cells and induction of apoptosis by a novel phenoxazinone, 2-amino-4,4alpha-dihydro-4alpha,7-dimethyl-3H-phenoxazine-3-one. Anticancer. Drugs *12*, 377–382.

Abeliovich, H., and Klionsky, D. J. (2001). Autophagy in Yeast: Mechanistic Insights and Physiological Function. Microbiol. Mol. Biol. Rev. *65*, 463–479.

Alberti, A., Bolognese, A., Guerra, M., Lavecchia, A., Macciantelli, D., Marcaccio, M., Novellino, E., and Paolucci, F. (2003). Antitumor agents 4. Characterization of free radicals produced during reduction of the antitumor drug 5H-pyridophenoxazin-5-one: an EPR study. Biochemistry *42*, 11924–11931.

Andersson, U. *et al.* (2000). High mobility group 1 protein (HMG-1) stimulates proinflammatory cytokine synthesis in human monocytes. J. Exp. Med. *192*, 565–570.

Aravind, L., Dixit, V. M., and Koonin, E. V (2001). Apoptotic molecular machinery: vastly increased complexity in vertebrates revealed by genome comparisons. Sci. (New York, NY) *291*, 1279–1284.

Austriaco Nicanor, O. P. (2012). Endoplasmic reticulum involvement in yeast cell death. Front. Oncol. *2*, 87.

Baehrecke, E. H. (2002). How death shapes life during development. Nat. Rev. Mol. Cell Biol. *3*, 779–787.

Baehrecke, E. H. (2005). Autophagy: dual roles in life and death? Nat. Rev. Mol. Cell Biol. *6*, 505–510.

Barkla, D. H., and Gibson, P. R. (1999). The fate of epithelial cells in the human large intestine. Pathology *31*, 230–238.

Bell, C. W., Jiang, W., Reich, C. F., and Pisetsky, D. S. (2006). The extracellular release of HMGB1 during apoptotic cell death. Am. J. Physiol. Cell Physiol. *291*, C1318–C1325.

Benes, P., Vetvicka, V., and Fusek, M. (2008). Cathepsin D–many functions of one aspartic protease. Crit. Rev. Oncol. Hematol. *68*, 12–28.

Beyer, C., Stearns, N. A., Giessl, A., Distler, J. H. W., Schett, G., and Pisetsky, D. S. (2012). The extracellular release of DNA and HMGB1 from Jurkat T cells during in vitro necrotic cell death. Innate Immun. *18*, 727–737.

Bianchi, M. E. (2007). DAMPs, PAMPs and alarmins: all we need to know about danger. J. Leukoc. Biol. *81*, 1–5.

Bianchi, M. E., and Agresti, A. (2005). HMG proteins: Dynamic players in gene regulation and differentiation. Curr. Opin. Genet. Dev. *15*, 496–506.

Blomgran, R., Zheng, L., and Stendahl, O. (2007). Cathepsin-cleaved Bid promotes apoptosis in human neutrophils via oxidative stress-induced lysosomal membrane permeabilization. J. Leukoc. Biol. *81*, 1213–1223.

Bolognese, A., Correale, G., Manfra, M., Lavecchia, A., Mazzoni, O., Novellino, E., Barone, V., La Colla, P., and Loddo, R. (2002). Antitumor agents. 2. Synthesis, structure - Activity relationships, and

biological evaluation of substituted 5H-pyridophenoxazin-5-ones with potent antiproliferative activity. J. Med. Chem. *45*, 5217–5223.

Bolognese, A., Correale, G., Manfra, M., Lavecchia, A., Novellino, E., and Pepe, S. (2006). Antitumor agents. 5. Synthesis, structure - activity relationships, and biological evaluation of dimethyl-5H-pyridophenoxazin-5-ones, tetrahydro-5H-benzopyridophenoxazin-5-ones, and 5H-benzopyridophenoxazin-5-ones with potent antiproliferative activity. J. Med. Chem. *49*, 5110–5118.

Bonaldi, T., Talamo, F., Scaffidi, P., Ferrera, D., Porto, A., Bachi, A., Rubartelli, A., Agresti, A., and Bianchi, M. E. (2003). Monocytic cells hyperacetylate chromatin protein HMGB1 to redirect it towards secretion. EMBO J. *22*, 5551–5560.

Boya, P. *et al.* (2005). Inhibition of macroautophagy triggers apoptosis. Mol. Cell. Biol. *25*, 1025–1040.

Boya, P., Andreau, K., Poncet, D., Zamzami, N., Perfettini, J.-L., Metivier, D., Ojcius, D. M., Jäättelä, M., and Kroemer, G. (2003). Lysosomal membrane permeabilization induces cell death in a mitochondrion-dependent fashion. J. Exp. Med. *197*, 1323–1334.

Boya, P., and Kroemer, G. (2008). Lysosomal membrane permeabilization in cell death. Oncogene *27*, 6434–6451.

Boya, P., Reggiori, F., and Codogno, P. (2013). Emerging regulation and functions of autophagy. Nat Cell Biol *15*, 713–720.

Braun, R. J., and Westermann, B. (2011). Mitochondrial dynamics in yeast cell death and aging. Biochem. Soc. Trans. *39*, 1520–1526.

Bursch, W. (2001). The autophagosomal-lysosomal compartment in programmed cell death. Cell Death Differ. *8*, 569–581.

Bustin, M. (2001). Revised nomenclature for high mobility group (HMG) chromosomal proteins. Trends Biochem. Sci. *26*, 152–153.

Buttner, S. *et al.* (2007). Endonuclease G regulates budding yeast life and death. Mol. Cell *25*, 233–246.

Carmona-Gutierrez, D., Eisenberg, T., Büttner, S., Meisinger, C., Kroemer, G., and Madeo, F. (2010a). Apoptosis in yeast: triggers, pathways, subroutines. Cell Death Differ. *17*, 763–773.

Carmona-Gutierrez, D., Ruckenstuhl, C., Bauer, M., Eisenberg, T., Bü Ttner, S., and Madeo, F. (2010b). Cell death in yeast: growing applications of a dying buddy. Cell Death Differ. *17*, 733–734.

Carvalho, R. E. S. (2011). Staining pattern and potential targets of a benzo[a]phenoxazinium chloride with antiproliferative activity. University of Minho.

Castino, R., Bellio, N., Nicotra, G., Follo, C., Trincheri, N. F., and Isidoro, C. (2007). Cathepsin D-Bax death pathway in oxidative stressed neuroblastoma cells. Free Radic. Biol. Med. *42*, 1305–1316.

Celona, B. *et al.* (2011). Substantial Histone reduction modulates Genomewide nucleosomal occupancy and global transcriptional output. PLoS Biol. *9*.

Choi, J. J., Reich, C. F., and Pisetsky, D. S. (2005). The role of macrophages in the in vitro generation of extracellular DNA from apoptotic and necrotic cells. Immunology *115*, 55–62.

Cohen, G. M., Sun, X. M., Fearnhead, H., MacFarlane, M., Brown, D. G., Snowden, R. T., and Dinsdale, D. (1994). Formation of large molecular weight fragments of DNA is a key committed step of apoptosis in thymocytes. J. Immunol. *153*, 507–516.

Coughlan, C. M., and Brodsky, J. L. (2003). Yeast as a model system to investigate protein conformational diseases. Methods Mol. Biol. *232*, 77–90.

Deiss, L. P., Galinka, H., Berissi, H., Cohen, O., and Kimchi, A. (1996). Cathepsin D protease mediates programmed cell death induced by interferon-gamma, Fas/APO-1 and TNF-alpha. EMBO J. *15*, 3861–3870.

Denton, D., Nicolson, S., and Kumar, S. (2012). Cell death by autophagy: facts and apparent artefacts. Cell Death Differ *19*, 87–95.

Deretic, V., and Levine, B. (2009). Autophagy, immunity, and microbial adaptations. Cell Host Microbe *5*, 527–549.

Droga-Mazovec, G., Bojic, L., Petelin, A., Ivanova, S., Romih, R., Repnik, U., Salvesen, G. S., Stoka, V., Turk, V., and Turk, B. (2008). Cysteine cathepsins trigger caspase-dependent cell death through cleavage of bid and antiapoptotic Bcl-2 homologues. J. Biol. Chem. *283*, 19140–19150.

Du, L., Su, Y., Sun, D., Zhu, W., Wang, J., Zhuang, X., Zhou, S., and Lu, Y. (2008). Formic acid induces Yca1p-independent apoptosis-like cell death in the yeast Saccharomyces cerevisiae. FEMS Yeast Res. *8*, 531–539.

De Duve, C., and Wattiaux, R. (1966). Functions of lysosomes. Annu. Rev. Physiol. *28*, 435–492.

Duve, D. E. (1967). L. D E T E R and C H R I S T I A N DE DUVE From The Rockefeller University, New York.

Eisenberg, T. *et al.* (2009). Induction of autophagy by spermidine promotes longevity. Nat. Cell Biol. *11*, 1305–1314.

Eisenberg, T., Carmona-Gutierrez, D., Büttner, S., Tavernarakis, N., and Madeo, F. (2010). Necrosis in yeast. Apoptosis *15*, 257–268.

Eskelinen, E. L. (2006). Roles of LAMP-1 and LAMP-2 in lysosome biogenesis and autophagy. Mol. Aspects Med. *27*, 495–502.

Eskelinen, E.-L., Tanaka, Y., and Saftig, P. (2003). At the acidic edge: emerging functions for lysosomal membrane proteins. Trends Cell Biol. *13*, 137–145.

Ferreira, J. C. C. (2014). Envolvimento da proteína HMGB1 na morte induzida pela Benzofenoxazina MSG-111-cd3. Universidade do Minho.

Frade, V. H. J., Sousa, M. J., Moura, J. C. V. P., and Gonçalves, M. S. T. (2007). Synthesis, characterisation and antimicrobial activity of new benzo[a]phenoxazine based fluorophores. Tetrahedron Lett. *48*, 8347–8352.

Frade, V. H. J., Sousa, M. J., Moura, J. C. V. P., and Gonçalves, M. S. T. (2008). Synthesis of naphtho[2,3-a]phenoxazinium chlorides: Structure-activity relationships of these heterocycles and benzo[a]phenoxazinium chlorides as new antimicrobials. Bioorganic Med. Chem. *16*, 3274–3282.

Galluzzi, L. *et al.* (2009a). Guidelines for the use and interpretation of assays for monitoring cell death in higher eukaryotes. Cell Death Differ. *16*, 1093–1107.

Galluzzi, L. *et al.* (2012). Molecular definitions of cell death subroutines: recommendations of the Nomenclature Committee on Cell Death 2012. Cell Death Differ. *19*, 107–120.

Galluzzi, L., Blomgren, K., and Kroemer, G. (2009b). Mitochondrial membrane permeabilization in neuronal injury. Nat. Rev. Neurosci. *10*, 481–494.

Galluzzi, L., Maiuri, M. C., Vitale, I., Zischka, H., Castedo, M., Zitvogel, L., and Kroemer, G. (2007). Cell death modalities: classification and pathophysiological implications. Cell Death Differ. *14*, 1237–1243.

Gardella, S., Andrei, C., Ferrera, D., Lotti, L. V., Torrisi, M. R., Bianchi, M. E., and Rubartelli, A. (2002). The nuclear protein HMGB1 is secreted by monocytes via a non-classical, vesicle-mediated secretory pathway. EMBO Rep. *3*, 995–1001.

Gerlitz, G., Hock, R., Ueda, T., and Bustin, M. (2009). The dynamics of HMG protein-chromatin interactions in living cells. Biochem. Cell Biol. *87*, 127–137.

Golstein, P., and Kroemer, G. (2007). Cell death by necrosis: towards a molecular definition. Trends Biochem. Sci. *32*, 37–43.

Green, D. R., Ferguson, T., Zitvogel, L., and Kroemer, G. (2009). Immunogenic and tolerogenic cell death. Nat. Rev. Immunol. *9*, 353–363.

Greenwood, M. T., and Ludovico, P. (2010). Expressing and functional analysis of mammalian apoptotic regulators in yeast. Cell Death Differ. *17*, 737–745.

Guicciardi, M. E., Leist, M., and Gores, G. J. (2004). Lysosomes in cell death. Oncogene *23*, 2881–2890.

Hardman, C. H., Broadhurst, R. W., Raine, a R., Grasser, K. D., Thomas, J. O., and Laue, E. D. (1995). Structure of the A-domain of HMG1 and its interaction with DNA as studied by heteronuclear three- and four-dimensional NMR spectroscopy. Biochemistry *34*, 16596–16607.

Hartwell, L. H. (2004). Yeast and Cancer. Biosci. Rep. *24*, 523–544.

Hendrzak-Henion, J. A., Knisely, T. L., Cincotta, L., Cincotta, E., and Cincotta, A. H. (1999). Role of the immune system in mediating the antitumor effect of benzophenothiazine photodynamic therapy. Photochem. Photobiol. *69*, 575–581.

Ichinose, S. *et al.* (2006). Lysosomal cathepsin initiates apoptosis, which is regulated by photodamage to Bcl-2 at mitochondria in photodynamic therapy using a novel photosensitizer, ATX-s10 (Na). Int. J. Oncol. *29*, 349–355.

Jacobson, M., Weil, M., and Raff, M. (1997). Programmed cell death in animal development. Cell *88*,

347–354.

Jose, J., and Burgess, K. (2006). Syntheses and properties of water-soluble Nile Red derivatives. J. Org. Chem. *71*, 7835–7839.

Kagedal, K., Johansson, A.-C., Johansson, U., Heimlich, G., Roberg, K., Wang, N. S., Jurgensmeier, J. M., and Ollinger, K. (2005). Lysosomal membrane permeabilization during apoptosis–involvement of Bax? Int. J. Exp. Pathol. *86*, 309–321.

Kagedal, K., Zhao, M., Svensson, I., and Brunk, U. T. (2001). Sphingosine-induced apoptosis is dependent on lysosomal proteases. Biochem. J. *359*, 335–343.

Kaminska, G. M., Niederkorn, J. Y., Murphy, R. B., Chader, J., Chader, J., Schwartz, J. P., Cristofalo, J., and Gillis, P. (1999). HMG-1 as a Late Mediator of Endotoxin Lethality in Mice. *285*, 248–251.

Kerr, J. F., Wyllie, A. H., and Currie, A. R. (1972). Apoptosis: a basic biological phenomenon with wide-ranging implications in tissue kinetics. Br. J. Cancer *26*, 239–257.

Kim, H., Kim, A., and Cunningham, K. W. (2012). Vacuolar H+-ATPase (V-ATPase) promotes vacuolar membrane permeabilization and nonapoptotic death in stressed yeast. J. Biol. Chem. *287*, 19029–19039.

Klionsky, D. J. (2005). The molecular machinery of autophagy: unanswered questions. J. Cell Sci. *118*, 7–18.

Klionsky, D. J. (2007). Autophagy: from phenomenology to molecular understanding in less than a decade. Nat. Rev. Mol. Cell Biol. *8*, 931–937.

Klionsky, D. J. *et al.* (2016). Guidelines for the use and interpretation of assays for monitoring autophagy (3rd edition). Autophagy *12*, 1–222.

Kolodrubetz, D., and Burgum, A. (1990). Duplicated NHP6 genes of Saccharomyces cerevisiae encode proteins homologous to bovine high mobility group protein 1. J. Biol. Chem. *265*, 3234–3239.

Kolodrubetz, D., Haggren, W., and Burgum, A. (1988). Amino-terminal sequence of a Saccharomyces cerevisiae nuclear protein, NHP6, shows significant identity to bovine HMG1. FEBS Lett. *238*, 175–179.

Krammer, P. H. (2000). CD95's deadly mission in the immune system. Nature *407*, 789–795.

Kroemer, G. *et al.* (2009). Classification of cell death: recommendations of the Nomenclature Committee on Cell Death 2009. Cell Death Differ *16*, 3–11.

Kumar, N., Sharma, A. K., Garg, R., and Yadav, A. K. (2006). Antimicrobial Screening and Synthesis of Some Novel Benzo[a]phenothiazines and Ribofuranosides. ChemInform *37*.

Lange, S. S., Mitchell, D. L., and Vasquez, K. M. (2008). High mobility group protein B1 enhances DNA repair and chromatin modification after DNA damage. Proc. Natl. Acad. Sci. U. S. A. *105*, 10320–10325.

Lee, M. C. S., Miller, E. A., Goldberg, J., Orci, L., and Schekman, R. (2004). Bi-directional protein transport between the ER and Golgi. Annu. Rev. Cell Dev. Biol. *20*, 87–123.

Levine, B., and Klionsky, D. J. (2004). Development by self-digestion: molecular mechanisms and biological functions of autophagy. Dev. Cell *6*, 463–477.

LEWIS, M. R., GOLAND, P. P., and SLOVITER, H. A. (1949). The action of oxazine dyes on tumors in mice. Cancer Res. *9*, 736–740.

Li, C.-N., Hsu, H.-L., Wu, T.-L., Tsao, K.-C., Sun, C.-F., and Wu, J. T. (2003). Cell-free DNA is released from tumor cells upon cell death: a study of tissue cultures of tumor cell lines. J. Clin. Lab. Anal. *17*, 103–107.

Ligr, M., Madeo, F., Fröhlich, E., Hilt, W., Fröhlich, K. U., and Wolf, D. H. (1998). Mammalian Bax triggers apoptotic changes in yeast. FEBS Lett. *438*, 61–65.

Lockshin, R. a., and Williams, C. M. (1964). Programmed cell death—II. Endocrine potentiation of the breakdown of the intersegmental muscles of silkmoths. J. Insect Physiol. *10*, 643–649.

Lockshin, R. a, and Williams, C. M. (1965). Programmed Cell Death–I. Cytology of Degeneration in the Intersegmental Muscles of the Pernyi Silkmoth. J. Insect Physiol. *11*, 123–133.

Lopes, C. (2015). Molecular pathways involved in the yeast cell death induced by a benzo[a]phenoxazine derivative. Universidade do Minho.

Lu, B. *et al.* (2012). Novel role of PKR in inflammasome activation and HMGB1 release. Nature *488*, 670–674.

Ludovico, P., Madeo, F., and Silva, M. (2005). Yeast programmed cell death: an intricate puzzle. IUBMB Life *57*, 129–135.

Ludovico, P., Sousa, M. J., Silva, M. T., Leão, C., and Côrte-Real, M. (2001). Saccharomyces cerevisiae commits to a programmed cell death process in response to acetic acid. Microbiology *147*, 2409–2415.

Luzio, J. P., Pryor, P. R., and Bright, N. a (2007). Lysosomes: fusion and function. Nat. Rev. Mol. Cell Biol. *8*, 622–632.

Ly, J. D., Grubb, D. R., and Lawen, A. (2003). The mitochondrial membrane potential (deltapsi(m)) in apoptosis; an update. Apoptosis *8*, 115–128.

Madeo, F. *et al.* (2002). A caspase-related protease regulates apoptosis in yeast. Mol. Cell *9*, 911–917.

Madeo, F., Fröhlich, E., and Fröhlich, K.-U. (1997). A Yeast Mutant Showing Diagnostic Markers of Early and Late Apoptosis . J. Cell Biol. *139*, 729–734.

Maiuri, M. C., Zalckvar, E., Kimchi, A., and Kroemer, G. (2007). Self-eating and self-killing: crosstalk between autophagy and apoptosis. Nat. Rev. Mol. Cell Biol. *8*, 741–752.

Marques, C., Oliveira, C. S. F., Alves, S., Chaves, S. R., Coutinho, O. P., Corte-Real, M., and Preto, A. (2013). Acetate-induced apoptosis in colorectal carcinoma cells involves lysosomal membrane permeabilization and cathepsin D release. Cell Death Dis. *4*, e507.

Martin, S. J., and Green, D. R. (1995). Protease activation during apoptosis: death by a thousand cuts?

Cell *82*, 349–352.

Mason, D. A., Shulga, N., Undavai, S., Ferrando-May, E., Rexach, M. F., and Goldfarb, D. S. (2005). Increased nuclear envelope permeability and Pep4p-dependent degradation of nucleoporins during hydrogen peroxide-induced cell death. FEMS Yeast Res. *5*, 1237–1251.

Melino, G., Knight, R. A., and Ameisen, J.-C. (2001). The Siren's Song: This Death That Makes Life Live. In: eLS, John Wiley & Sons, Ltd.

Mizushima, N., Levine, B., Cuervo, A. M., and Klionsky, D. J. (2008). Autophagy fights disease through cellular self-digestion. Nature *451*, 1069–1075.

Modjtahedi, N., Giordanetto, F., Madeo, F., and Kroemer, G. (2006). Apoptosis-inducing factor: vital and lethal. Trends Cell Biol. *16*, 264–272.

Motohashi, N., Sakagami, H., Kamata, K., and Yamamoto, Y. (1991). Cytotoxicity and differentiation-inducing activity of phenothiazine and benzo[a]phenothiazine derivatives. Anticancer Res. *11*, 1933–1937.

Muller, S., Ronfani, L., and Bianchi, M. E. (2004). Regulated expression and subcellular localization of HMGB1, a chromatin protein with a cytokine function. J. Intern. Med. *255*, 332–343.

Nakano, A. (2004). Yeast Golgi apparatus–dynamics and sorting. Cell. Mol. Life Sci. *61*, 186–191.

Nakatogawa, H., Ohbayashi, S., Sakoh-Nakatogawa, M., Kakuta, S., Suzuki, S. W., Kirisako, H., Kondo-Kakuta, C., Noda, N. N., Yamamoto, H., and Ohsumi, Y. (2012). The autophagy-related protein kinase Atg1 interacts with the ubiquitin-like protein Atg8 via the Atg8 family interacting motif to facilitate autophagosome formation. J. Biol. Chem. *287*, 28503–28507.

Nemeth, M. J., Curtis, D. J., Kirby, M. R., Garrett-Beal, L. J., Seidel, N. E., Cline, A. P., and Bodine, D. M. (2003). Hmgb3: an HMG-box family member expressed in primitive hematopoietic cells that inhibits myeloid and B-cell differentiation. Blood *102*, 1298–1306.

Nickel, W., and Rabouille, C. (2009). Mechanisms of regulated unconventional protein secretion. Nat. Rev. Mol. Cell Biol. *10*, 148–155.

Nishida, K., Yamaguchi, O., and Otsu, K. (2008). Crosstalk between autophagy and apoptosis in heart disease. Circ. Res. *103*, 343–351.

Orrenius, S., Zhivotovsky, B., and Nicotera, P. (2003). Regulation of cell death: the calcium-apoptosis link. Nat. Rev. Mol. Cell Biol. *4*, 552–565.

Pal, S., Konkimalla, V. B., Kathawate, L., Rao, S. S., Gejji, S. P., Puranik, V. G., Weyhermüller, T., and Salunke-Gawali, S. (2015). Targeting a chemorefractory COLO205 (BRAF V600E) cell line using substituted benzo[α]phenoxazines. RSC Adv. *5*, 82549–82563.

Papinski, D. *et al.* (2014). Early Steps in Autophagy Depend on Direct Phosphorylation of Atg9 by the Atg1 Kinase. Mol. Cell *53*, 471–483.

Paquet, C., Sane, A.-T., Beauchemin, M., and Bertrand, R. (2005). Caspase- and mitochondrial dysfunction-dependent mechanisms of lysosomal leakage and cathepsin B activation in DNA damage-

induced apoptosis. Leukemia *19*, 784–791.

Patil, V. S., Padalkar, V. S., Phatangare, K. R., Umape, P. G., Borase, B. N., and Sekar, N. (2015). Synthesis, Characterization, and Antibacterial Activity of Novel (1H-Benzo[d]imidazole-2-yl)-6-(diethylamino)-3H-one-xanthene, Phenoxazine, and Oxazine. J. Heterocycl. Chem. *52*, 124–129.

Pereira, C., Chaves, S., Alves, S., Salin, B., Camougrand, N., Manon, S., Sousa, M. J., and Corte-Real, M. (2010). Mitochondrial degradation in acetic acid-induced yeast apoptosis: the role of Pep4 and the ADP/ATP carrier. Mol. Microbiol. *76*, 1398–1410.

Piper, R. C., and Katzmann, D. J. (2007). Biogenesis and function of multivesicular bodies. Annu. Rev. Cell Dev. Biol. *23*, 519–547.

Pisetsky, D. (2014). The Expression of HMGB1 on Microparticles Released during Cell Activation and Cell Death In Vitroand In Vivo. Mol. Med. *20*, 1.

Puertollano, R. (2014). mTOR and lysosome regulation. F1000Prime Rep. *6*, 52.

Reiners, J. J. J., Caruso, J. A., Mathieu, P., Chelladurai, B., Yin, X.-M., and Kessel, D. (2002). Release of cytochrome c and activation of pro-caspase-9 following lysosomal photodamage involves Bid cleavage. Cell Death Differ. *9*, 934–944.

Renault, T. T., Dejean, L. M., and Manon, S. (2016). A brewing understanding of the regulation of Bax function by Bcl-xL and Bcl-2. Mech. Ageing Dev.

Roach, H. I., and Clarke, N. M. (2000). Physiological cell death of chondrocytes in vivo is not confined to apoptosis. New observations on the mammalian growth plate. J. Bone Joint Surg. Br. *82*, 601–613.

Ronfani, L., Ferraguti, M., Croci, L., Ovitt, C. E., Scholer, H. R., Consalez, G. G., and Bianchi, M. E. (2001). Reduced fertility and spermatogenesis defects in mice lacking chromosomal protein Hmgb2. Development *128*, 1265–1273.

Rovere-Querini, P. *et al.* (2004). HMGB1 is an endogenous immune adjuvant released by necrotic cells. EMBO Rep. *5*, 825–830.

Rubinsztein, D. C., Shpilka, T., and Elazar, Z. (2012). Mechanisms of autophagosome biogenesis. Curr. Biol. *22*, R29-34.

Sagulenko, V., Muth, D., Sagulenko, E., Paffhausen, T., Schwab, M., and Westermann, F. (2008). Cathepsin D protects human neuroblastoma cells from doxorubicin-induced cell death. Carcinogenesis *29*, 1869–1877.

Salomi, B. S. B., Mitra, C. K., and Gorton, L. (2005). Electrochemical and spectrophotometric studies on dyes and proteins labelled with dyes. Synth. Met. *155*, 426–429.

Santos, J., Sousa, M. J., and Leão, C. (2012). Ammonium Is Toxic for Aging Yeast Cells, Inducing Death and Shortening of the Chronological Lifespan. PLoS One *7*, e37090.

Sastry, P. S., and Rao, K. S. (2000). Apoptosis and the nervous system. J. Neurochem. *74*, 1–20.

Scaffidi, P., Misteli, T., and Bianchi, M. E. (2002). Release of chromatin protein HMGB1 by necrotic cells triggers inflammation. Nature *418*, 191–195.

Schmidt, O., and Teis, D. (2012). The ESCRT machinery. Curr. Biol. *22*, R116–R120.

Schweichel, J. U., and Merker, H. J. (1973). The morphology of various types of cell death in prenatal tissues. Teratology *7*, 253–266.

Serrano-Puebla, A., and Boya, P. (2016). Lysosomal membrane permeabilization in cell death: new evidence and implications for health and disease. Ann. N. Y. Acad. Sci. *1371*, 30–44.

Shimamoto, T., Tomoda, A., Ishida, R., and Ohyashiki, K. (2001). Antitumor effects of a novel phenoxazine derivative on human leukemia cell lines in vitro and in vivo. Clin. Cancer Res. *7*, 704–708.

Shintani, T., and Klionsky, D. J. (2004). Cargo proteins facilitate the formation of transport vesicles in the cytoplasm to vacuole targeting pathway. J. Biol. Chem. *279*, 29889–29894.

Shirato, K., Imaizumi, K., Abe, A., and Tomoda, A. (2007). Phenoxazine derivatives 2-amino-4,4alpha-dihydro-4alpha-phenoxazine-3-one and 2-aminophenoxazine-3-one-induced apoptosis through a caspase-independent mechanism in human neuroblastoma cell line NB-1 cells. Biol. Pharm. Bull. *30*, 331–336.

Shpilka, T., Weidberg, H., Pietrokovski, S., and Elazar, Z. (2011). Atg8: an autophagy-related ubiquitin-like protein family. Genome Biol *12*, 226.

Silva, G. A., Costa, L. M. M., Brito, F. C. F., Miranda, A. L. P., Barreiro, E. J., and Fraga, C. A. M. (2004). New class of potent antinociceptive and antiplatelet 10H-phenothiazine-1-acylhydrazone derivatives. Bioorg. Med. Chem. *12*, 3149–3158.

Soto, C. Y., Andreu, N., Gibert, I., and Luquin, M. (2002). Simple and Rapid Differentiation of Mycobacterium tuberculosis H37Ra from M . tuberculosis Clinical Isolates through Two Cytochemical Tests Using Neutral Red and Nile Blue Stains Simple and Rapid Differentiation of Mycobacterium tuberculosis H37Ra from M . Society *40*, 3021–3024.

Stewart, A., and Deacon, J. W. (1995). Vital fluorochromes as tracers for fungal growth studies. Biotech. Histochem. *70*, 57–65.

Štros, M. (2010). HMGB proteins: Interactions with DNA and chromatin. Biochim. Biophys. Acta - Gene Regul. Mech. *1799*, 101–113.

Stunkard, A. J. (2009). NIH Public Access. Psychiatry Interpers. Biol. Process. *162*, 214–220.

Suen, D., Norris, K. L., and Youle, R. J. (2008). Mitochondrial dynamics and apoptosis Mitochondrial dynamics and apoptosis. 1577–1590.

Suzuki, F., Hashimoto, K., Ishihara, M., Westman, G., Samuelsson, K., Kawase, M., Motohashi, N., and Sakagami, H. (2007). Tumor-specificity and type of cell death induced by phenoxazines. Anticancer Res. *27*, 4233–4238.

Swaminathan, S., and Sunnerhagen, P. (2005). Degradation of Saccharomyces cervisiae Rck2 upon exposure of cells to high levels of zinc is dependent on Pep4. Mol. Genet. Genomics *273*, 433–439.

Taylor, R. C., Cullen, S. P., and Martin, S. J. (2008). Apoptosis: controlled demolition at the cellular

level. Nat. Rev. Mol. Cell Biol. *9*, 231–241.

Terman, a, Kurz, T., Gustafsson, B., and Brunk, U. T. (2006). Lysosomal labilization. IUBMB Life *58*, 531–539.

Thomas, J. O., and Travers, A. A. (2001). HMG1 and 2, and related "architectural" DNA-binding proteins. Trends Biochem. Sci. *26*, 167–174.

Thompson, C. B. (1995). Apoptosis in the pathogenesis and treatment of disease. Science *267*, 1456–1462.

Turk, B., Stoka, V., Rozman-Pungercar, J., Cirman, T., Droga-Mazovec, G., Oresic, K., and Turk, V. (2002). Apoptotic pathways: involvement of lysosomal proteases. Biol. Chem. *383*, 1035–1044.

Turk, B., and Turk, V. (2009). Lysosomes as "suicide bags" in cell death: Myth or reality? J. Biol. Chem. *284*, 21783–21787.

Turk, V., Stoka, V., Vasiljeva, O., Renko, M., Sun, T., Turk, B., and Turk, D. (2012). Cysteine cathepsins: from structure, function and regulation to new frontiers. Biochim. Biophys. Acta *1824*, 68–88.

Vellai, T., Takacs-Vellai, K., Sass, M., and Klionsky, D. J. (2009). The regulation of aging: does autophagy underlie longevity? Trends Cell Biol. *19*, 487–494.

Villalpando Rodriguez, G. E., and Torriglia, A. (2013). Calpain 1 induce lysosomal permeabilization by cleavage of lysosomal associated membrane protein 2. Biochim. Biophys. Acta *1833*, 2244–2253.

Vande Walle, L., Kanneganti, T.-D., and Lamkanfi, M. (2011). HMGB1 release by inflammasomes. Virulence *2*, 162–165.

Weir, H. M., Kraulis, P. J., Hill, C. S., Raine, a R., Laue, E. D., and Thomas, J. O. (1993). Structure of the HMG box motif in the B-domain of HMG1. EMBO J. *12*, 1311–1319.

Werneburg, N., Guicciardi, M. E., Yin, X.-M., and Gores, G. J. (2004). TNF-alpha-mediated lysosomal permeabilization is FAN and caspase 8/Bid dependent. Am. J. Physiol. Gastrointest. Liver Physiol. *287*, G436-43.

Wissing, S. *et al.* (2004). An AIF orthologue regulates apoptosis in yeast. J. Cell Biol. *166*, 969 LP-974.

Yang, H., Antoine, D. J., Andersson, U., and Tracey, K. J. (2013). The many faces of HMGB1: molecular structure-functional activity in inflammation, apoptosis, and chemotaxis. J. Leukoc. Biol. *93*, 865–873.

Youle, R. J., and Strasser, A. (2008). The BCL-2 protein family: opposing activities that mediate cell death. Nat. Rev. Mol. Cell Biol. *9*, 47–59.

Young, A. R. J. *et al.* (2009). Autophagy mediates the mitotic senescence transition. Genes Dev. *23*, 798–803.

Zhivotovsky, B., and Orrenius, S. (2011). Calcium and cell death mechanisms: A perspective from the cell death community. Cell Calcium *50*, 211–221.

Ziegler, U. (2004). Morphological Features of Cell Death. News Physiol. Sci. *19*, 124–128.

Zitvogel, L., Casares, N., Pequignot, M. O., Chaput, N., Albert, M. L., and Kroemer, G. (2004). Immune response against dying tumor cells. Adv. Immunol. *84*, 131–179.